MRIと最新の実験室天体プラズマ

Takayoshi Sano

(ILE, Osaka U, Japan)

【MHD2017】

磁気流体プラズマで探る高エネルギー天体現象研究会

August 28, 2017 (東京)

Since I moved to Osaka, ...

- MHD Simulation + Laser Experiment
- Keywords: Plasma Physics, Magnetic Field
- Target: Boundary between Laboratory (Laser) Plasma and Astrophysical Plasma
  - MHD Turbulence (MRI, Dynamo)
  - High-Pressure Physics (H EOS) Jupiter, ICF
  - Interfacial Instability (RMI, RTI) ISM, ICF
  - Particle Acceleration (PIC) LPI + B


コズミックフロント☆NEXT
木星誕生のミステリー
佐野 孝好 助教
大阪大学


コズミックフロント☆
NEXT


コズミックフロント☆
NEXT
木星誕生のミステリー
佐野 孝好 助教
大阪大学

To understand the saturation of MRI is an ultimate goal of accretion disk study.

- What is the origin of "alpha"?
  - Local Shearing Box
  - Non-ideal MHD Effects (Ohmic & Hall)
  - Pressure Dependence?
- What determines the saturation?
  - Magnetic Field Geometry
  - Dissipation
  - Magnetic Prandtl Number
  - Global Effect (Wind)
  - Convection?

MRI turbulence is the most promising mechanism of angular momentum transport.

- Origin of Turbulence in Accretion Disks
- Key Ingredients
  - (Weak) Seed Field
  - Differential Rotation

$$d\Omega/dr < 1$$

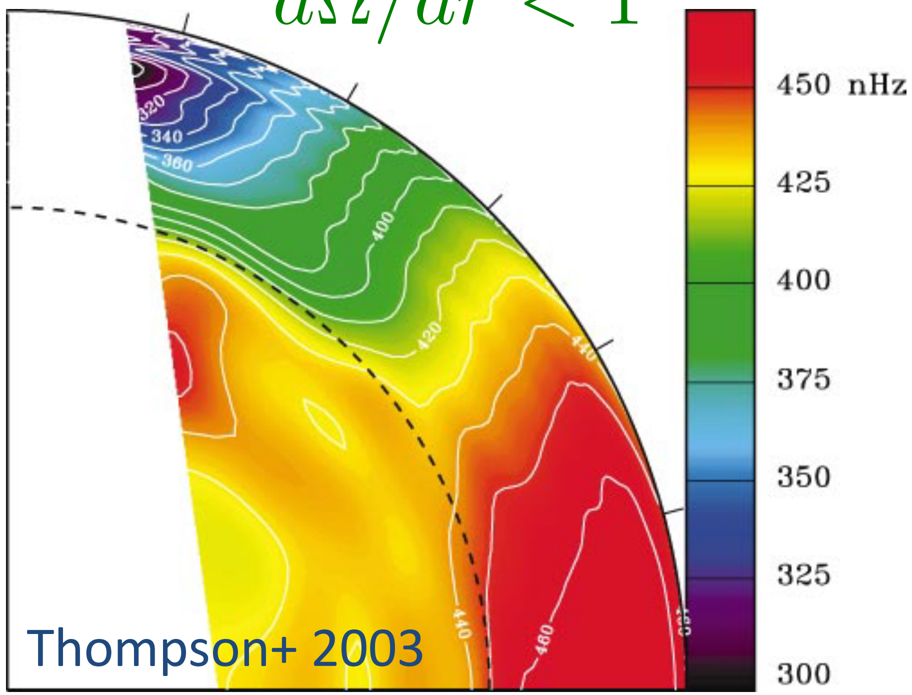

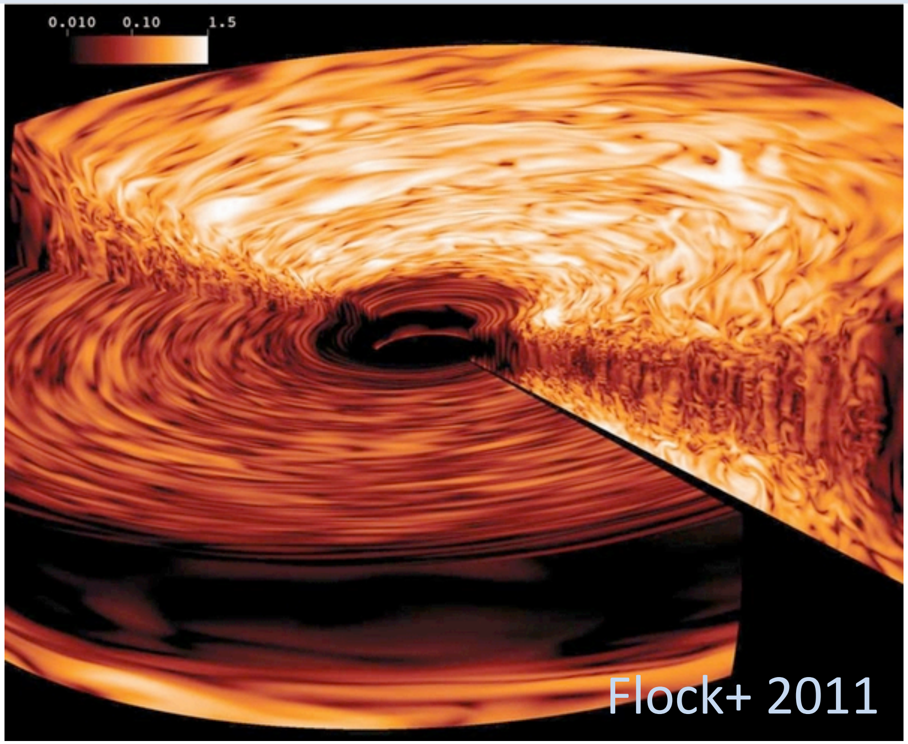

- Field Amplification (Dynamo)
- Different Rotation in the Sun → Unstable?

Convection zone in the Sun could be unstable for MRI.

- Higher Latitude Tachocline
- Near Surface Shear Layer (NSSL)

$$q = -\frac{d\ln\Omega}{d\ln r} \approx 1$$

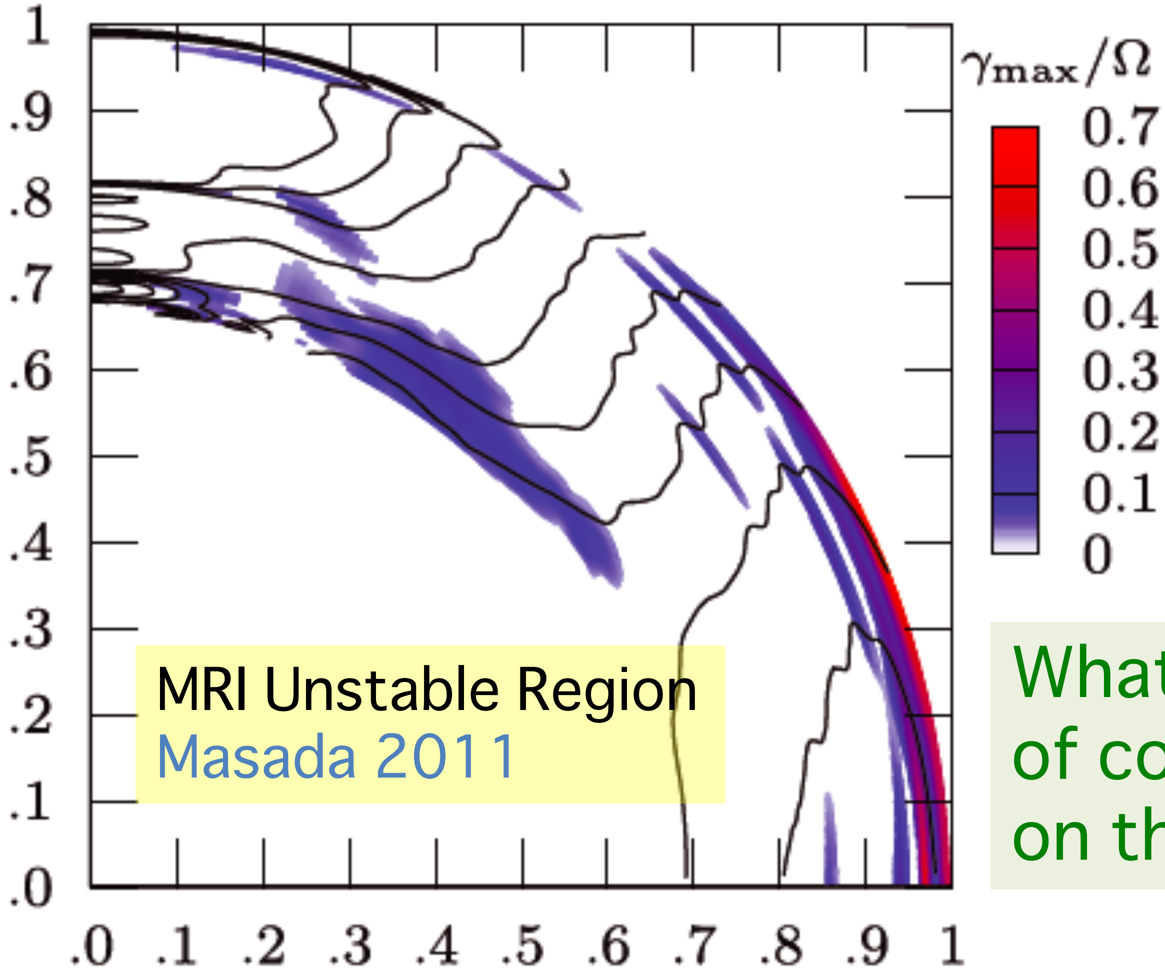

What about the effects of convective motion on the MRI?

Linear stability for MRI is examined with a radial shear in the vertical velocity.

Unperturbed State

- Uniform Density & Pressure
- Differential Rotation & Vertical Shear Flow

$$\boldsymbol{v}_0 = (0, -q\Omega x, v_{z0}(x))$$

- Sinusoidal Shear

$$v_{z0} = v_0 \cos(k_0 x)$$

- Uniform Vertical Magnetic Field

$$\boldsymbol{B}_0 = (0, 0, B_0)$$

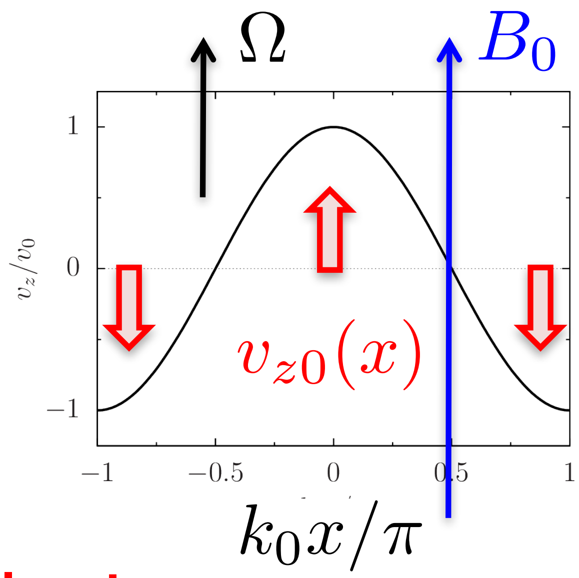

Two Major Parameters of This Analysis

$$K_0 = \frac{v_{A0} k_z}{\Omega} \quad \& \quad V_0 = \frac{v_0}{v_{A0}}$$

The growth rate is given by complex eigen-values of 2nd order dispersion equations.

$$D\left(\frac{\delta P}{\rho_0} + v_{A0}^2 \frac{\delta B_z}{B_0}\right) = \frac{\left(\sigma^2 - v_{A0}^2 k_z^2\right)^2 - \kappa^2 \left(\sigma^2 - v_{A0}^2 k_z^2\right) - 4\Omega^2 v_{A0}^2 k_z^2}{\sigma\left(\sigma^2 - v_{A0}^2 k_z^2\right)} \left(i\delta v_x\right)$$

$$D\left(i\delta v_x\right) = -\left(D v_{z0}\right) \frac{k_z}{\sigma} \left(i\delta v_x\right) + \frac{\sigma k_z^2}{\sigma^2 - v_{A0}^2 k_z^2} \left(\frac{\delta P}{\rho_0} + v_{A0}^2 \frac{\delta B_z}{B_0}\right)$$

$$\sigma \equiv \omega - v_{z0} k_z \qquad v_{A0}^2 \equiv \frac{B_0^2}{4\pi\rho_0}$$

- Periodic Boundary Condition

$$i\delta v_x = 0 \quad \text{or} \quad D(i\delta v_x) = 0 \quad \text{at} \quad k_0 x = \pm\pi$$

- Eigenvalue Problem for Growth Rate ω
  - Searched in Complex Space

KHI in the shearing box is suppressed by differential rotation.

Growth Rate
$\sim v_0 k_0$

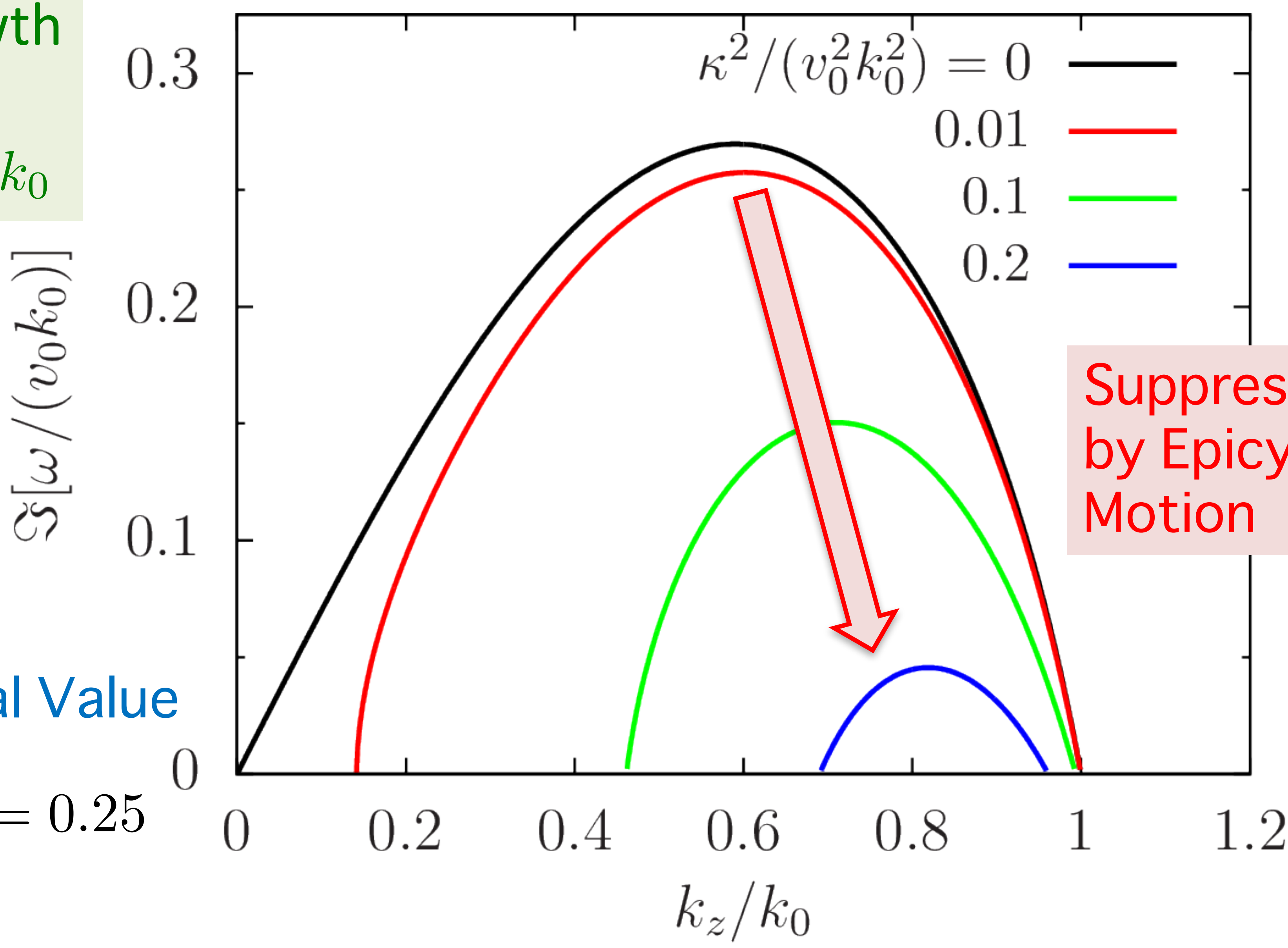

Suppression by Epicyclic Motion

Critical Value

$$\frac{\kappa^2}{v_0^2 k_0^2} = 0.25$$

If the shear velocity exceeds the Alfven speed, the growth of MRI is reduced significantly.

- Reduction of MRI Growth
- Appearance of KHI Mode

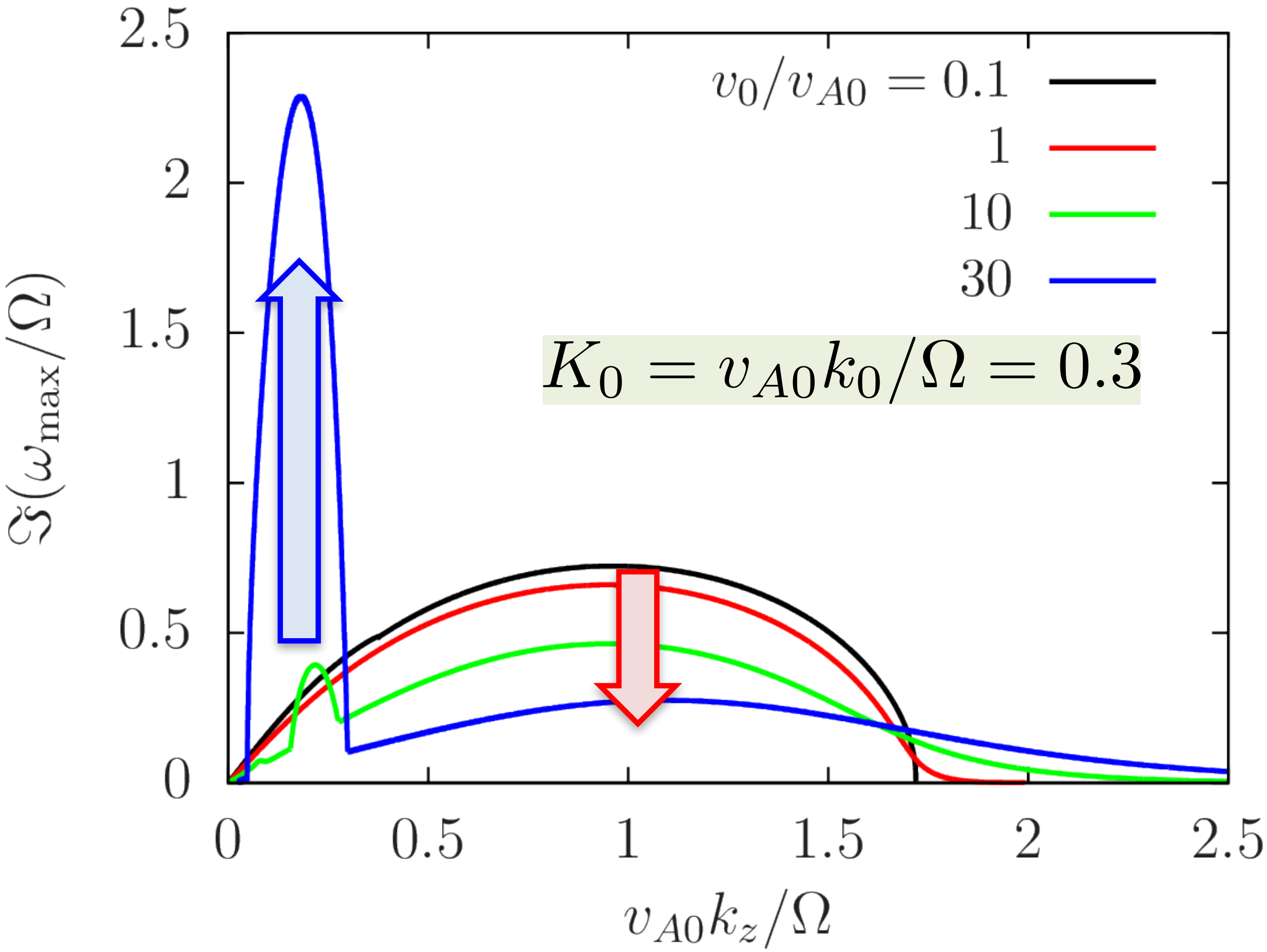

Linear growth of MRI is killed or regulated by convection (turbulent) motion.

Conditions:

- Shear wavelength is comparable to v_{A0}/Ω
- Shear velocity is 10 times faster than Alfven speed.

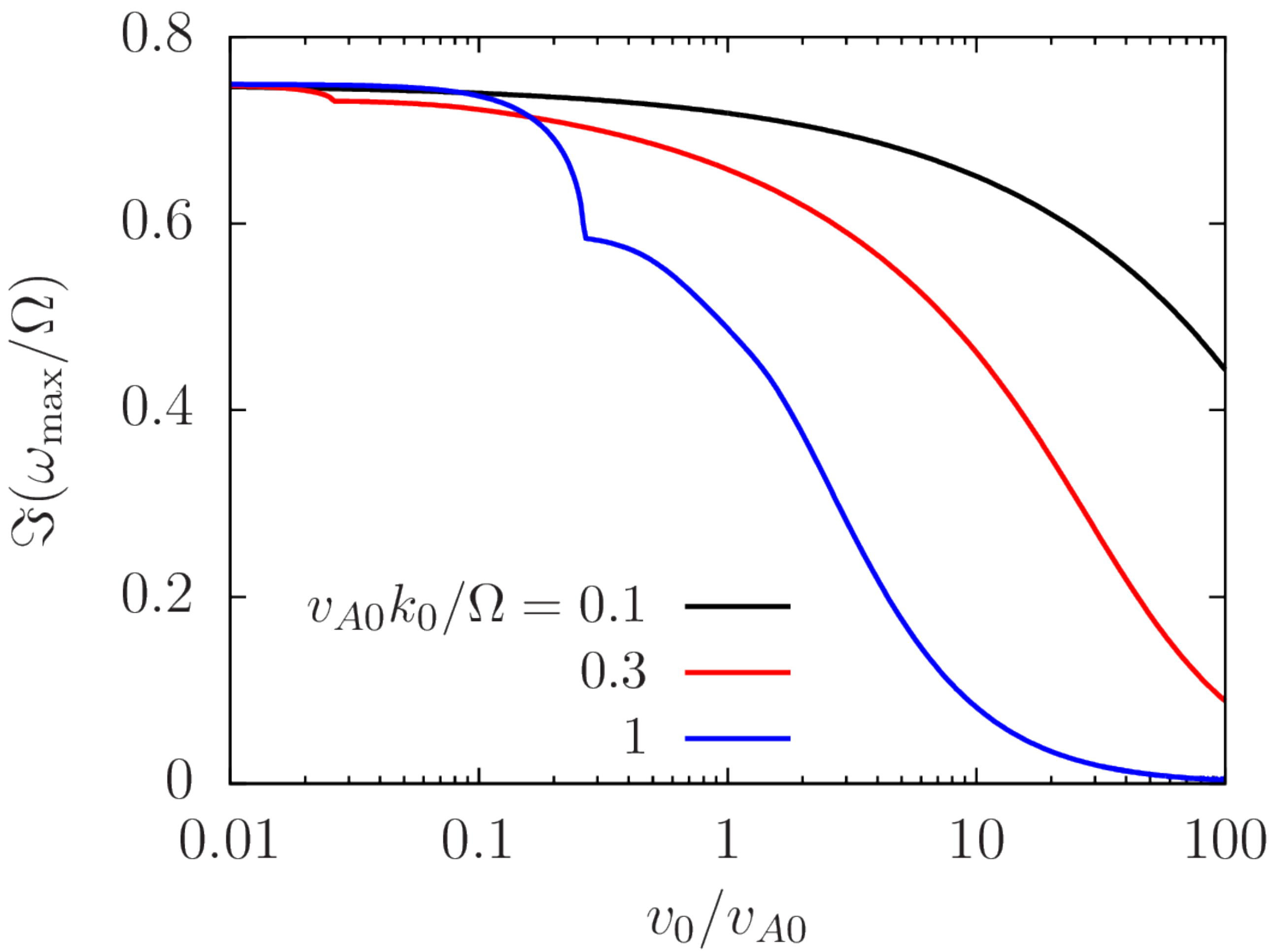

Maximum Growth Rate at $v_{A0}k_z/\Omega = 1$

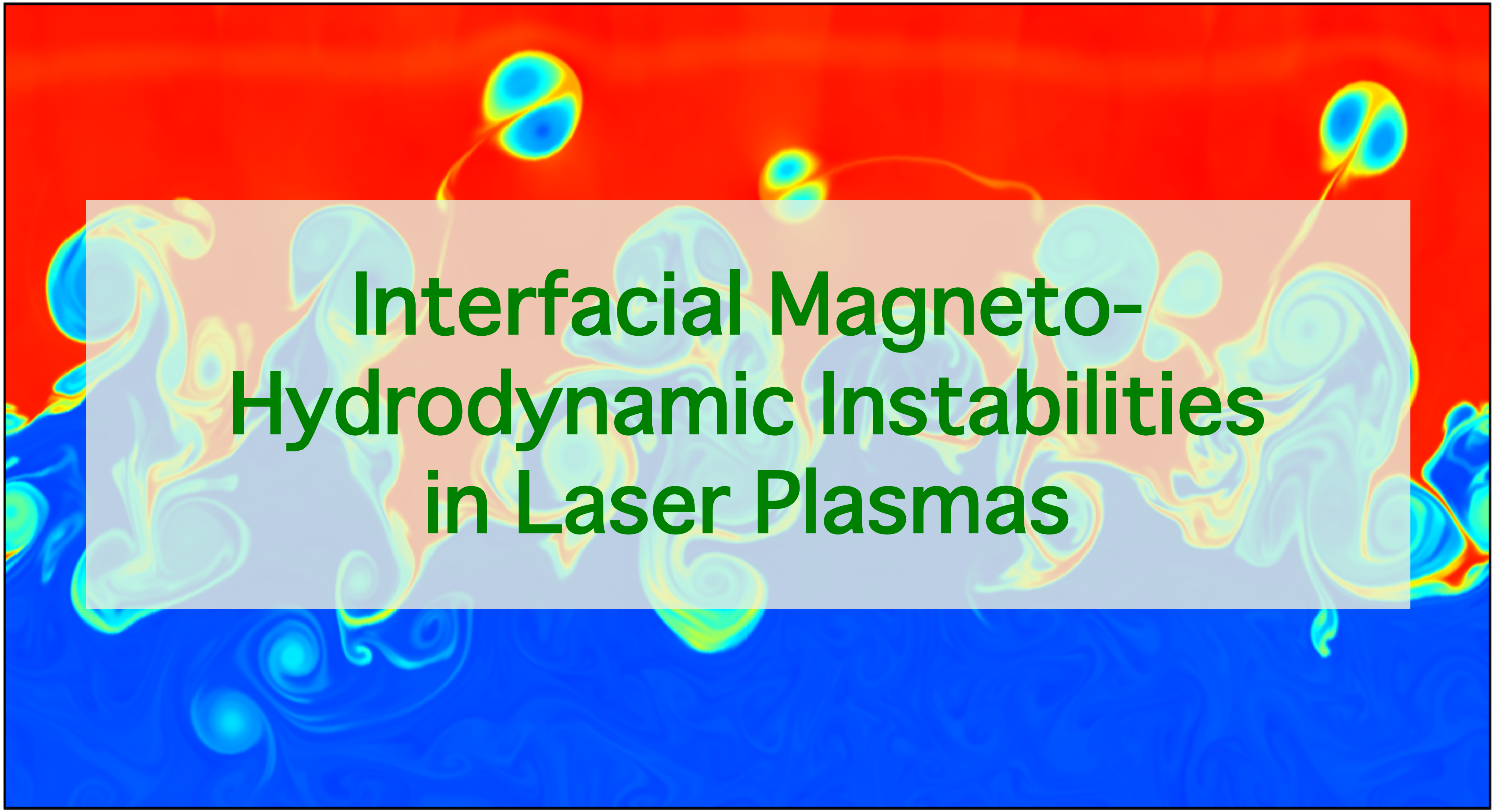
Interfacial Magneto-
Hydrodynamic Instabilities
in Laser Plasmas

Collaborators

- Simulation & Theory
  - K. Nishihara (Osaka U)
  - C. Matsuoka (Osaka City U)
  - T. Inoue (Nagoya U)
  - J. G. Wouchuk (UCLM, Spain)

- Laser Experiment
  - Y. Sakawa, S. Fujioka, K. Shigemori, S. Tamatani, M. Murakami, R. Kumar, K. Matsuo (Osaka U)
  - T. Morita (Kyushu U)
  - M. Koenig, B. Albertazzi, T. Michel, G. Rigon (LULI, France)
  - A. Casner (CEA, France)

Laser Experiment

GEKKO XII Laser at ILE, Osaka U

Laser Wavelength: 0.35 [um], Laser Energy: 1 [kJ]
Pulse Duration: 2.5 [ns], Spot Diameter: 600 [um]

Outline

- Backgrounds
  - Why RMI? Why Magnetic Field?
- MHD RMI
- Effects of Magnetic Field
  1. Suppression of RMI (Theory)
  2. Field Amplification (Theory/Experiment)
  3. Anisotropic Thermal Conduction (Experiment)
- Summary

MHD Simulations

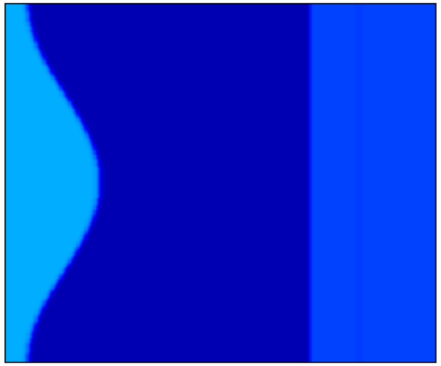

Laser Experiment

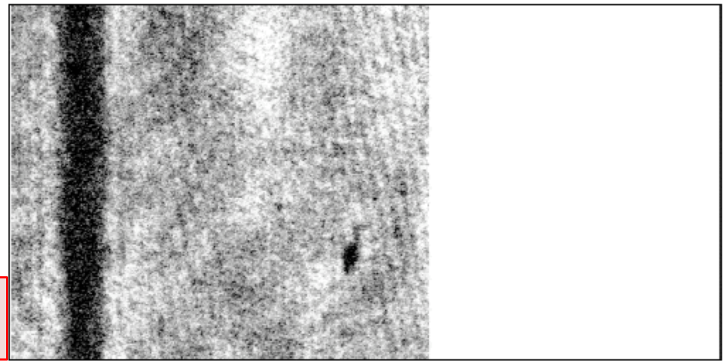

Backgrounds

RMI-driven turbulence plays an important role in various plasma phenomena.

Astrophysical Plasmas

- Supernova Shocks + Inhomogeneous Interstellar Medium
  - Origin of IS Turbulence
  - Magnetic Field Amplification

Laboratory Plasmas

- Implosion in Laser Fusion Plasma
  - "Mixing" by RMI & RTI
  - External Magnetic Field

RMI + Magnetic Field = ???

Supernova Remnant

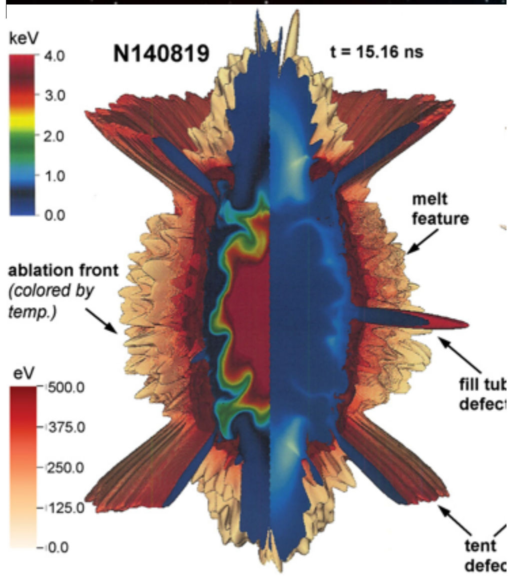

Clark+ 2016

Generation of kilo-Tesla magnetic fields has been achieved by high-power lasers.

- Strong B Field Available in Laser Exp.
- Method (Using GEKKO Laser in Osaka)
  - Coil + Compression
  - Capacitor Coil

cf.) 1kT = 10MG, Permanent Magnet ～1T

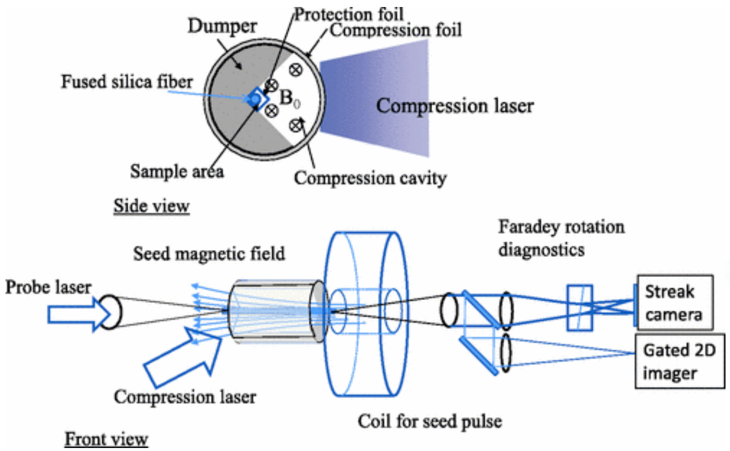

Yoneda+ 2012

Fujioka+ 2013

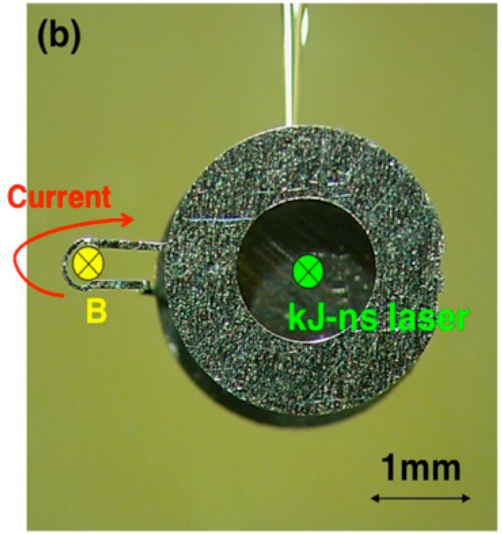

Korneev+ 2015

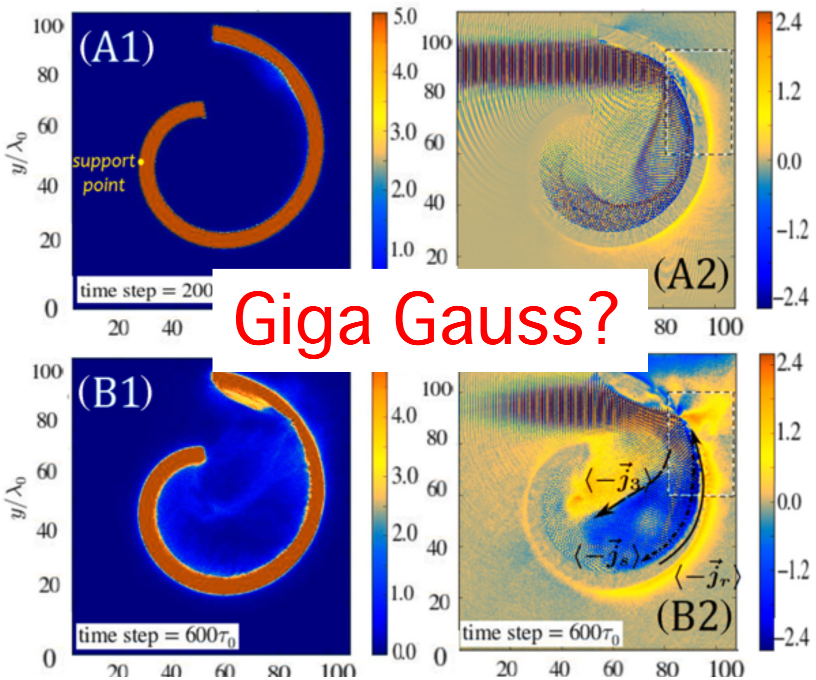

Giga Gauss?

Laser experiments can treat RMI in high-energy-density plasmas.

- "Low Energy Density" RMI

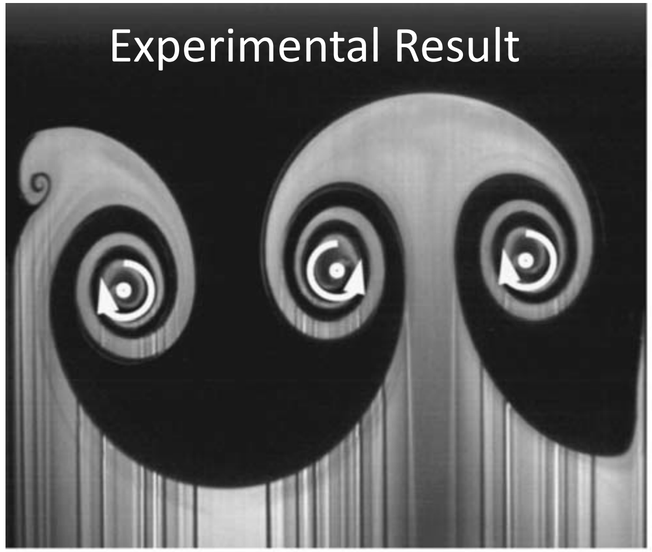

Chapmann & Jacobs 2006

Laser experiments can treat RMI in high-energy-density plasmas.

- "Low Energy Density" RMI
- "High Energy Density" RMI
  - High Mach Number Shock
  - Plasma Flow
  - Magnetic Field
- Laser Plasma RMI
  - Ablative RM-type Instability
  - Classical RMI (Heavy-to-Light)

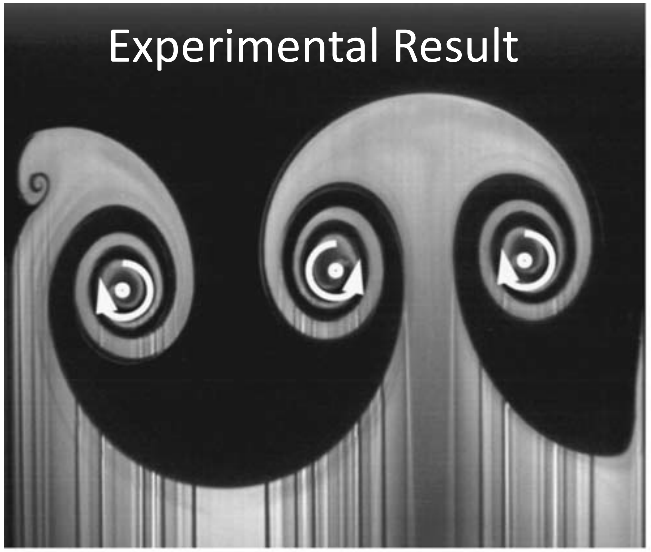

Chapmann & Jacobs 2006

Glendinning+ 2003

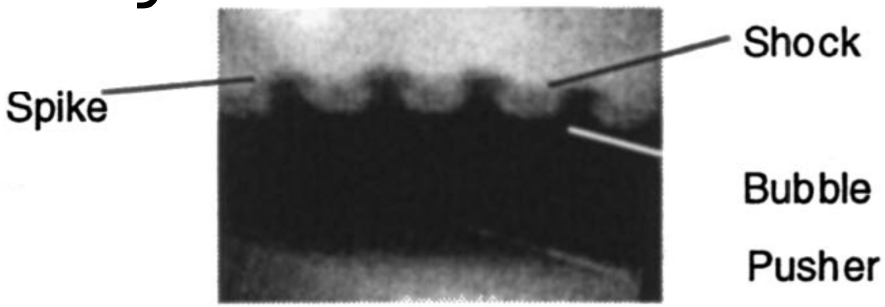

The key ingredients of RMI is a shock wave and corrugated contact discontinuity.

Minimum Setup for RMI
(Single-Mode Analysis)

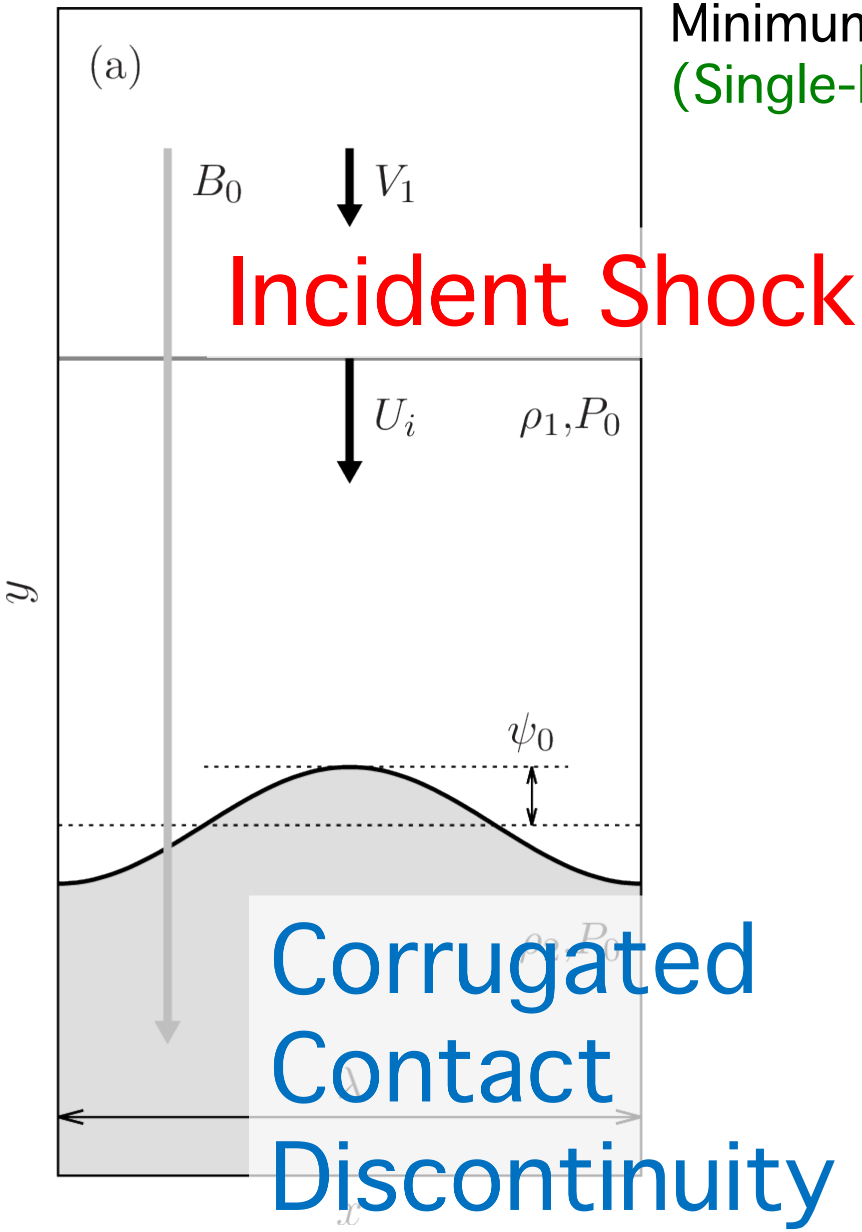

Density

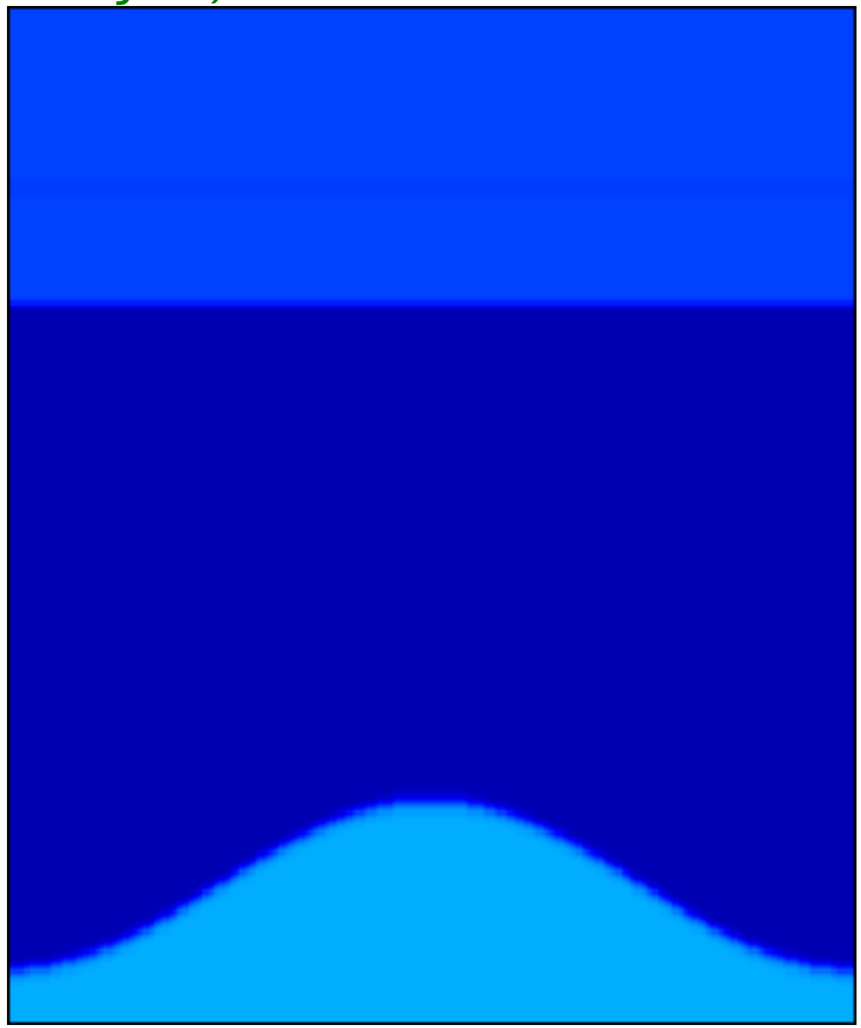

RMI: Growth of a Mushroom-Shaped Spike in Density Distribution

Driving engine of RMI is the vorticity deposited at the corrugated interface.

- Mechanism: Tangential Flows Caused by Refraction Motion at Oblique Shock Surface

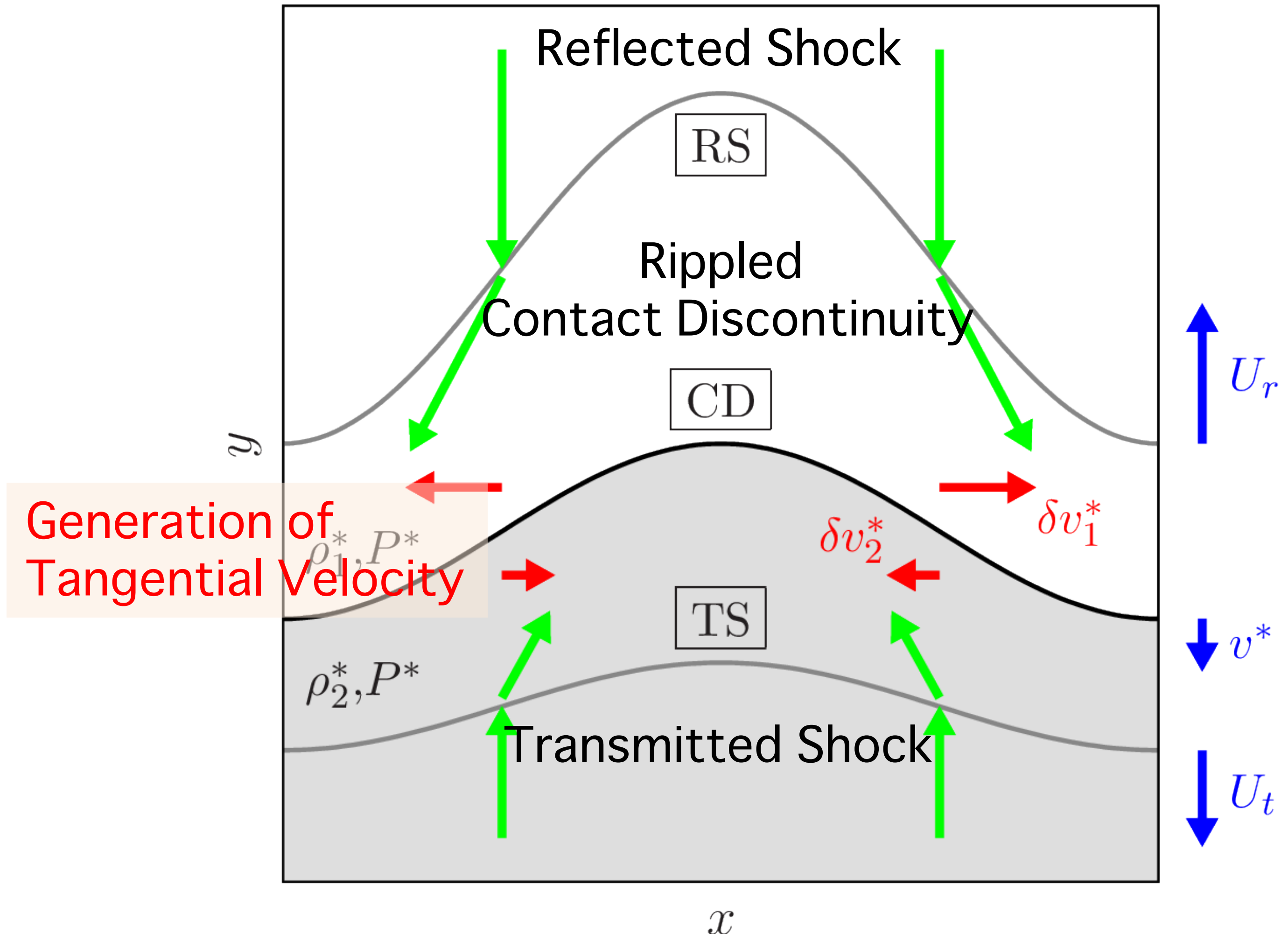

Driving engine of RMI is the vorticity deposited at the corrugated interface.

- Mechanism: Tangential Flows Caused by Refraction Motion at Oblique Shock Surface
- Growth Velocity

$$v_{\text{lin}} = \frac{\rho_1^* \delta v_1^* - \rho_2^* \delta v_2^*}{\rho_1^* + \rho_2^*}$$

Wouchuk & Nishihara 1996; 1997

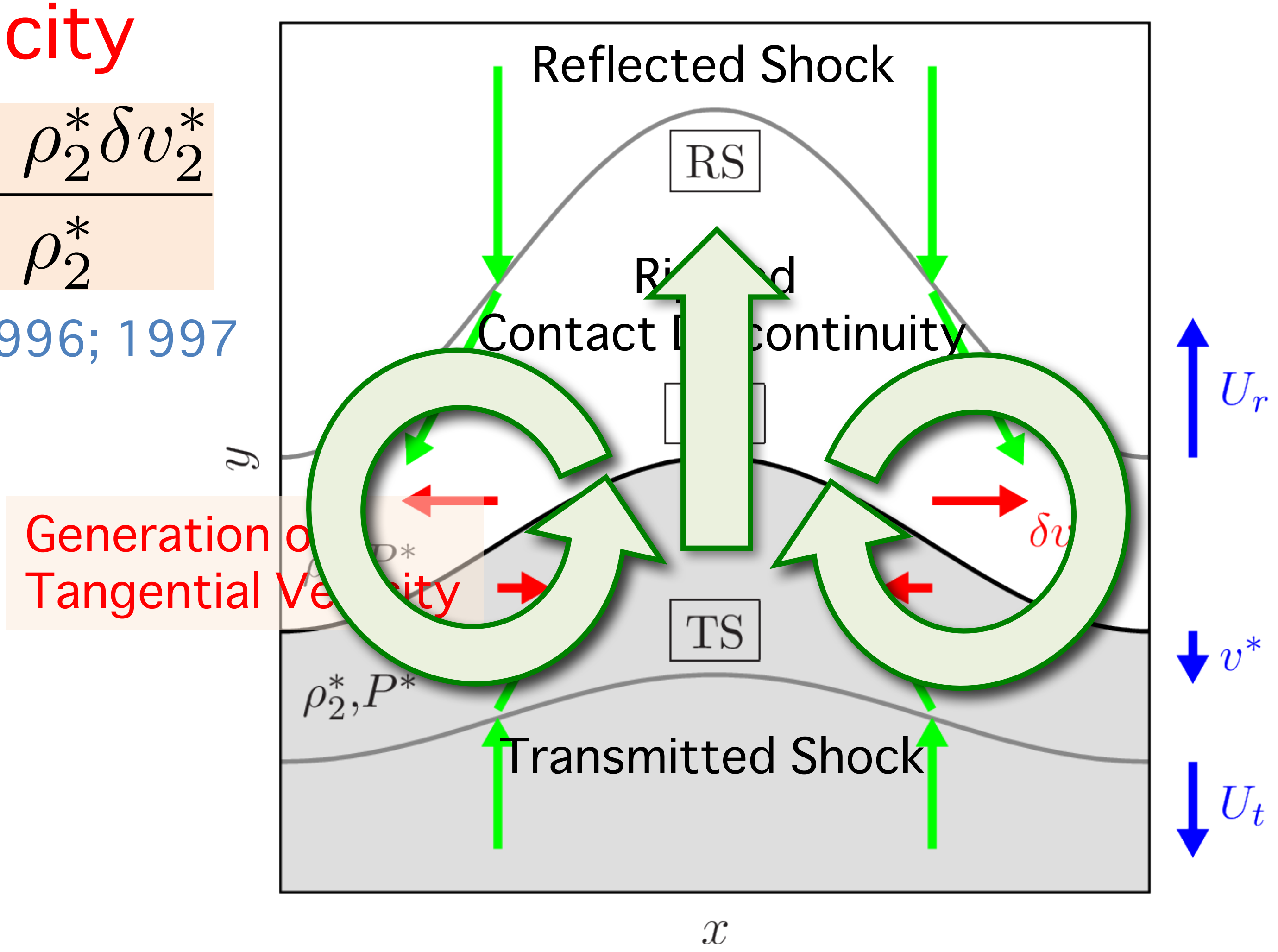

Driving engine of RMI is the vorticity deposited at the corrugated interface.

- Mechanism: Tangential Flows Caused by Refraction Motion at Oblique Shock Surface

- Growth Velocity

$$v_{\rm lin} = \frac{\rho_1^* \delta v_1^* - \rho_2^* \delta v_2^*}{\rho_1^* + \rho_2^*}$$

Wouchuk & Nishihara 1996; 1997

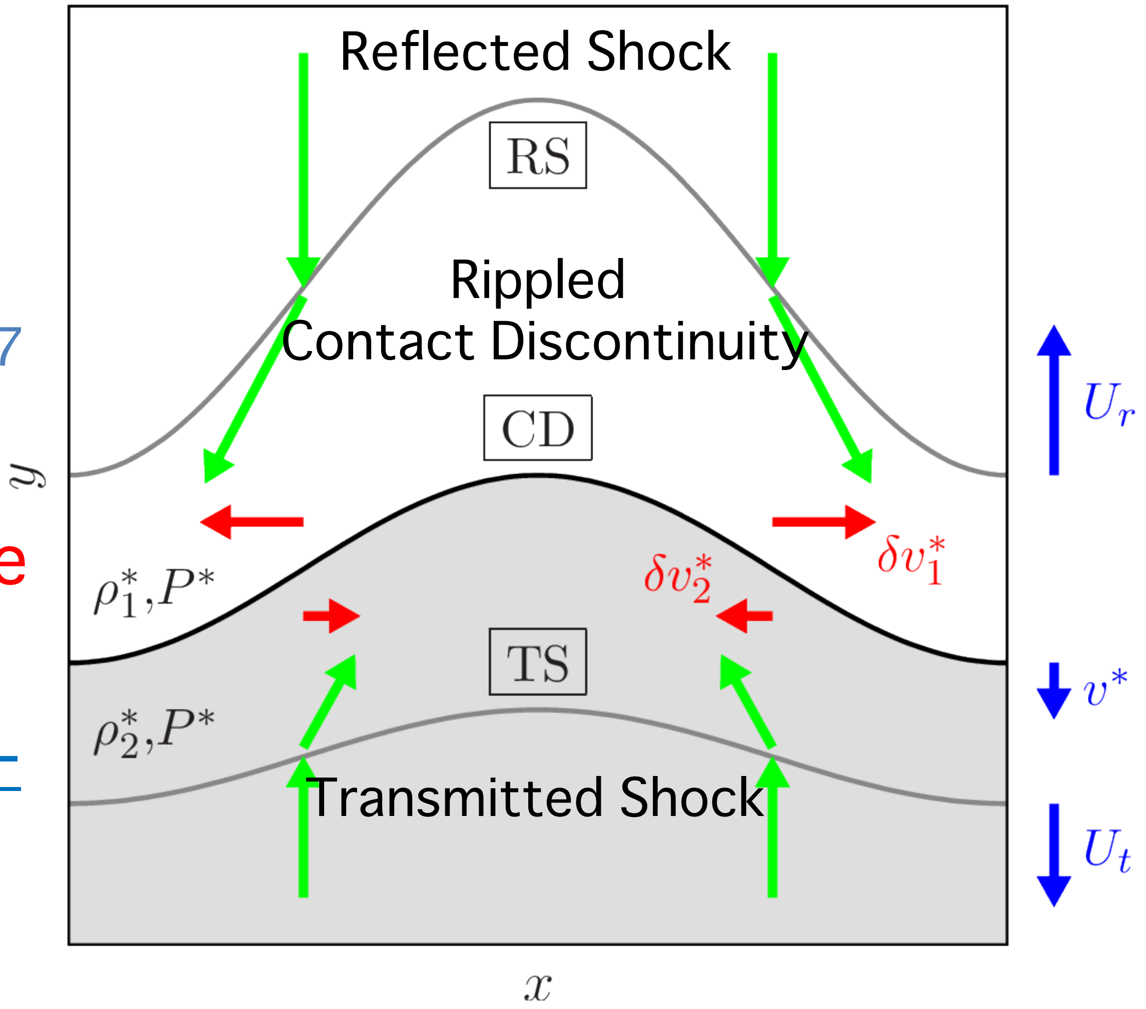

Characteristics of RMI

- Linear Growth with Time
- Without Gravity
- Unstable for Both Light-to-Heavy & Heavy-to-Light Configurations

There are some formula predicting the linear growth velocity of RMI theoretically.

- Asymptotic Growth Velocity

Wouchuk & Nishihara 1997

$$v_{\text{lin}} = \frac{\rho_2^* \delta v_2^* - \rho_1^* \delta v_1^*}{\rho_2^* + \rho_1^*} - \frac{\rho_2^* F_2 - \rho_1^* F_1}{\rho_2^* + \rho_1^*}$$

  - Sonic Interaction Parameter "F"

- Simpler Formula
  - Richtmyer (1960)

$$v_{\text{IM}} = A^* k \psi_0^* v_i$$

Interface Velocity

  - Meyer & Blewett (1972)

$$v_{\text{MB}} = A^* k \frac{\psi_0 + \psi_0^*}{2} v_i$$

Atwood Number after the Interaction

$$A^* = \frac{\rho_2^* - \rho_1^*}{\rho_2^* + \rho_1^*}$$

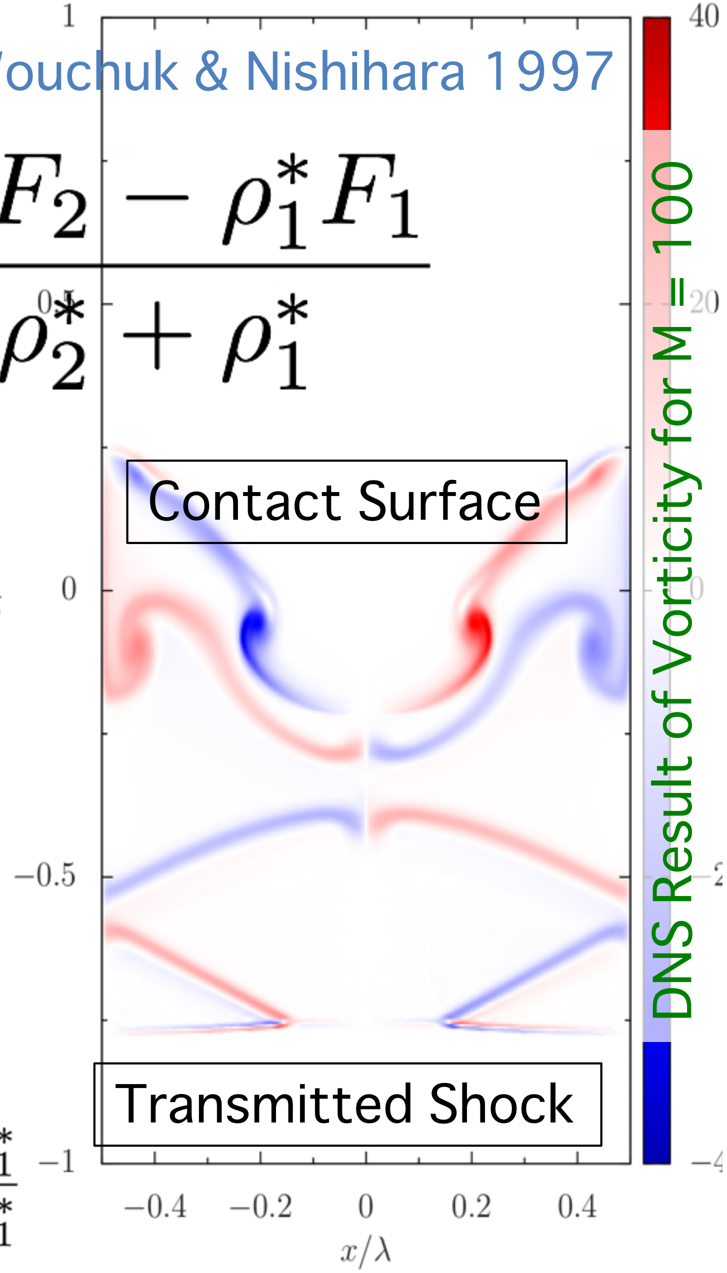

There are some formula predicting the linear growth velocity of RMI theoretically.

- Asymptotic Growth Velocity

Wouchuk & Nishihara 1997

$$v_{\text{lin}} = \frac{\rho_2^* \delta v_2^* - \rho_1^* \delta v_1^*}{\rho_2^* + \rho_1^*} - \frac{\rho_2^* F_2 - \rho_1^* F_1}{\rho_2^* + \rho_1^*}$$

  - Sonic Interaction Parameter "F"

    ··· Reduces the Growth Velocity

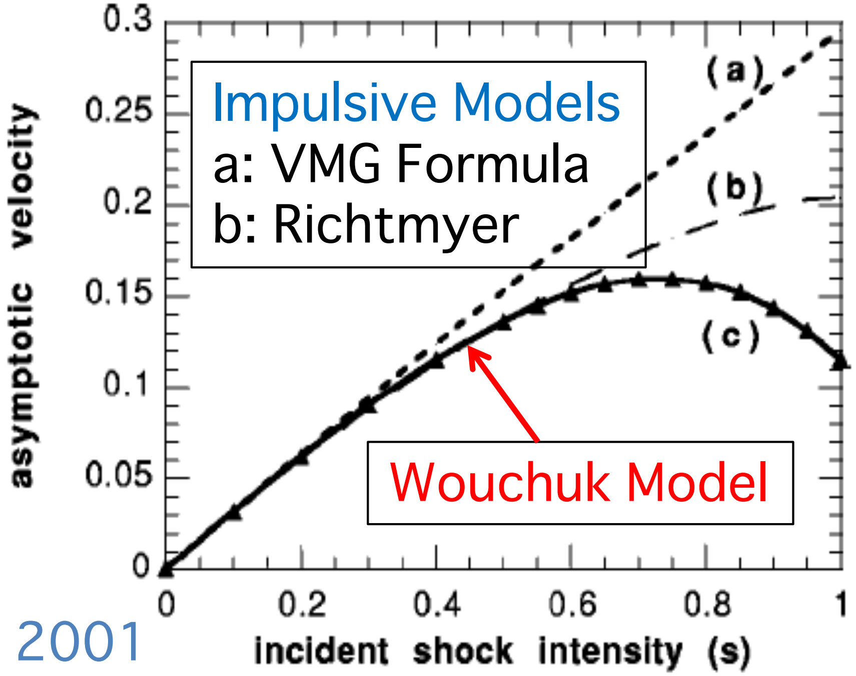

Wouchuk 2001

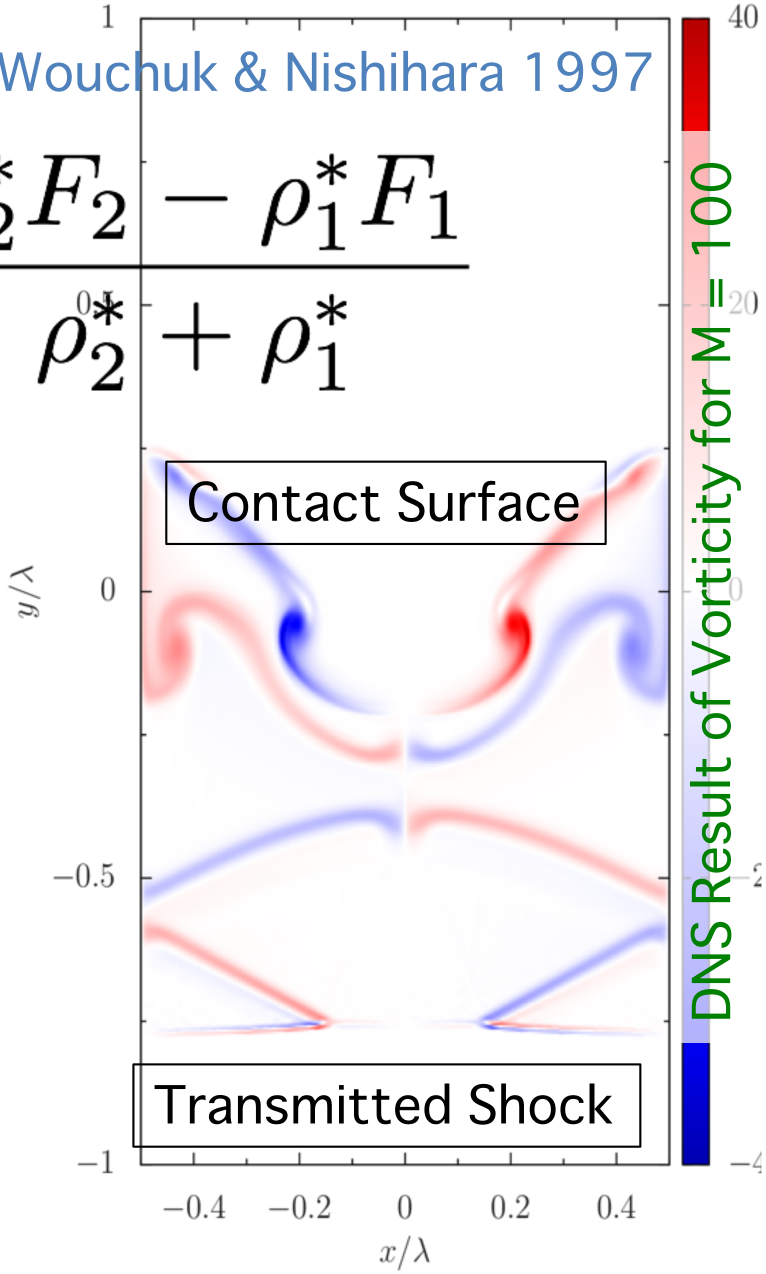

Important effects of B fields on RMI have shown by simulations and experiments.

1. Suppression of RMI Growth by a Strong Magnetic Field
2. Amplification of a Magnetic Field by RMI Turbulent Motions
3. Energy Confinement Due to Anisotropic Thermal Conduction

1. Suppression of RMI

MHD Simulations

Samtaney 2003
Wheatley et al. 2005; 2009
Sano+ PRL 2013

Basic equations for numerical RMI simulations are standard ideal MHD equations.

SIM

- Ideal MHD Equations

$$\frac{\partial \rho}{\partial t} + \boldsymbol{\nabla} \cdot (\rho \boldsymbol{v}) = 0$$

$$\frac{\partial \rho \boldsymbol{v}}{\partial t} + \boldsymbol{\nabla} \cdot \left[\left(P + \frac{B^2}{8\pi} \right) \boldsymbol{I} + \rho \boldsymbol{v}\boldsymbol{v} - \frac{\boldsymbol{B}\boldsymbol{B}}{4\pi} \right] = 0$$

$$\frac{\partial e}{\partial t} + \boldsymbol{\nabla} \cdot \left[\left(e + P + \frac{B^2}{8\pi} \right) \boldsymbol{v} - \frac{(\boldsymbol{B} \cdot \boldsymbol{v}) \boldsymbol{B}}{4\pi} \right] = 0$$

$$\frac{\partial \boldsymbol{B}}{\partial t} = \boldsymbol{\nabla} \times (\boldsymbol{v} \times \boldsymbol{B}) \qquad e = \frac{P}{\gamma - 1} + \frac{\rho v^2}{2} + \frac{B^2}{8\pi}$$

- Numerical MHD Scheme
  - Godunov-type Grid-base Scheme with an Approximate MHD Riemann Solver (Sano+ ApJ 1998)
  - CMoC-CT for the Field Evoluton (Clarke 1996)

Initial setup for the single-mode analysis is characterized by only 4 parameters.

SIM

- 2D Initial Configuration
- 4 Non-Dimensional Parameters

1. Mach Number

$$M = |U_i|/c_{s1}$$

2. Density Jump

$$\rho_2/\rho_1$$

3. Corrugation Amplitude

$$\psi_0/\lambda$$

4. Field Strength

$$\beta_0 = 8\pi P_0/B_0^2$$

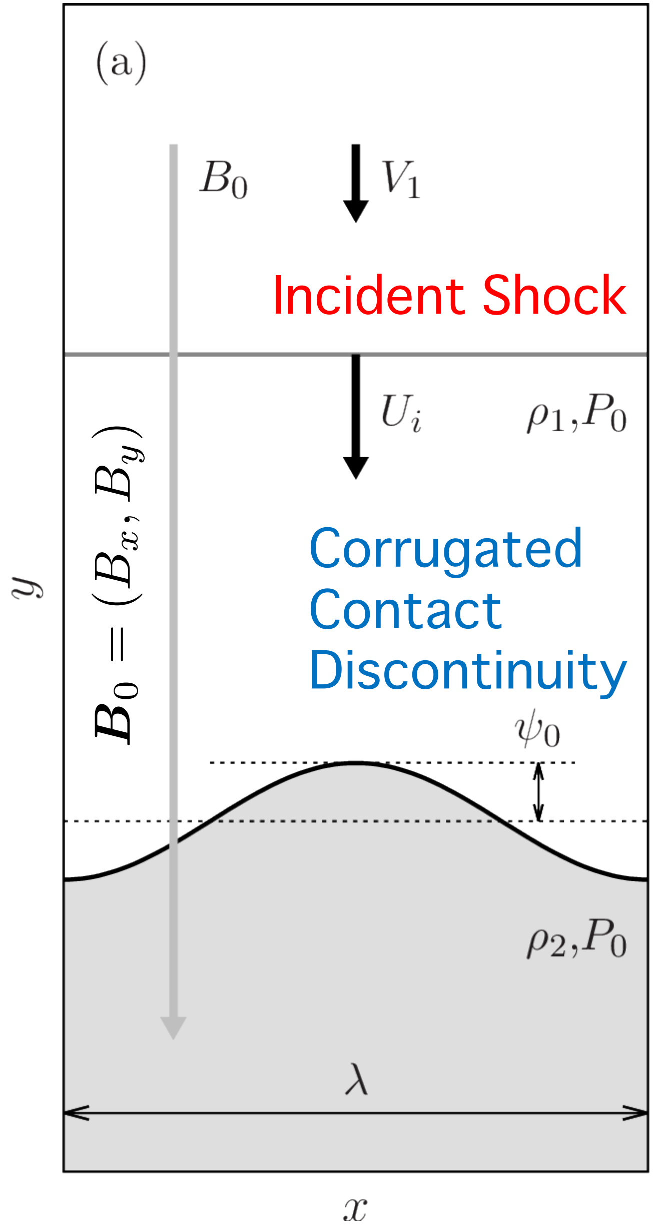

RMI growth can be reduced if a magnetic field is larger than a critical value.

SIM

- Plasma beta gives the criteria?

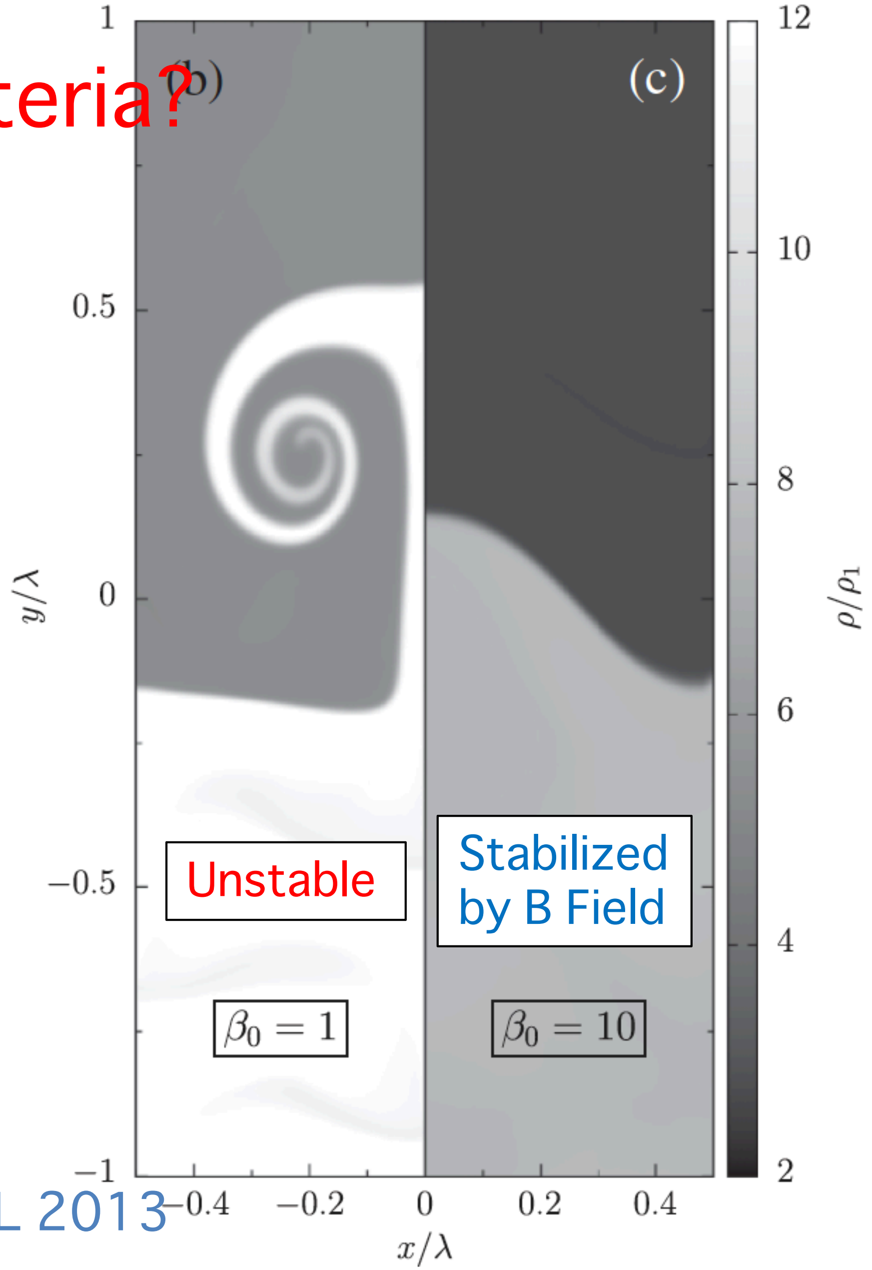

Sano+ PRL 2013

RMI growth can be reduced if a magnetic field is larger than a critical value.

SIM

- Plasma beta gives the criteria?
- No, not so simple…
- Critical strength depends on the Mach number of incident shock.

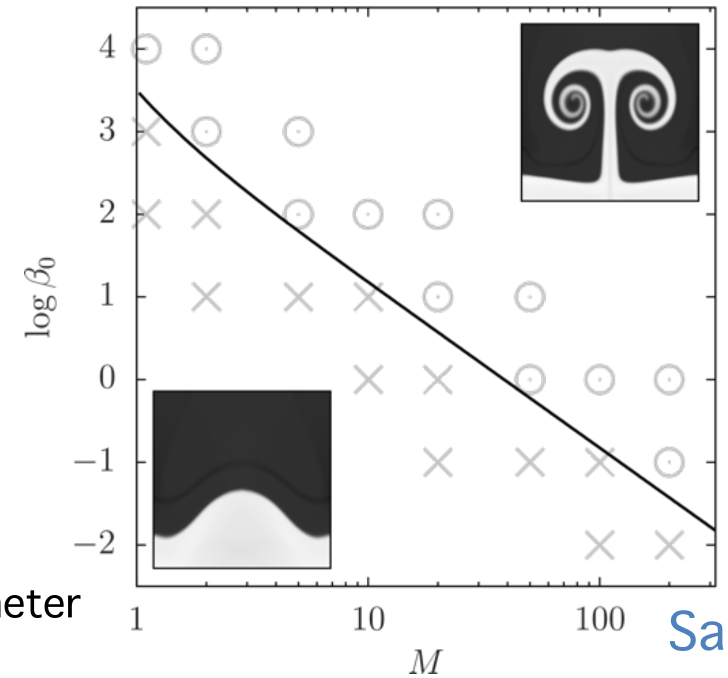

Initial Parameter Space

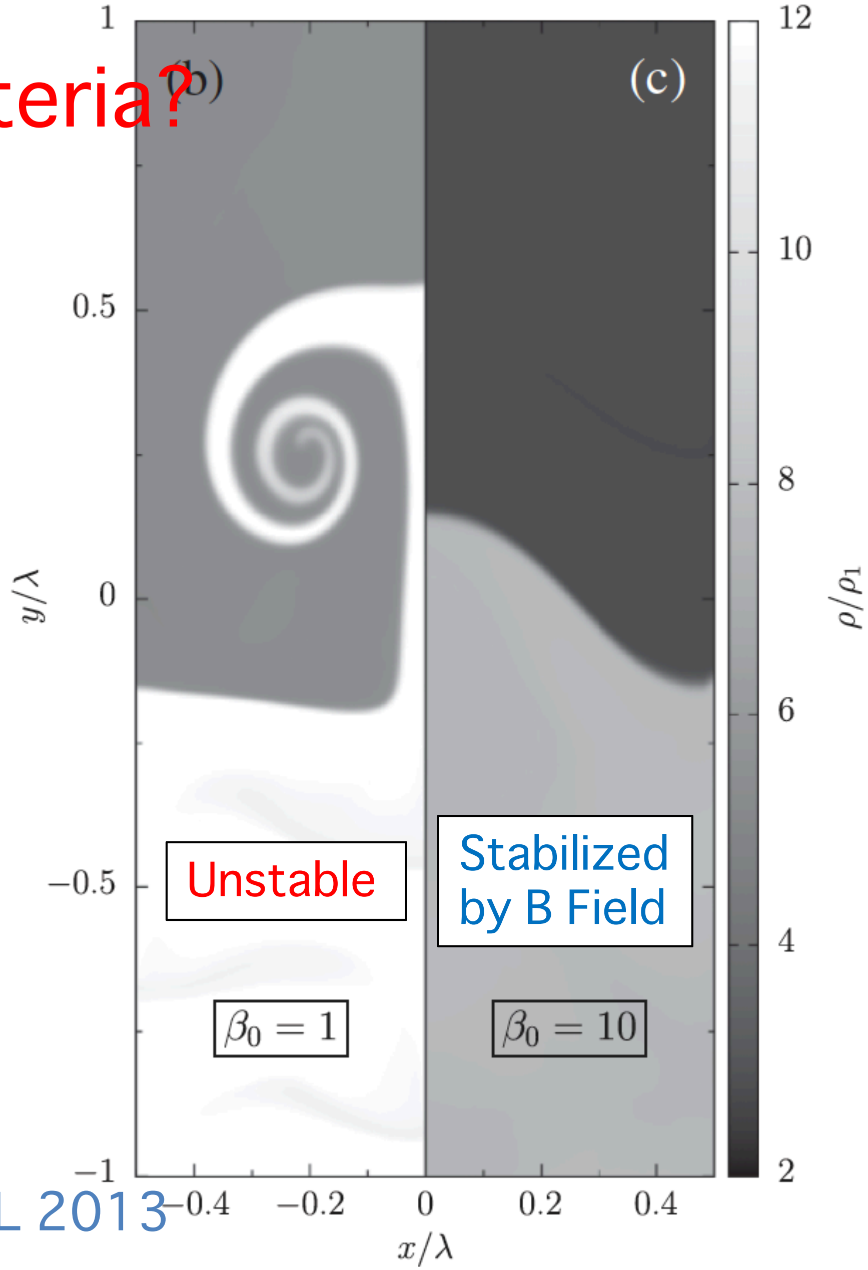

Sano+ PRL 2013

RMI growth can be reduced if a magnetic field is larger than a critical value.

SIM

- Plasma beta gives the criteria?
- No, not so simple...
- Critical strength depends on the Mach number of incident shock.
- Key Process: Extraction of the Vorticity from the Interface

Samtaney 2003
Wheatley et al. 2005; 2009

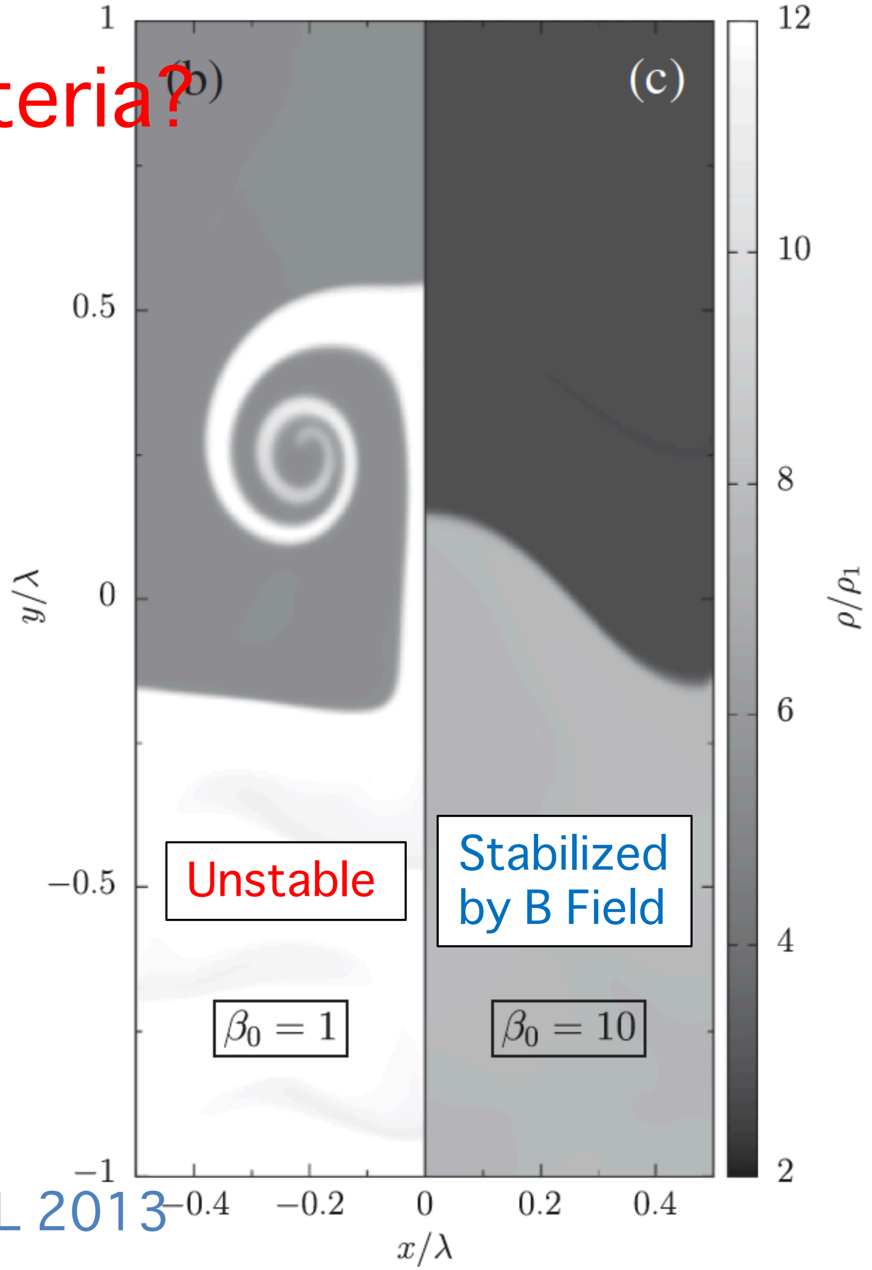

Sano+ PRL 2013

For HD cases, the vorticity deposited at the interface stays there and drives RMI.

SIM

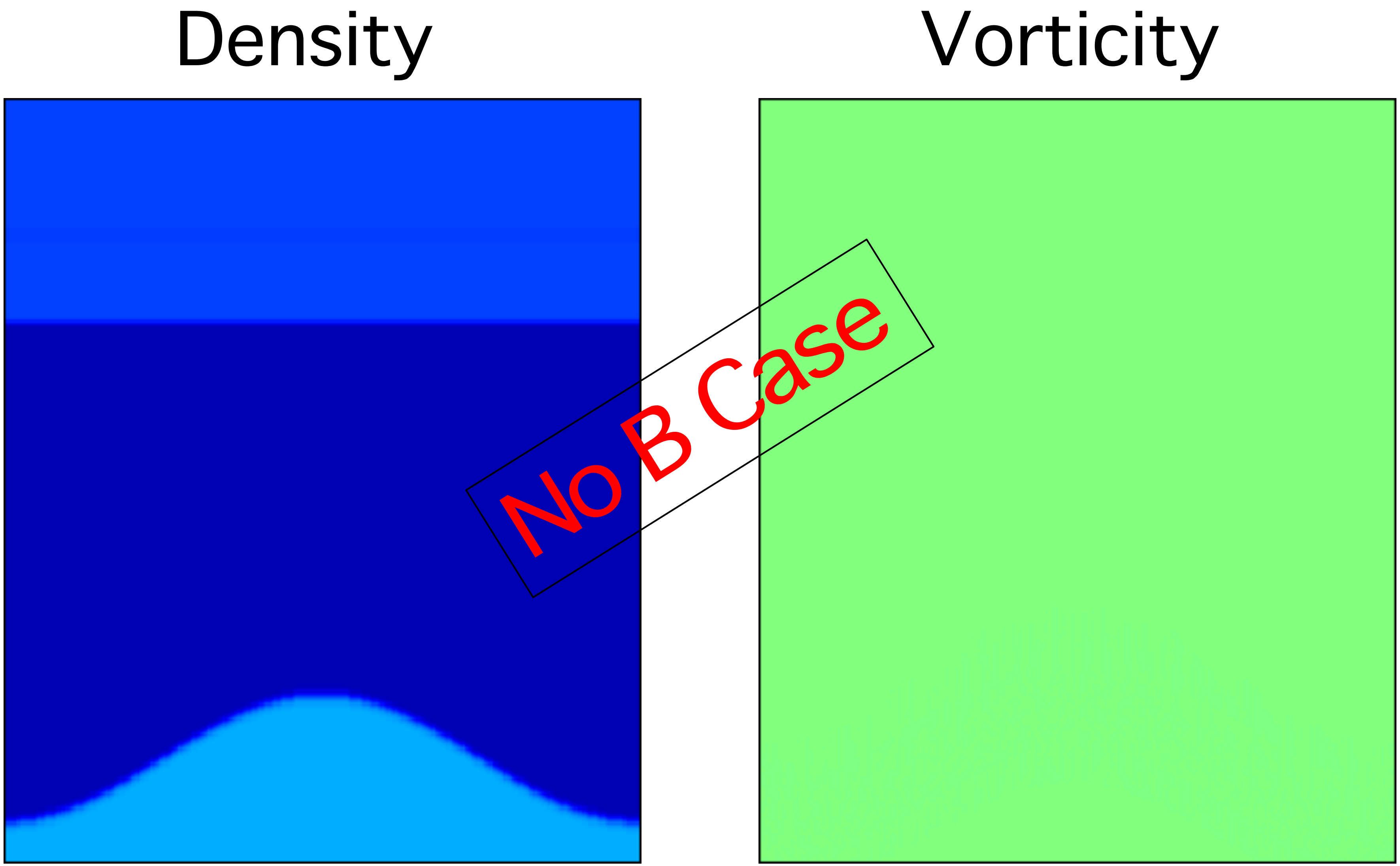

During the growth of the RMI, vorticity is always associated with the CD.

When B fields exist, the vorticity travels away from the interface by Alfven wave.

SIM

- Vortex sheet is moving away from the contact surface!

Sano+ PRL 2013

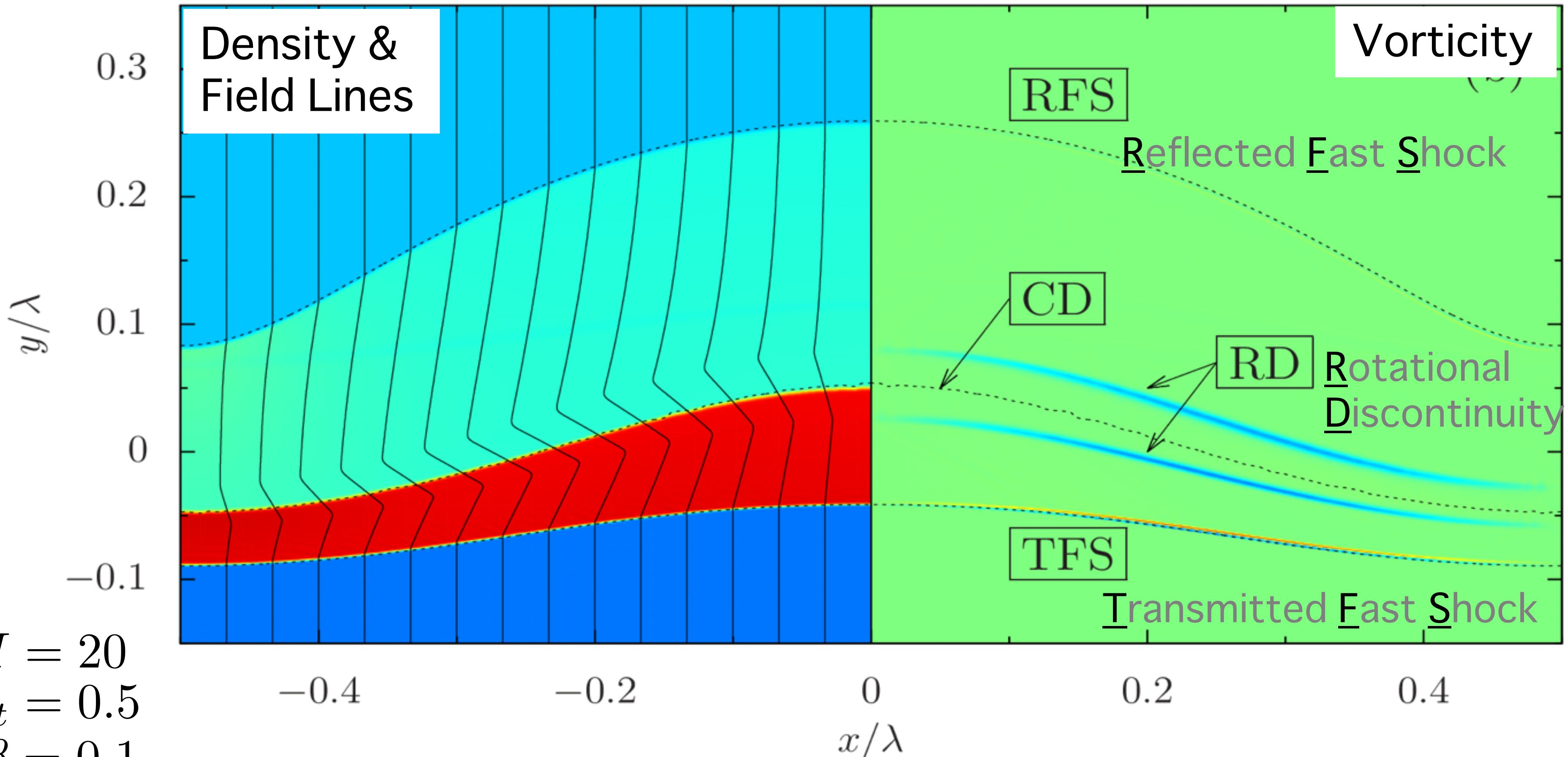

$M = 20$
$A_t = 0.5$
$\beta = 0.1$

We could not see any growth of RMI for this model.

When B fields exist, the vorticity travels away from the interface by Alfven wave.

SIM

- Vortex sheet is moving away from the contact surface!

Sano+ PRL 2013

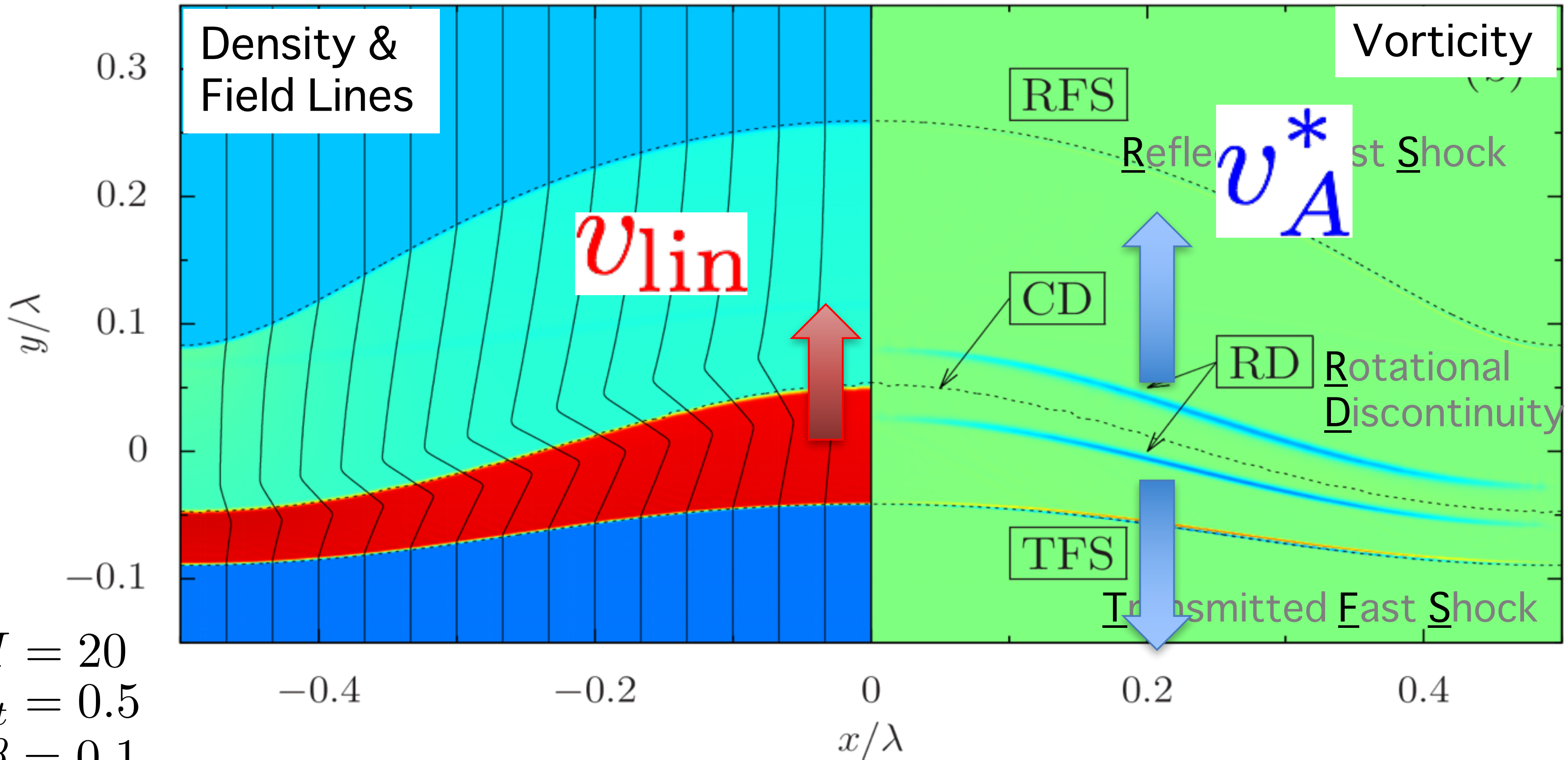

$M = 20$
$A_t = 0.5$
$\beta = 0.1$

We could not see any growth of RMI for this model.

Critical stability condition is determined by the Alfven (Mach) number for RMI.

SIM

- Alfven Number for RMI

$$R_A \equiv \frac{v_{\mathrm{lin}}}{v_A^*}$$

WN Formula

Critical stability condition is determined by the Alfven (Mach) number for RMI.

SIM

- Alfven Number for RMI

$$R_A \equiv \frac{v_{\rm lin}}{v_A^*}$$ ← WN Formula

- Critical Value ~ 10
  - Independent of Mach Number, Density Ratio, Perturbation Amplitude, and Field Direction!

$$\begin{aligned}(\rho_2/\rho_1, \psi_0/\lambda) &= (0.1, 0.1)\ \&\ B_y \\ &= (0.5, 0.1)\ \&\ B_y \\ &= (0.1, 0.03)\ \&\ B_y \\ &= (0.1, 0.1)\ \&\ B_x \\ &= (10, 0.1)\ \&\ B_y\end{aligned}$$

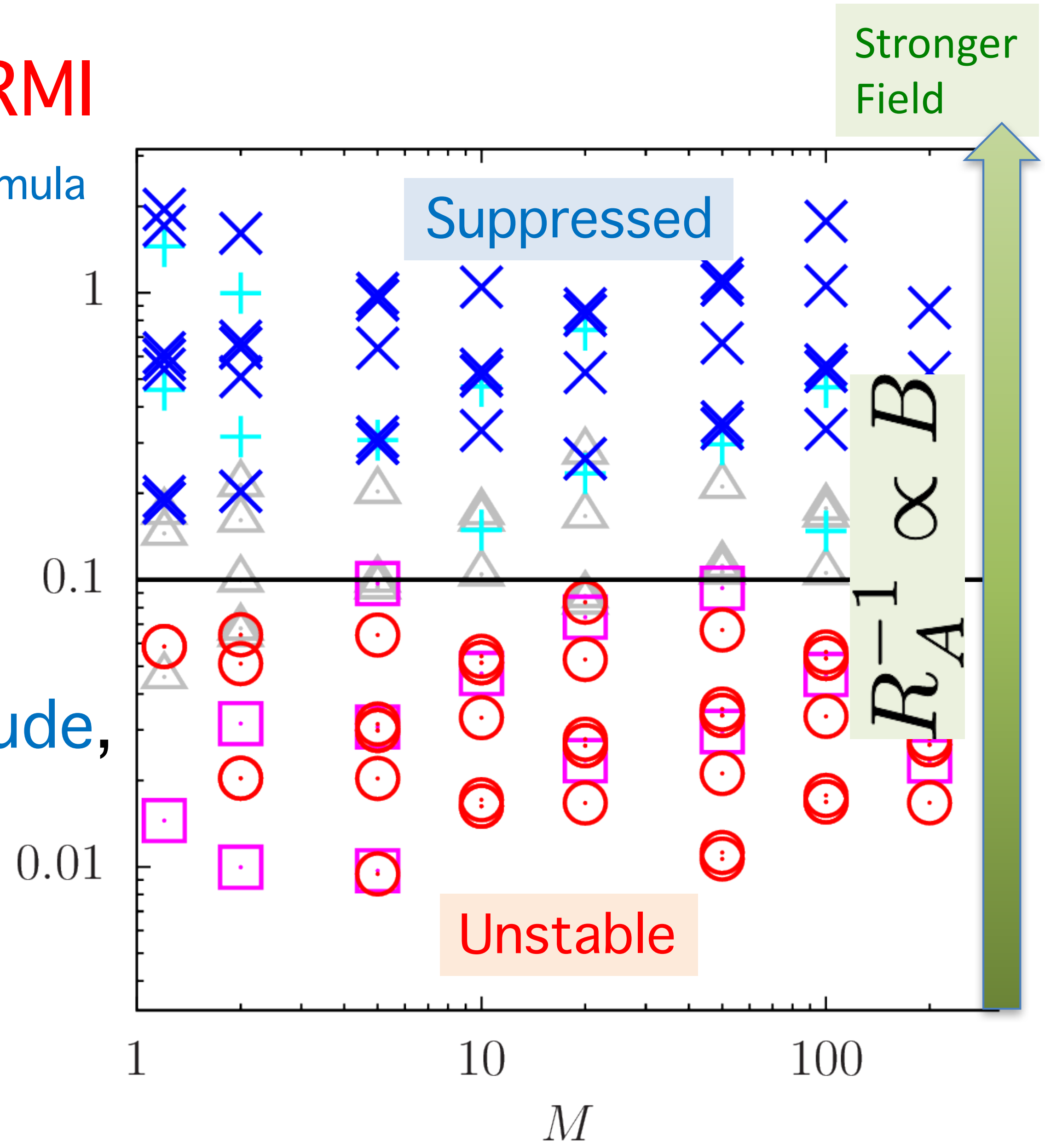

Critical stability condition is determined by the Alfven (Mach) number for RMI.

SIM

- Alfven Number for RMI

$$R_A \equiv \frac{v_{\mathrm{lin}}}{v_A^*}$$ ← WN Formula

- Critical Value ~ 10
  - Independent of Mach Number, Density Ratio, Perturbation Amplitude, and Field Direction!
- Consistent with Current-Vortex Sheet Model

Matsuoka+ JNS 2017

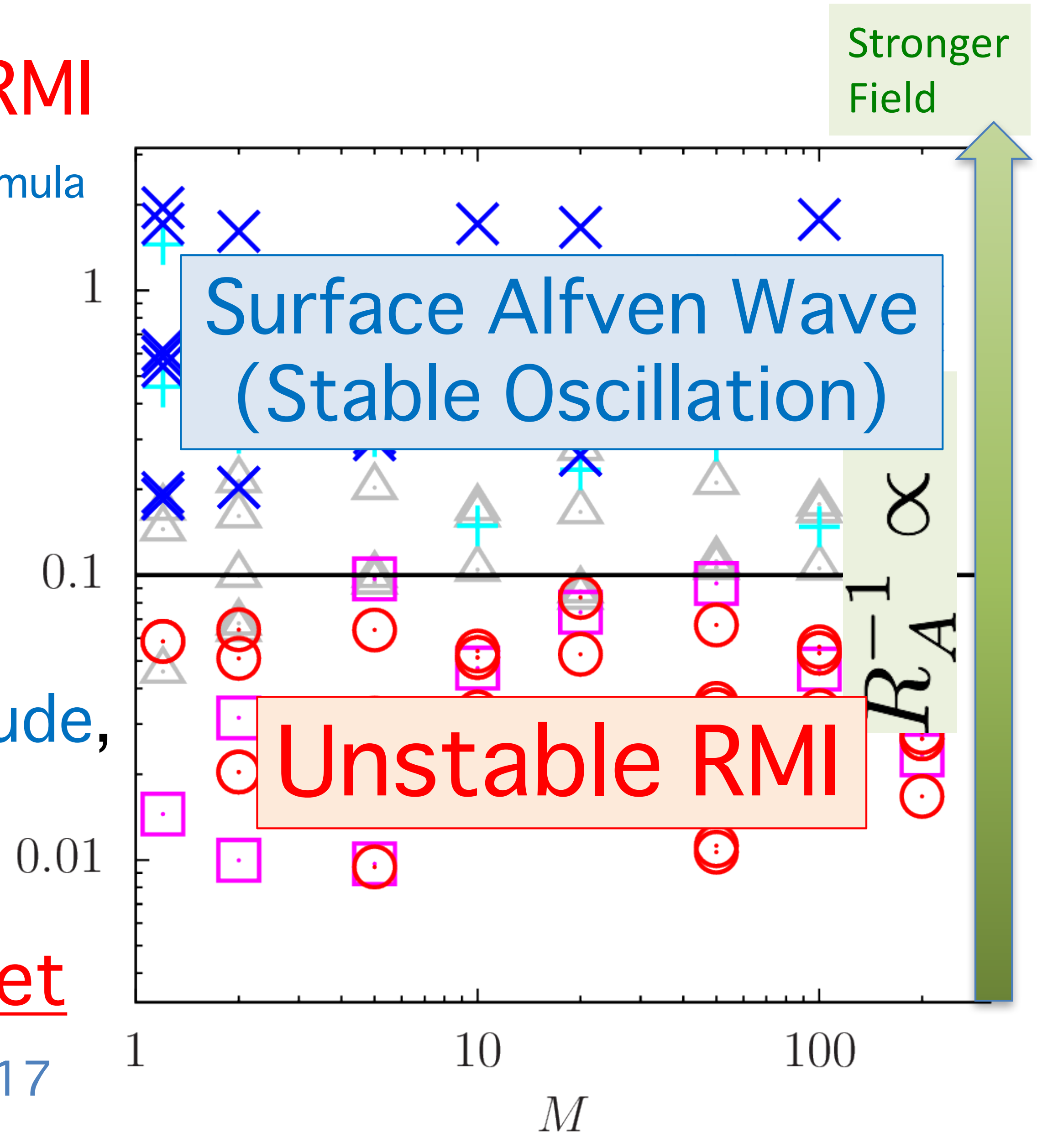

Critical field strength for the suppression in laser plasma is estimated as about 10T.

SIM

- This will be tested experimentally soon.
- For Stability (Laser Exp. Condition) $R_A < 10$

$$B > B_c \approx 0.1 \times (4\pi\rho^*)^{1/2} v_{\rm lin}$$

$$\sim 10^5 \left(\frac{\rho}{1\ {\rm g/cm^3}}\right)^{1/2} \left(\frac{v_{\rm lin}}{3\ {\rm km/s}}\right)\ [{\rm G}]$$

$$\sim 10\ [{\rm T}]$$

$$v_{\rm lin} \sim 0.1 U_i$$

Wouchuk & Sano PRE 2015

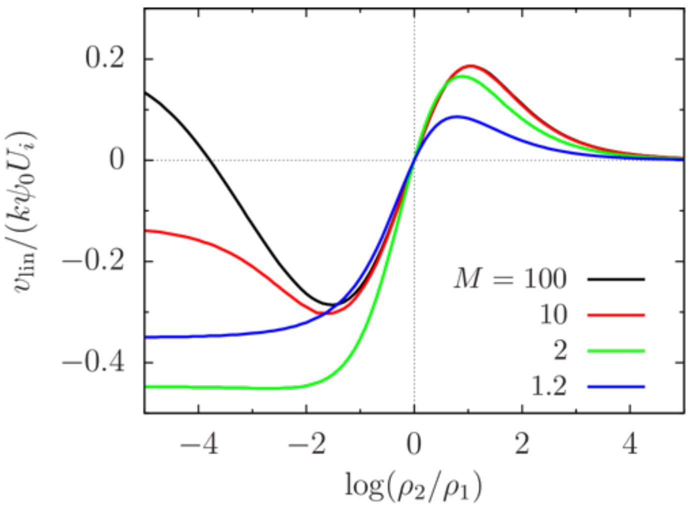

2-1. Amplification of a Magnetic field

MHD Simulations & Current-Vortex Sheet Model

Sano+ ApJ 2012
Matsuoka+ JNS 2017

SIM

Ambient magnetic fields can be amplified dramatically by RMI motions.

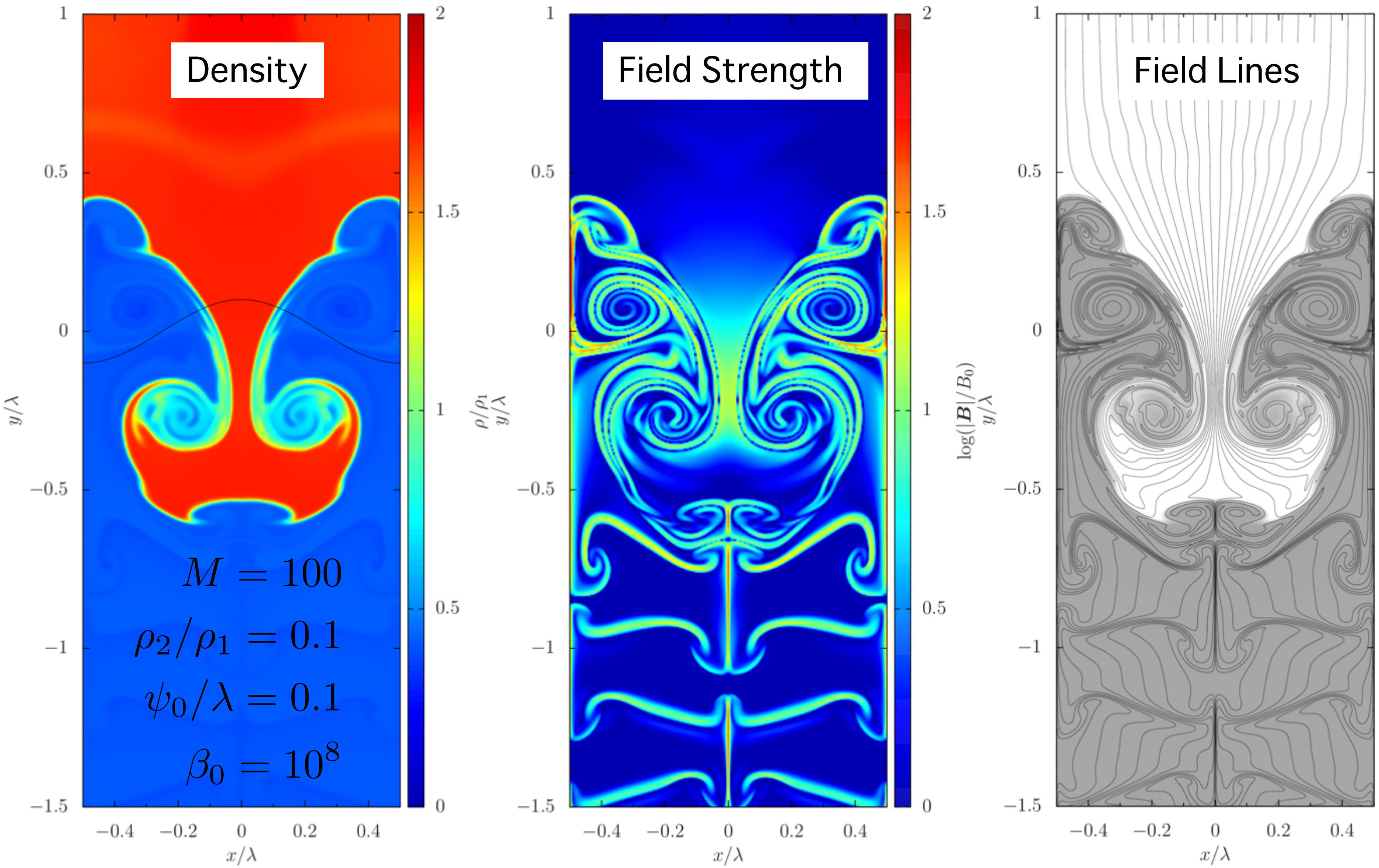

Ambient magnetic fields can be amplified dramatically by RMI motions.

SIM

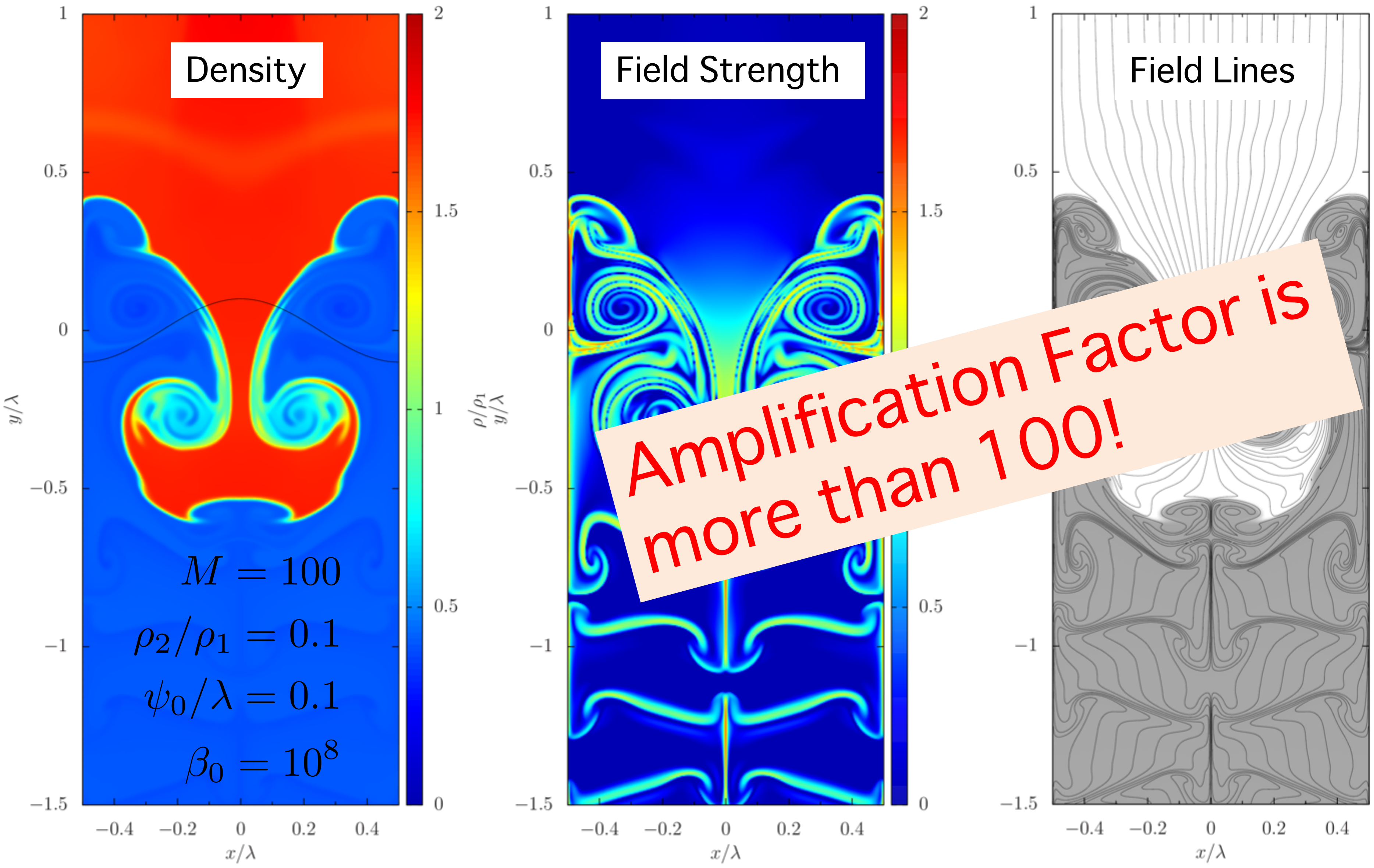

Growth rate of B field agrees fairly well with the stretching rate of interface.

SIM

- Amplification by Stretching Term in Induction Eq.

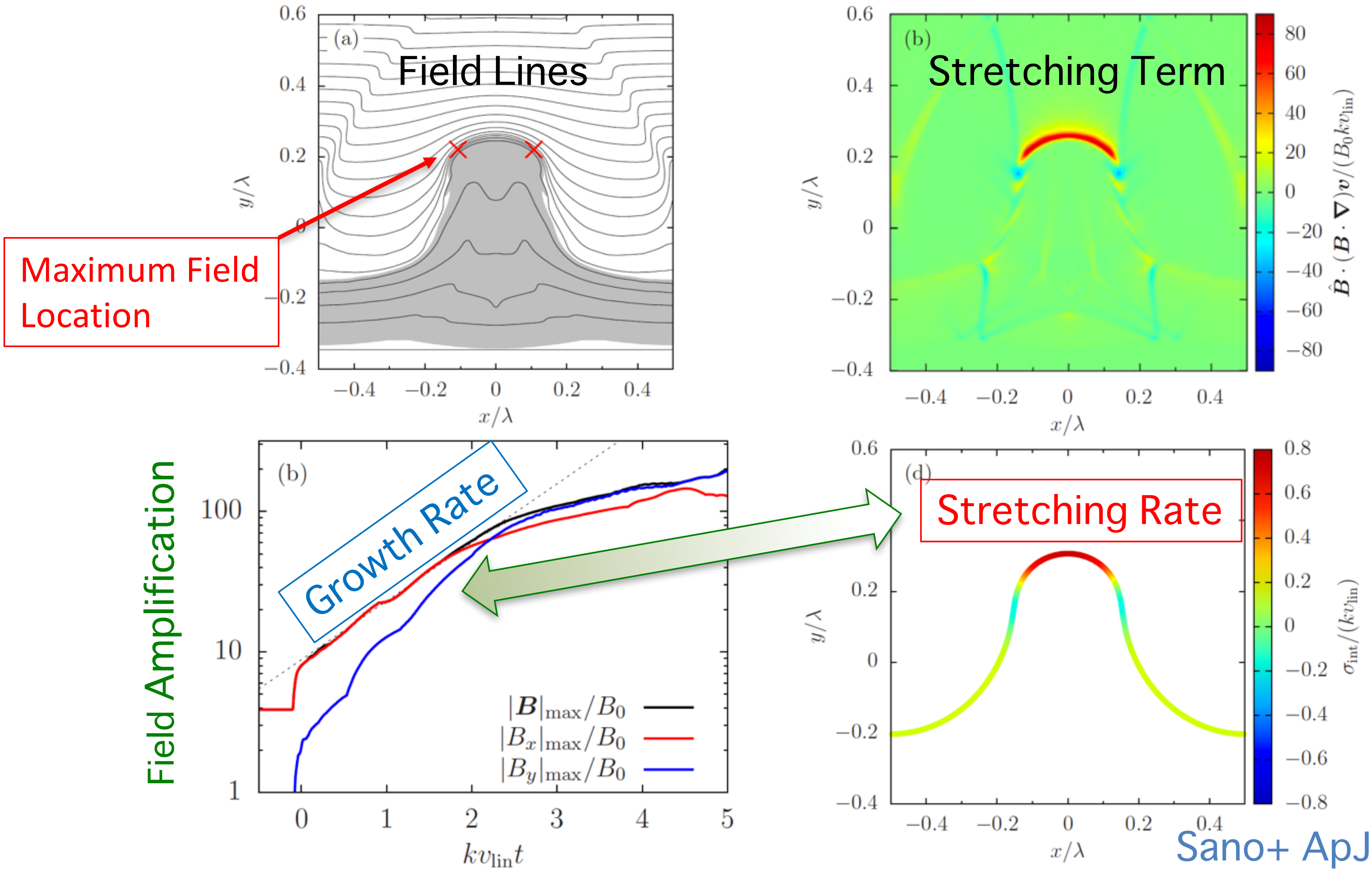

Sano+ ApJ 2012

Field amplification process is independent of the initial field direction.

SIM

- Saturation level is independent of any parameters; Mach number, density jump, & fluctuation amplitude.

$B \parallel$ interface

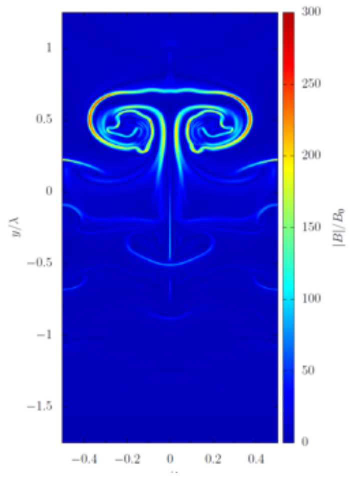

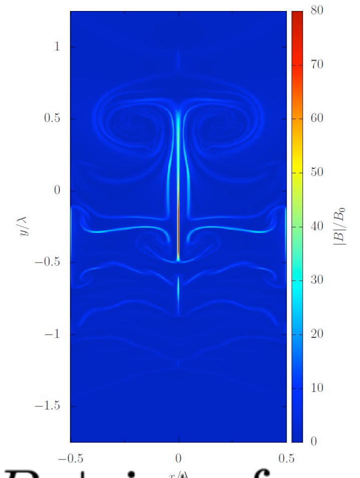

$B \perp$ interface

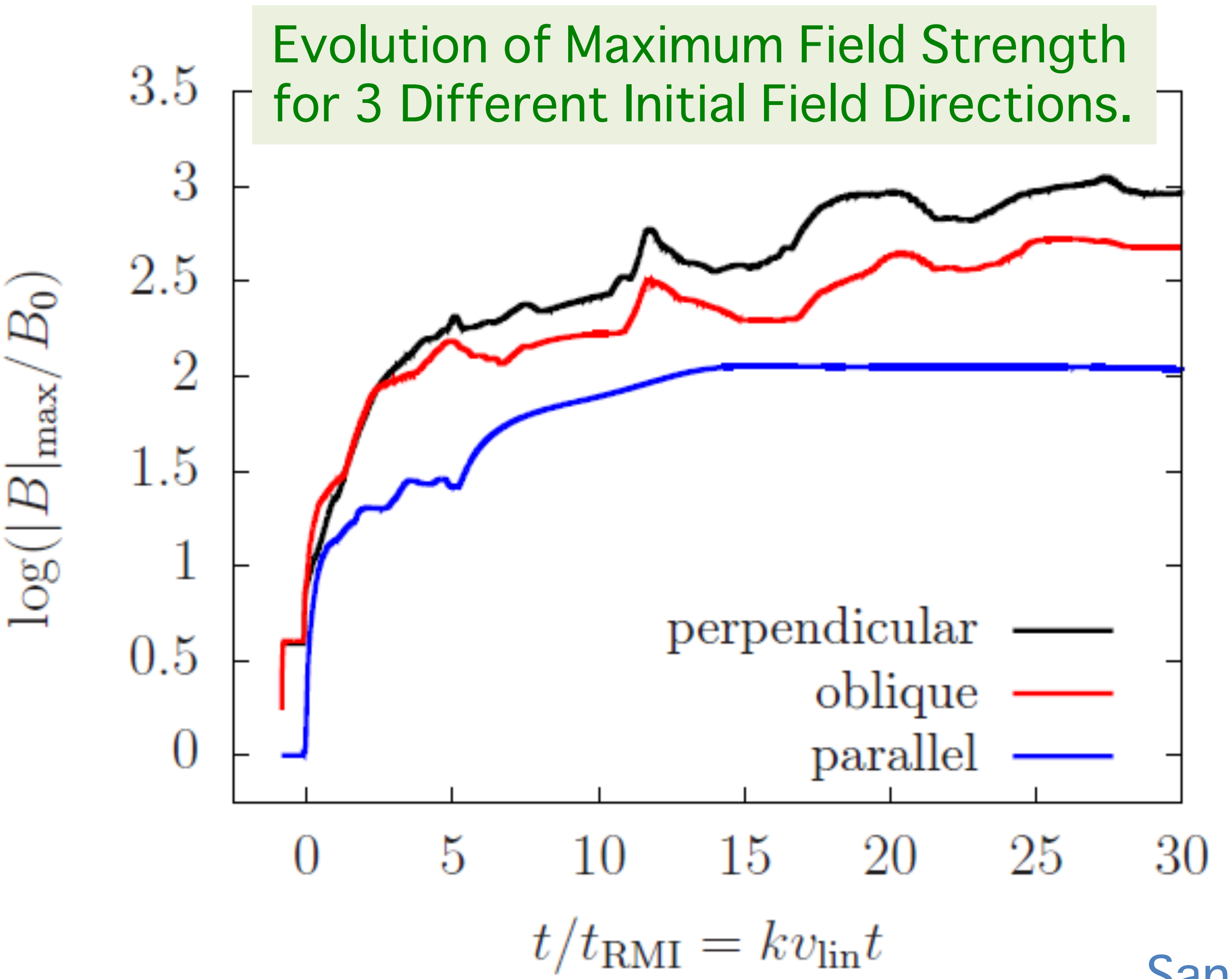

oblique B

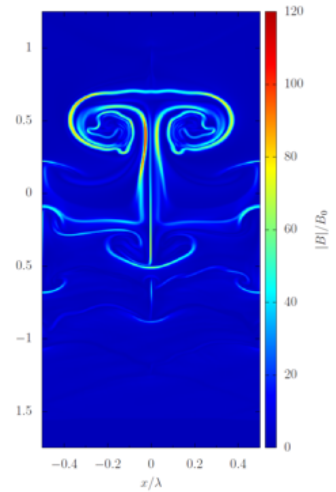

Sano+ ApJ 2012

Saturation level of field strength is of the order of turbulent kinetic energy.

SIM

- The maximum field strength is limited by the growth (turbulent) velocity of RMI.

Evolution of the "Maximum Field"

$$\frac{B_{\max}^2}{8\pi} \Big/ \left(\frac{1}{2}\rho_1^* v_{\rm lin}^2\right)$$

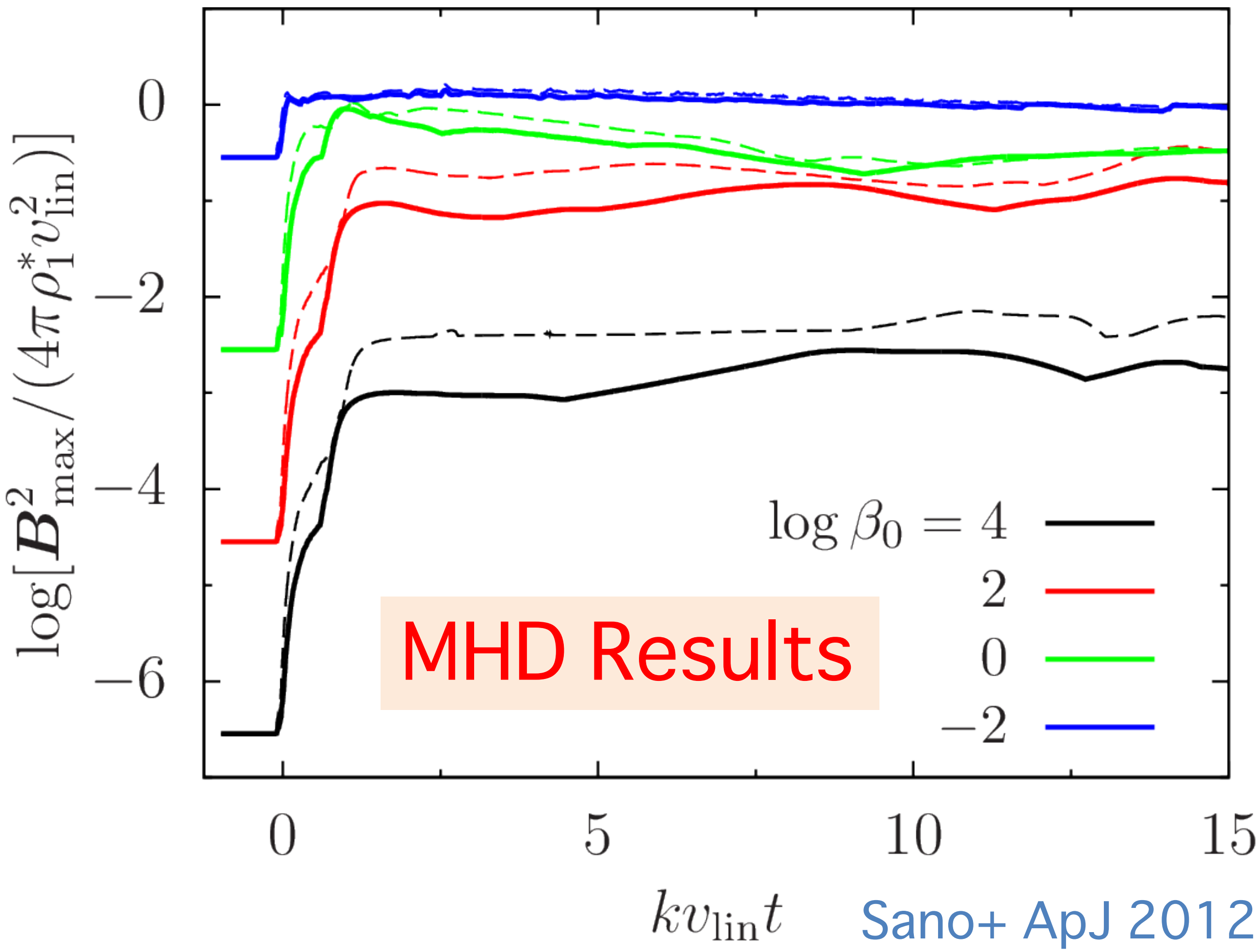

Sano+ ApJ 2012

Saturation level of field strength is of the order of turbulent kinetic energy.

SIM

- The maximum field strength is limited by the growth (turbulent) velocity of RMI.

Evolution of the "Maximum Field"

$$\frac{B_{\rm max}^2}{8\pi} \Big/ \left(\frac{1}{2}\rho_1^* v_{\rm lin}^2\right)$$

MHD simulations and the current-vortex sheet model give the same results for the saturation amplitude.

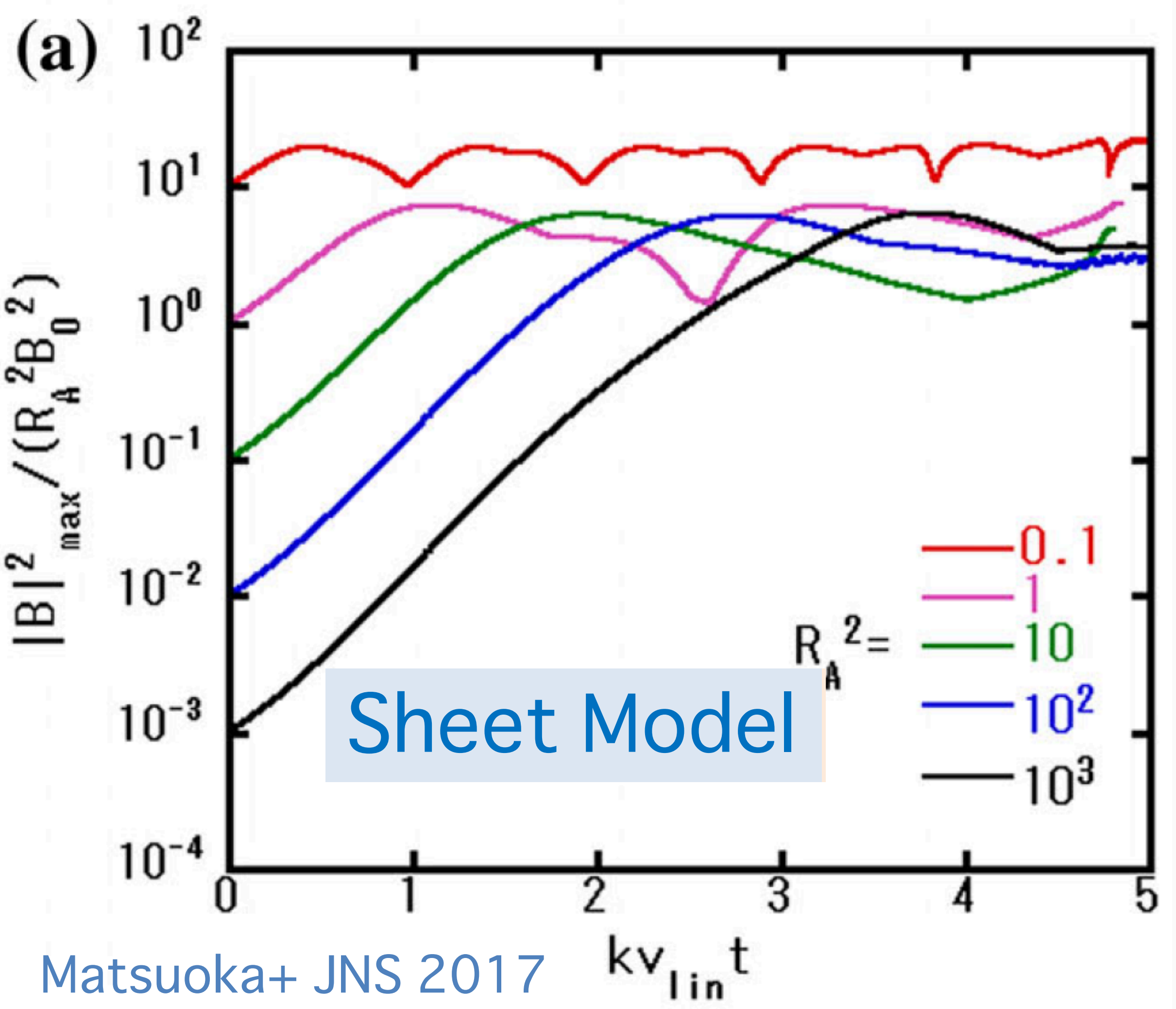

Matsuoka+ JNS 2017

Magnetic field amplification occurs also in 3D RMI, and the amplitude is slightly larger.

SIM

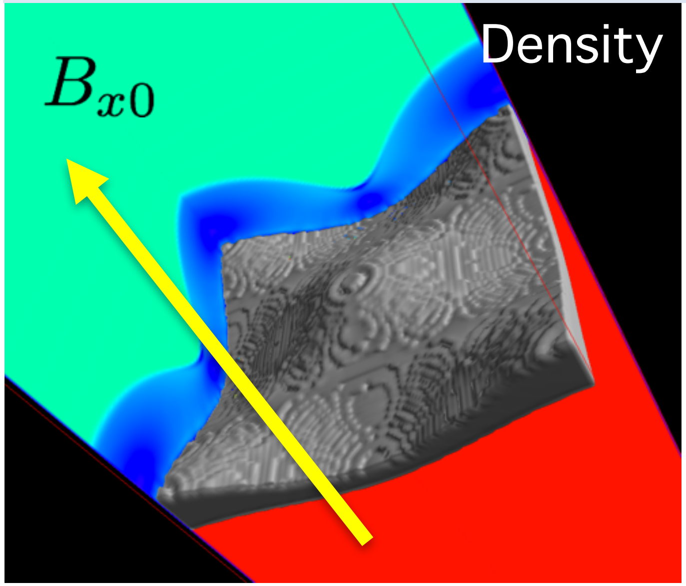

Initial Modulation Function

$$\psi_{3D} = \psi_0 \cos(ky)\cos(kz)$$

Magnetic field amplification occurs also in 3D RMI, and the amplitude is slightly larger.

SIM

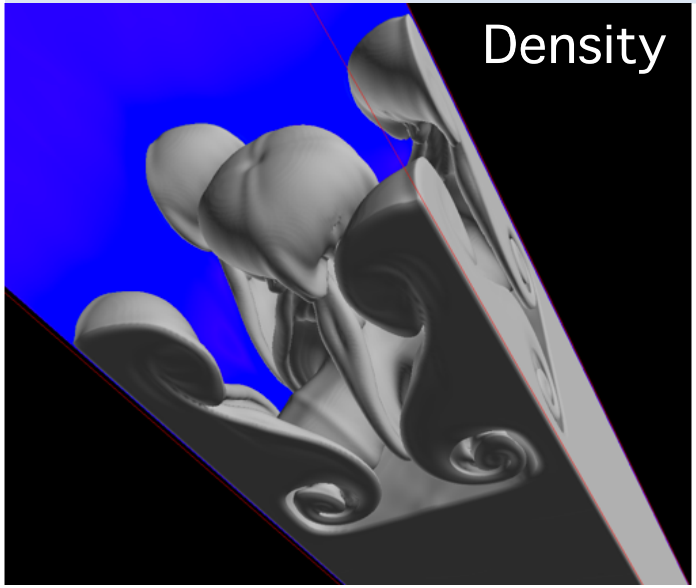

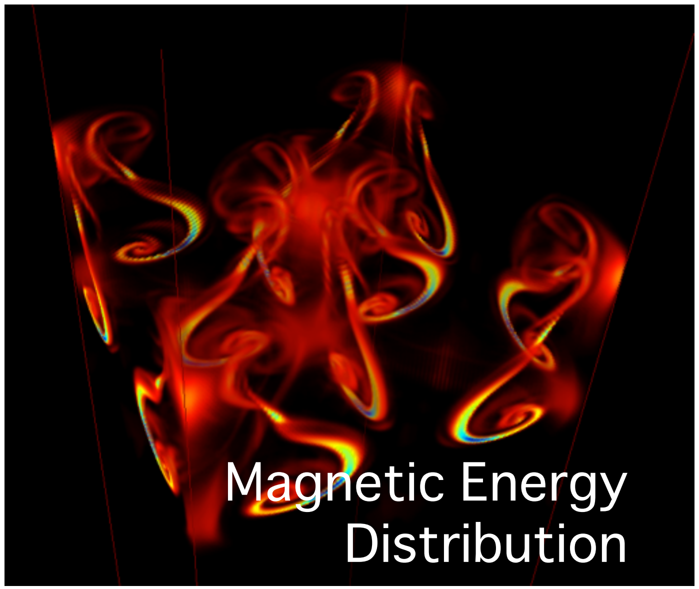

Time Evolution of Field Strength in 2D & 3D RMI Growth

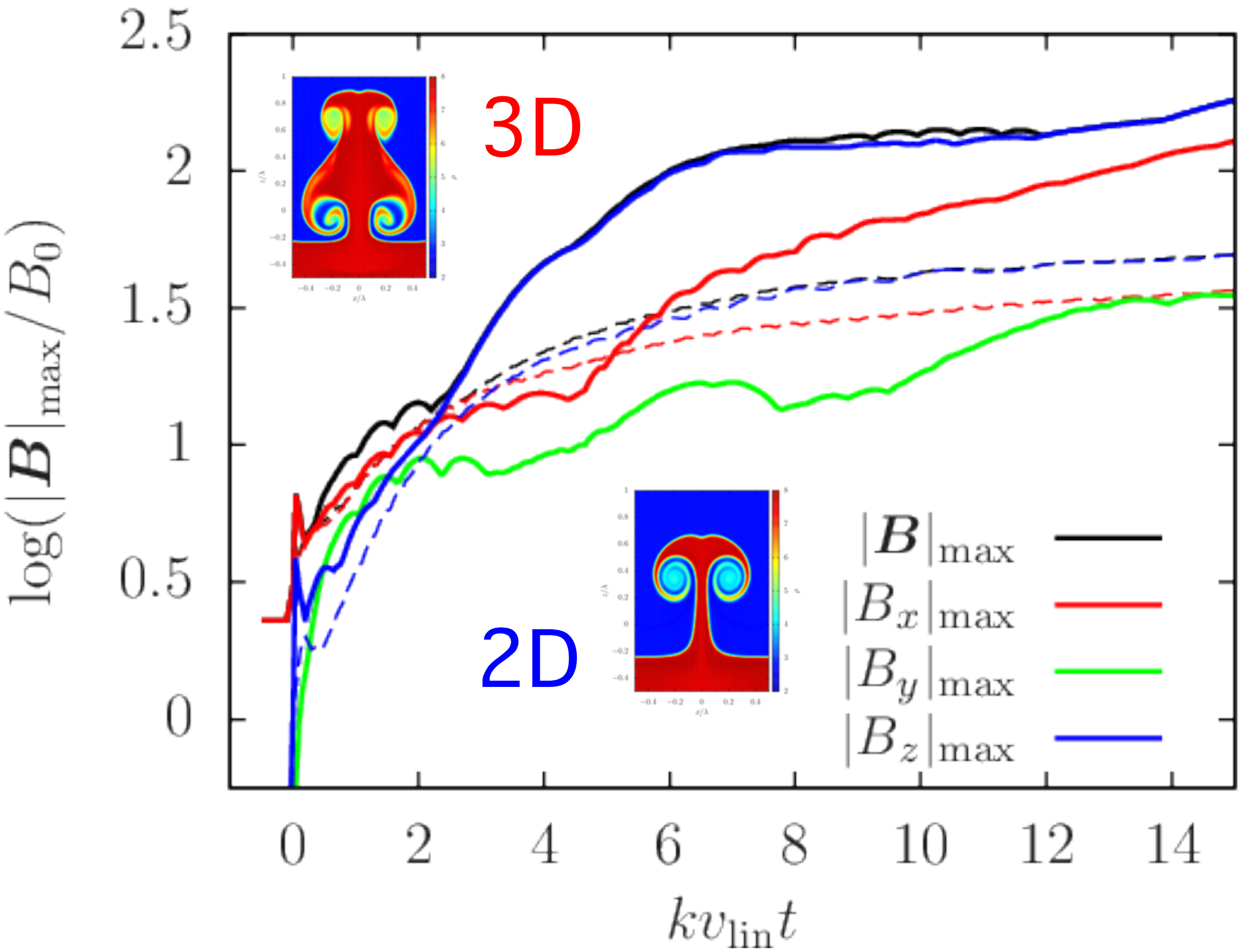

Complicated "filamentary" field structures are formed in multi-mode fluctuation cases.

SIM

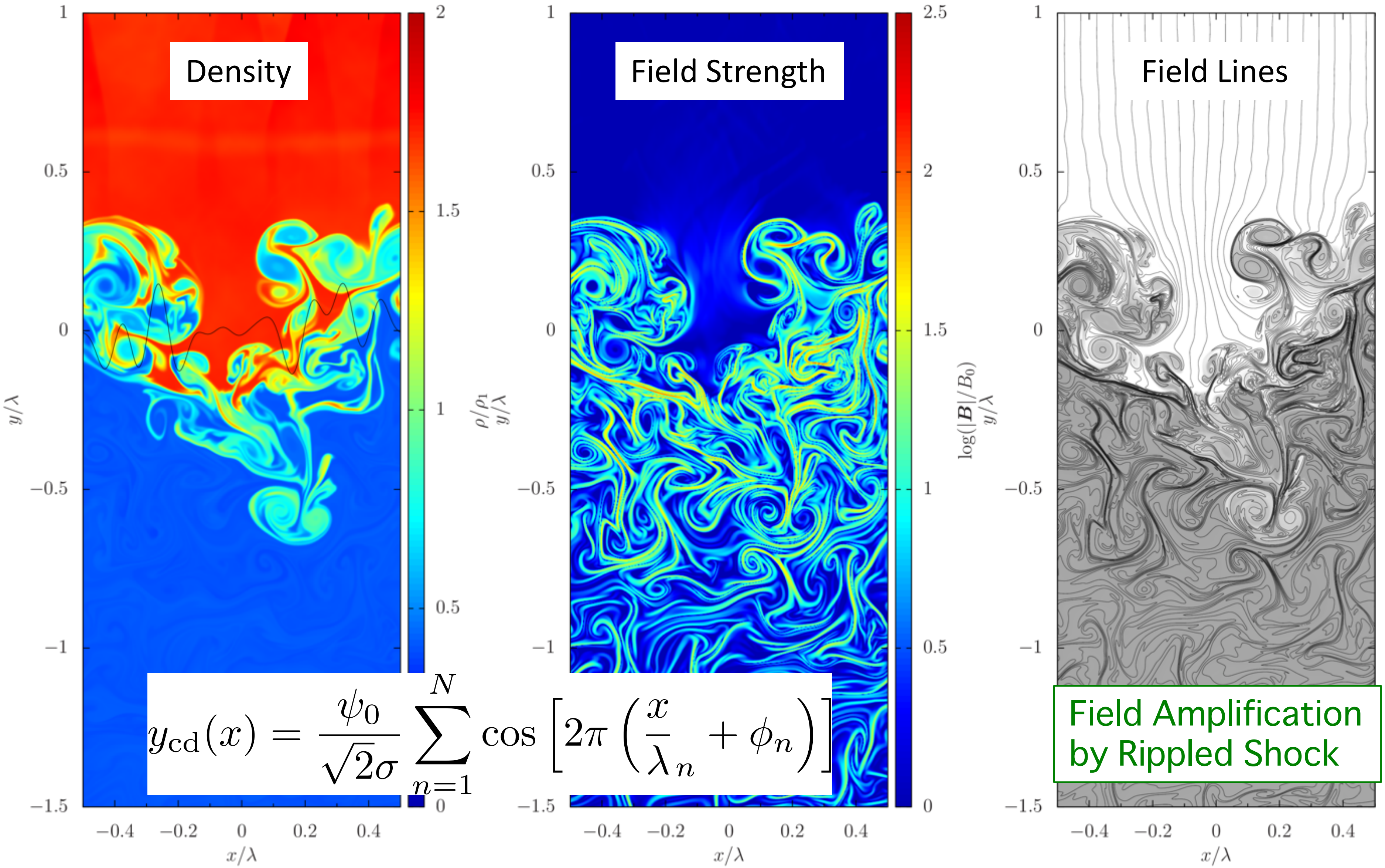

$$y_{\rm cd}(x) = \frac{\psi_0}{\sqrt{2}\sigma}\sum_{n=1}^{N}\cos\left[2\pi\left(\frac{x}{\lambda_n}+\phi_n\right)\right]$$

Filamentary structures in RMI remind us interstellar turbulence driven by SN shocks.

SIM

- Supernova Shock + Density Fluctuation in ISM
- RMI turbulence shows many similarities to Interstellar turbulence.

Good Application

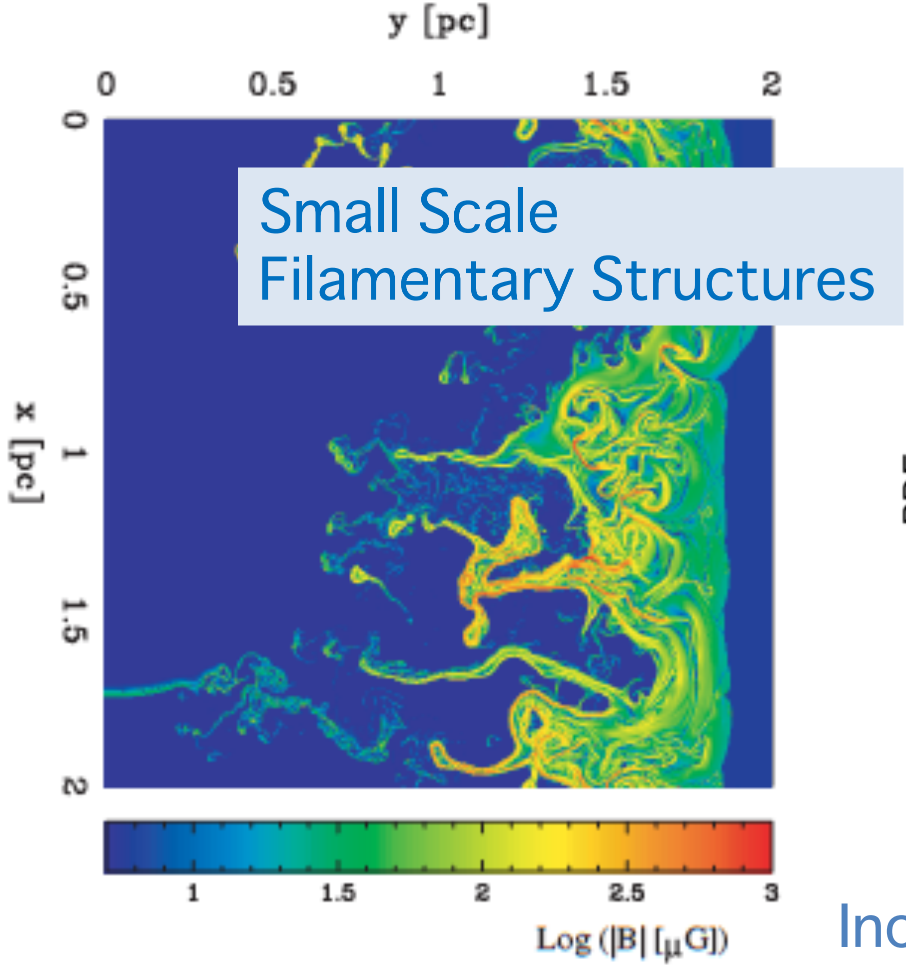

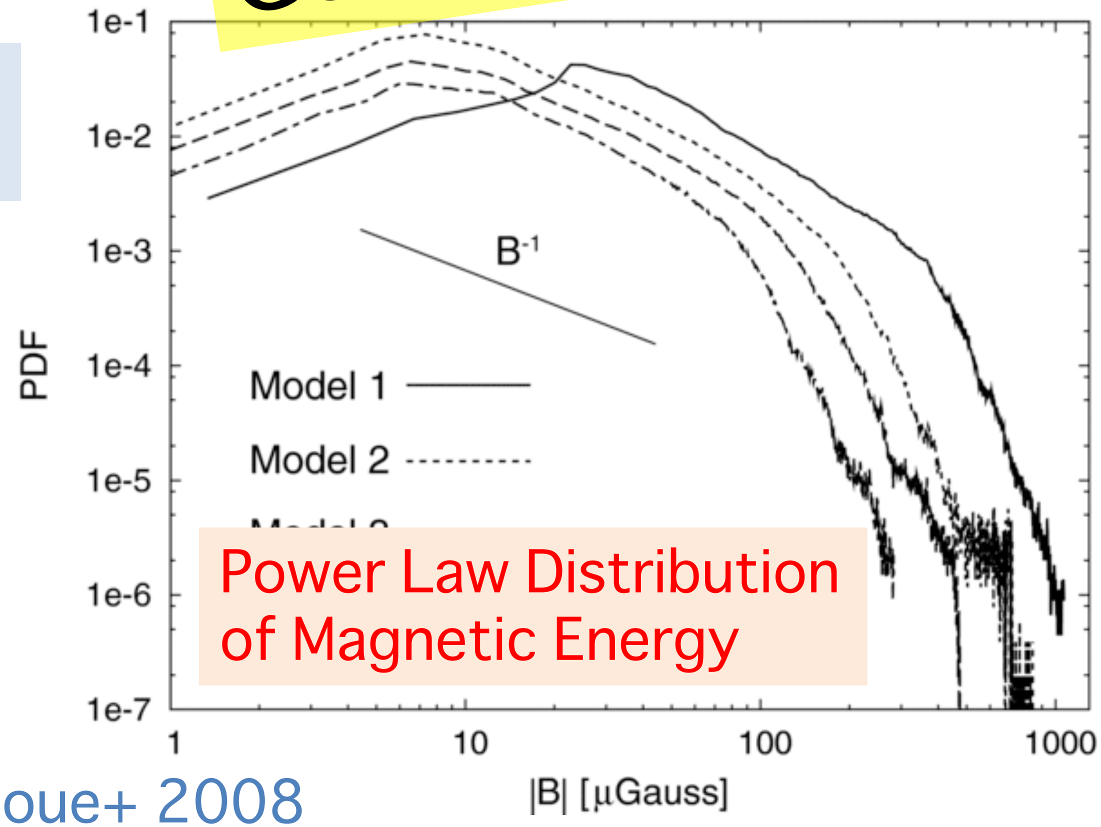

Inoue+ 2008

2-2. Amplification of a Magnetic field

Experimental Results by GEKKO Laser in Osaka

Preliminary

Classical RMI experiment using high-power lasers have been carried out by many groups.

EXP

- NOVA Laser
  - Be/Foam, Be/CH

  Dimonte & Remington 1993

  Farley+ 1996
- OMEGA Laser
  - CHBr/Foam

  Glendinning+ 2003
- Nike Laser
  - Foam/CH

  e.g., Aglitskiy+ 2006
- X-ray Diagnostics

Farley+1999

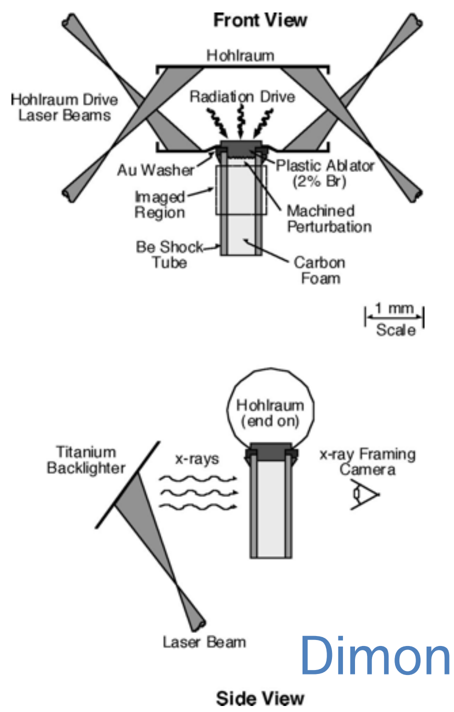

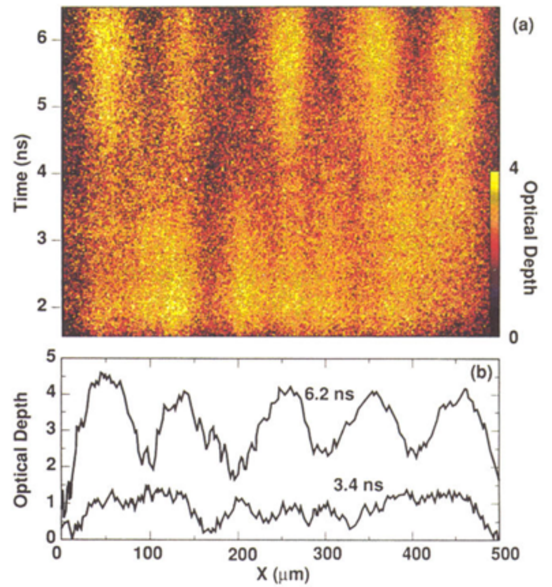

FIG. 3. (a) Face-on radiograph of Be/AGAR target showing instability growth. (b) Optical depth profiles averaged over 0.4 ns. Initial perturbations have $\lambda = 100\ \mu m$, $\eta_0 = 14\ \mu m$.

Dimonte & Remington 1993

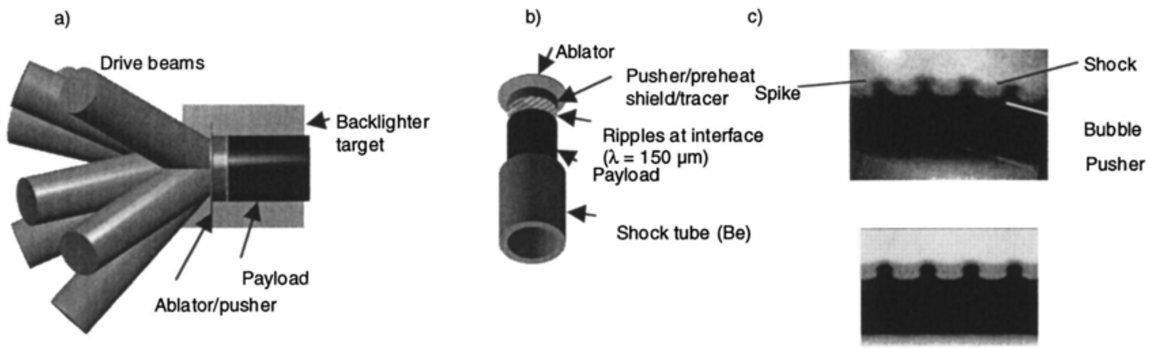

Glendinning+2003

Classical RMI experiment using high-power lasers have been carried out by many groups.

EXP

- NOVA Laser
  - Be/Foam, Be/CH

    Dimonte & Remington 1993

    Farley+ 1996
- OMEGA Laser
  - CHBr/Foam

    Glendinning+ 2003
- Nike Laser
  - Foam/CH

    e.g., Aglitskiy+ 2006
- X-ray Diagnostics

- GEKKO Laser at Osaka
  - CH/N2 Gas
  - Inclusion of B Field
  - Optical Measurement

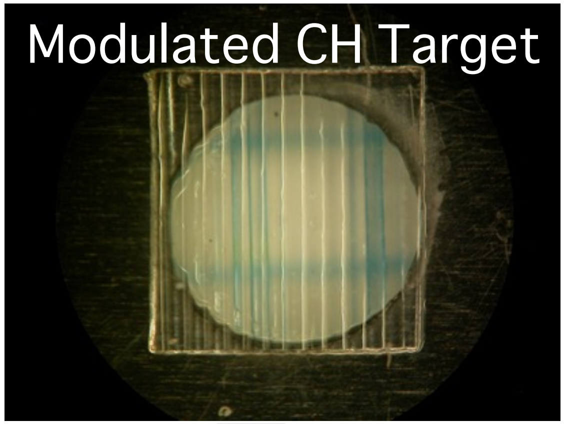

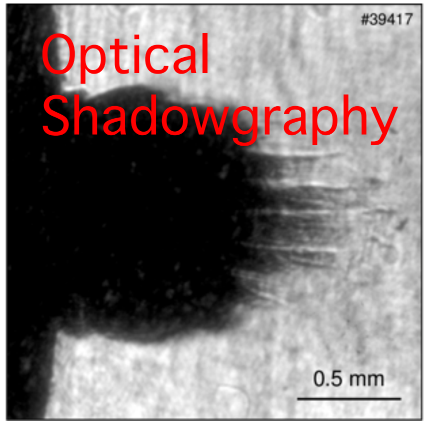

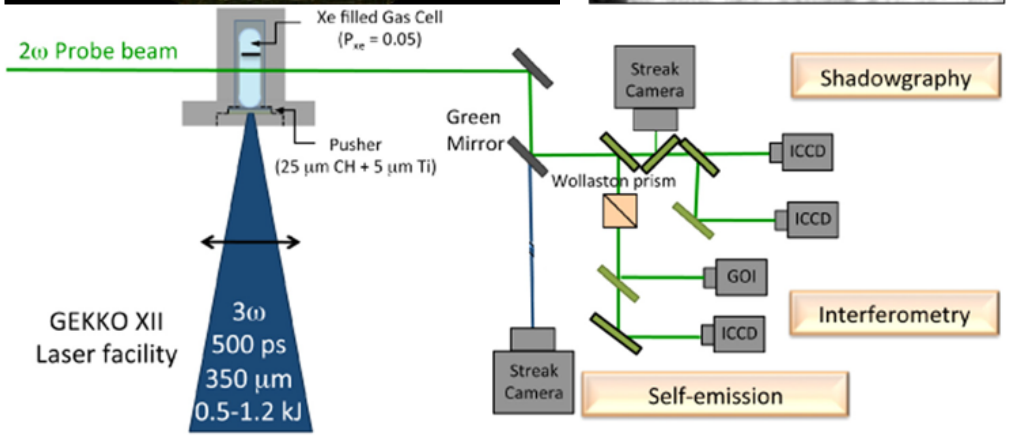

Koenig+ PoP 2017

Laser experiment on self-generated field is one of the hot topics in "laser astrophysics".

EXP

1. Generation of B Field
   – Biermann Battery Process

$$-\nabla n_e \times \nabla p_e / e n_e^2$$

2. Field Amplification
   – Amplification of Self-Generated Field by Turbulence Driven by Shock + "Mesh"

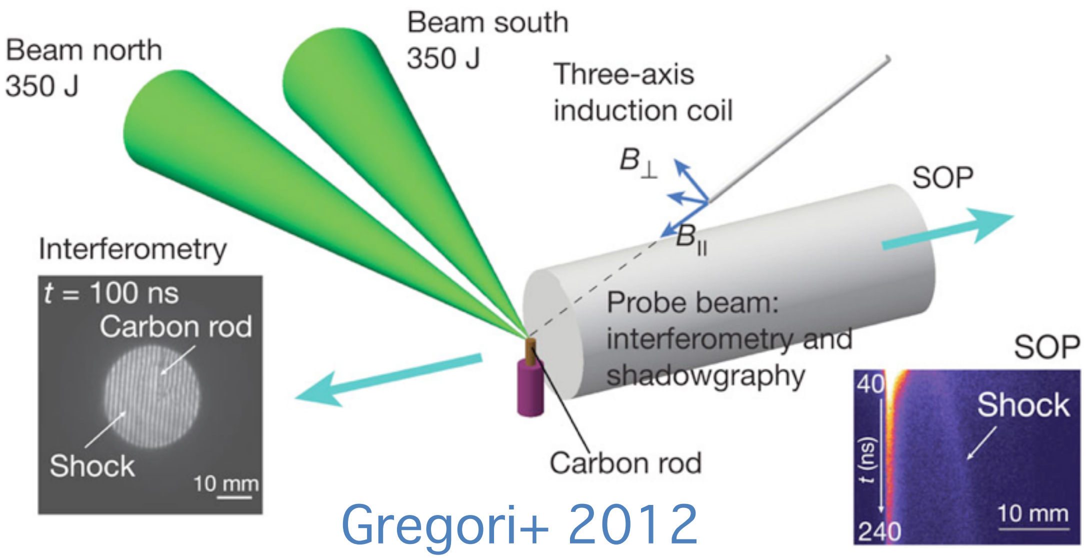

Gregori+ 2012

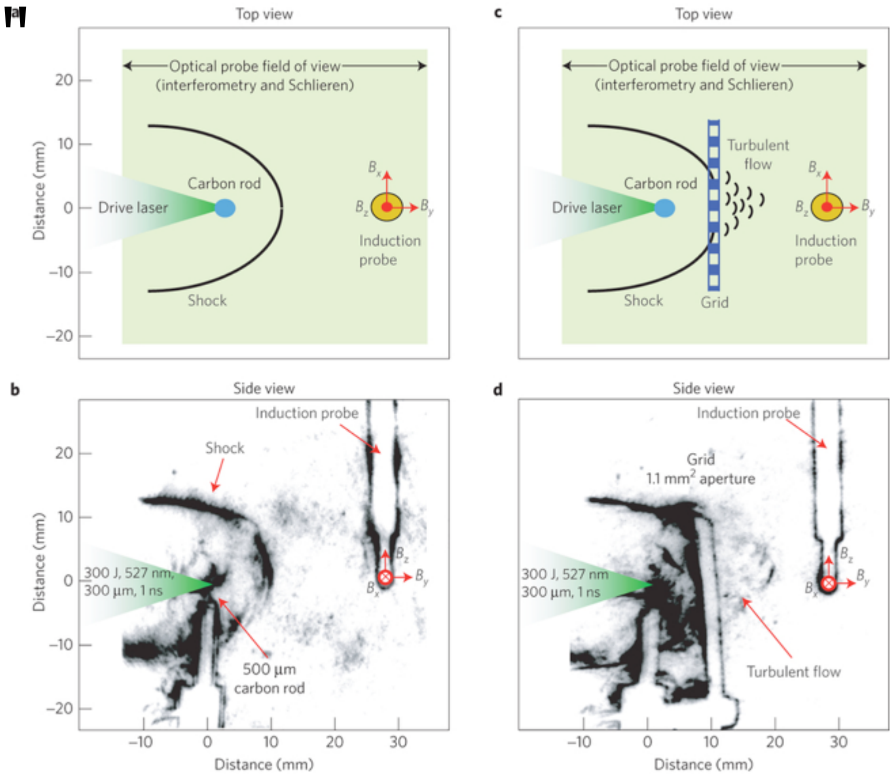

Meinecke+ 2014

EXP

Laser experiment on self-generated field is one of the hot topics in "laser astrophysics".

1. Generation of B Field
   - Biermann Battery Process

$$-\nabla n_e \times \nabla p_e / e n_e^2$$

2. Field Amplification
   - Amplification of Self-Generated Field by Turbulence Driven by Shock + "Mesh"
   - Amplification of an External Seed Field by Turbulence Driven by RMI

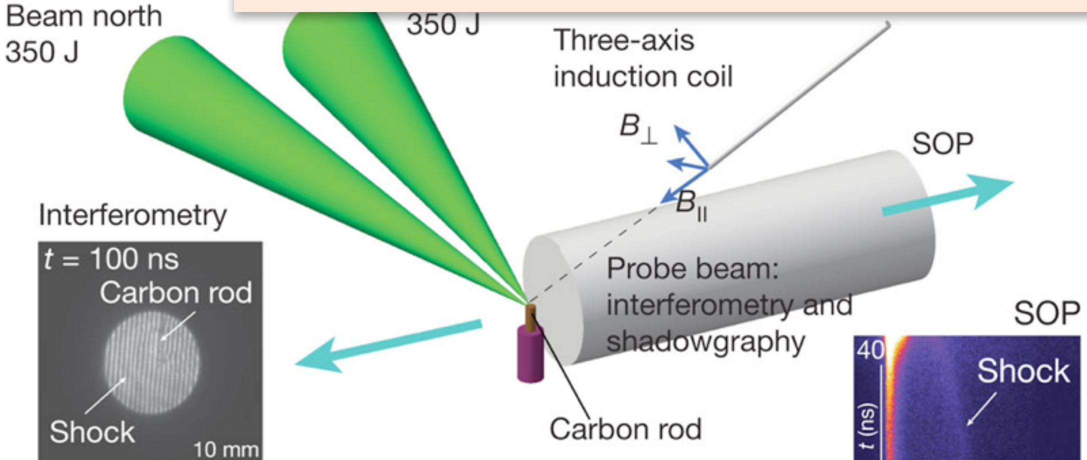

Gregori+ 2012

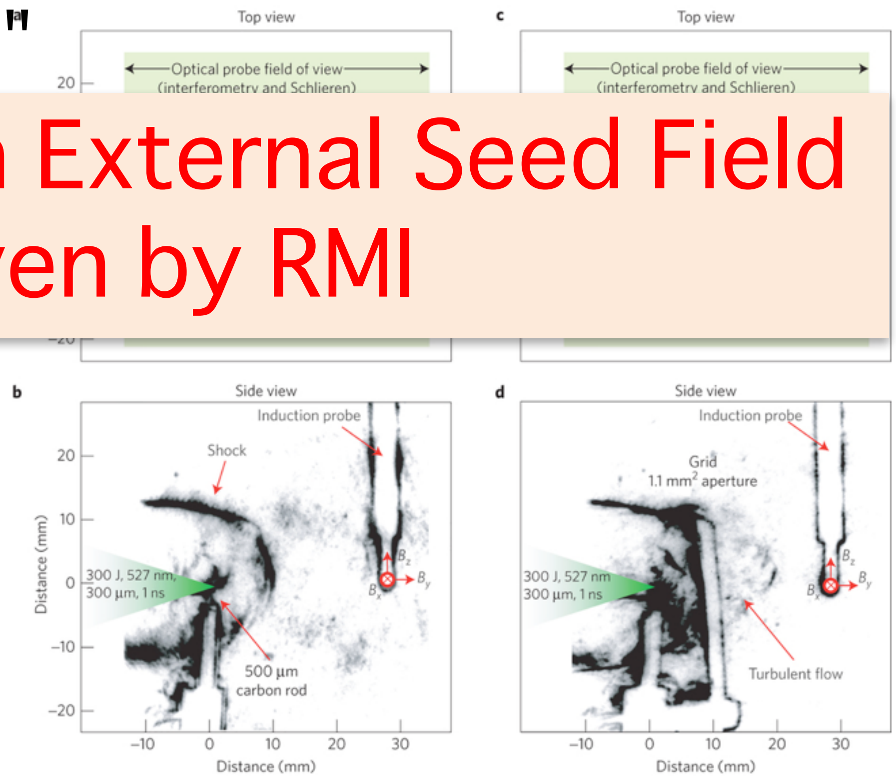

Meinecke+ 2014

Why laser experiment? --- It is because of magnetized plasma and high Mach number.

EXP

- Initial Interface
  - Modulated CH Foil (50 umt)
    - Wavelength: 150 um
    - Amplitude: 7.5 um
  - Nitrogen Gas
    - Pressure: 5 Torr
- Experimental Setup

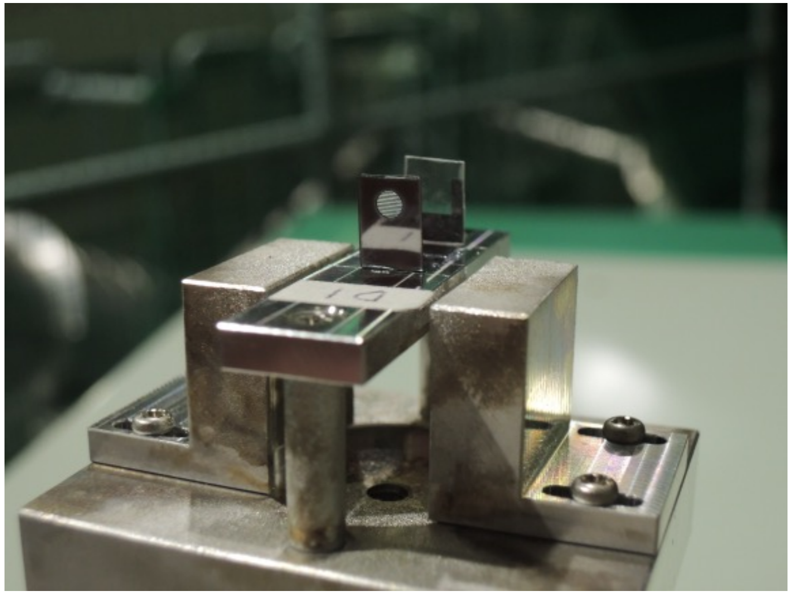

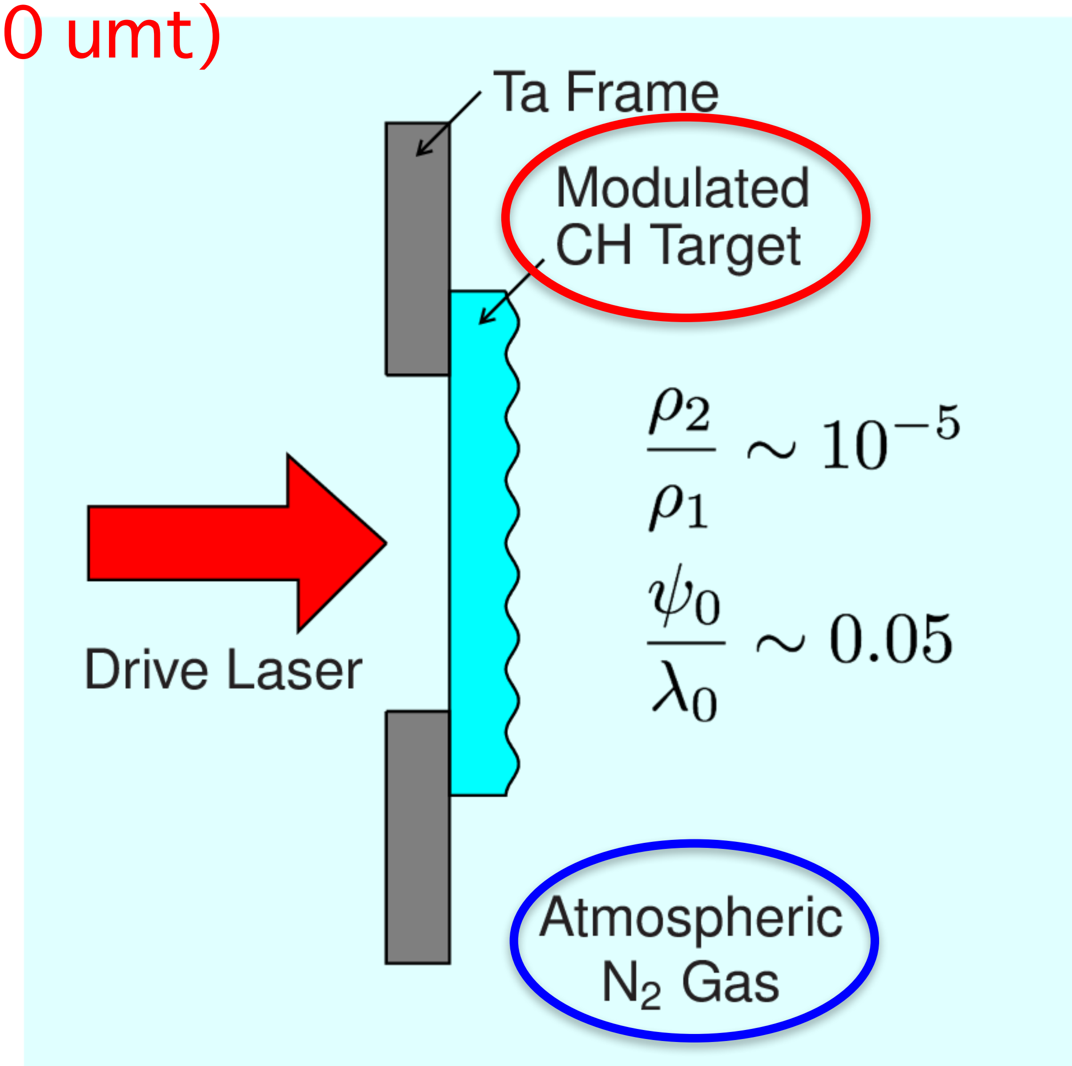

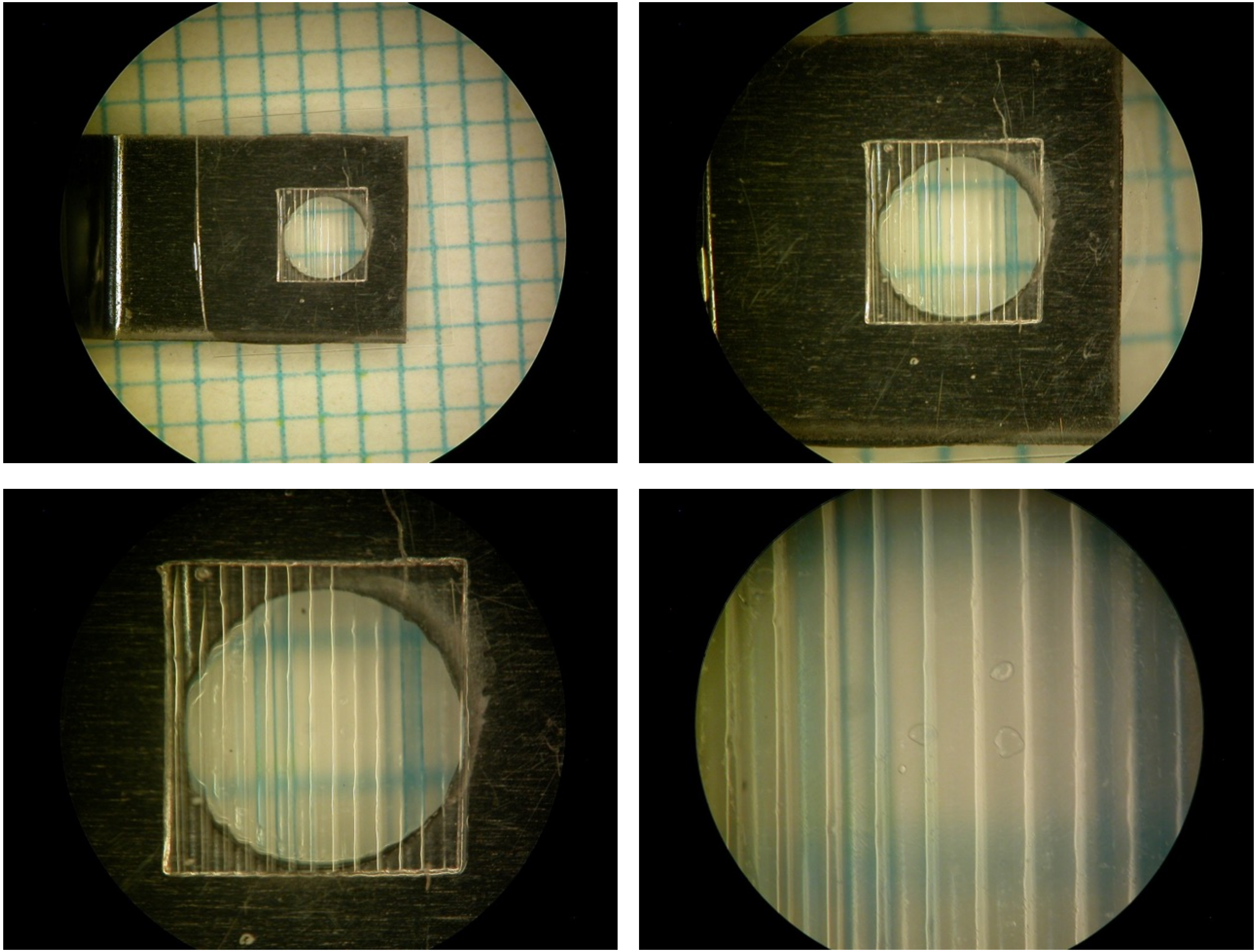

2016 FM02

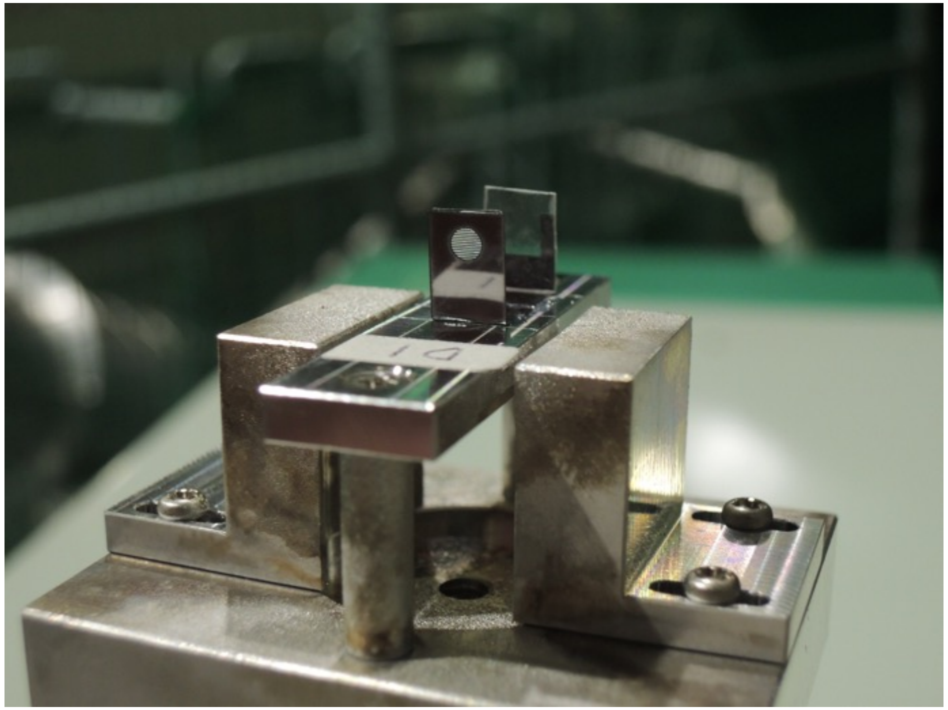

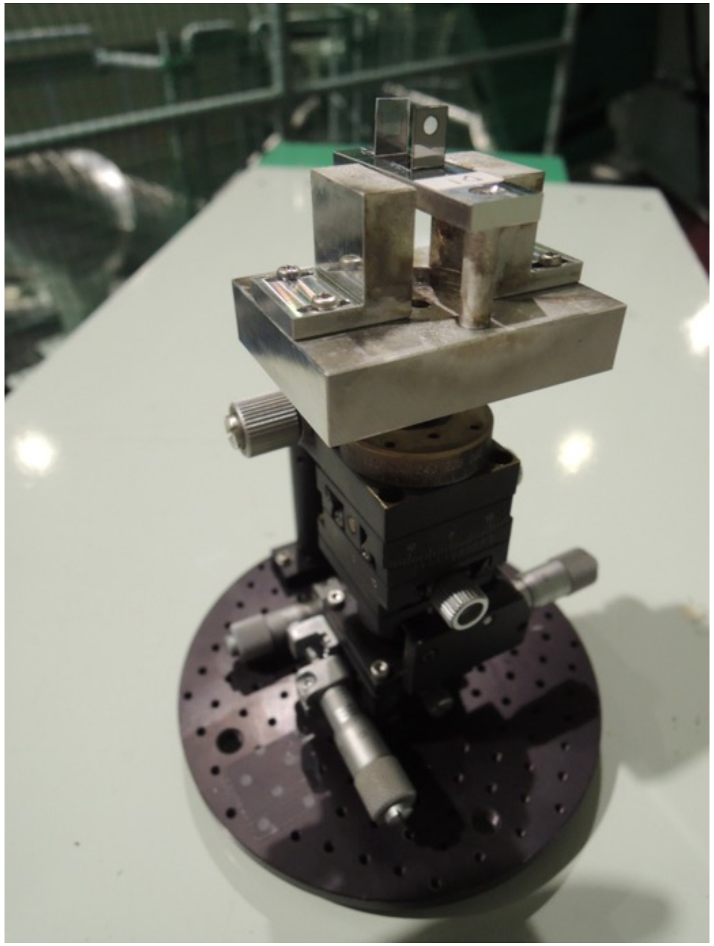

2016 FM02

Why laser experiment? --- It is because of magnetized plasma and high Mach number.

EXP

- Initial Interface
  - Modulated CH Foil (50 umt)
    - Wavelength: 150 um
    - Amplitude: 7.5 um
  - Nitrogen Gas
    - Pressure: 5 Torr
- Magnetic Field
  - Neodymium Magnet
    - Strength: 0.2 T
- Experimental Setup

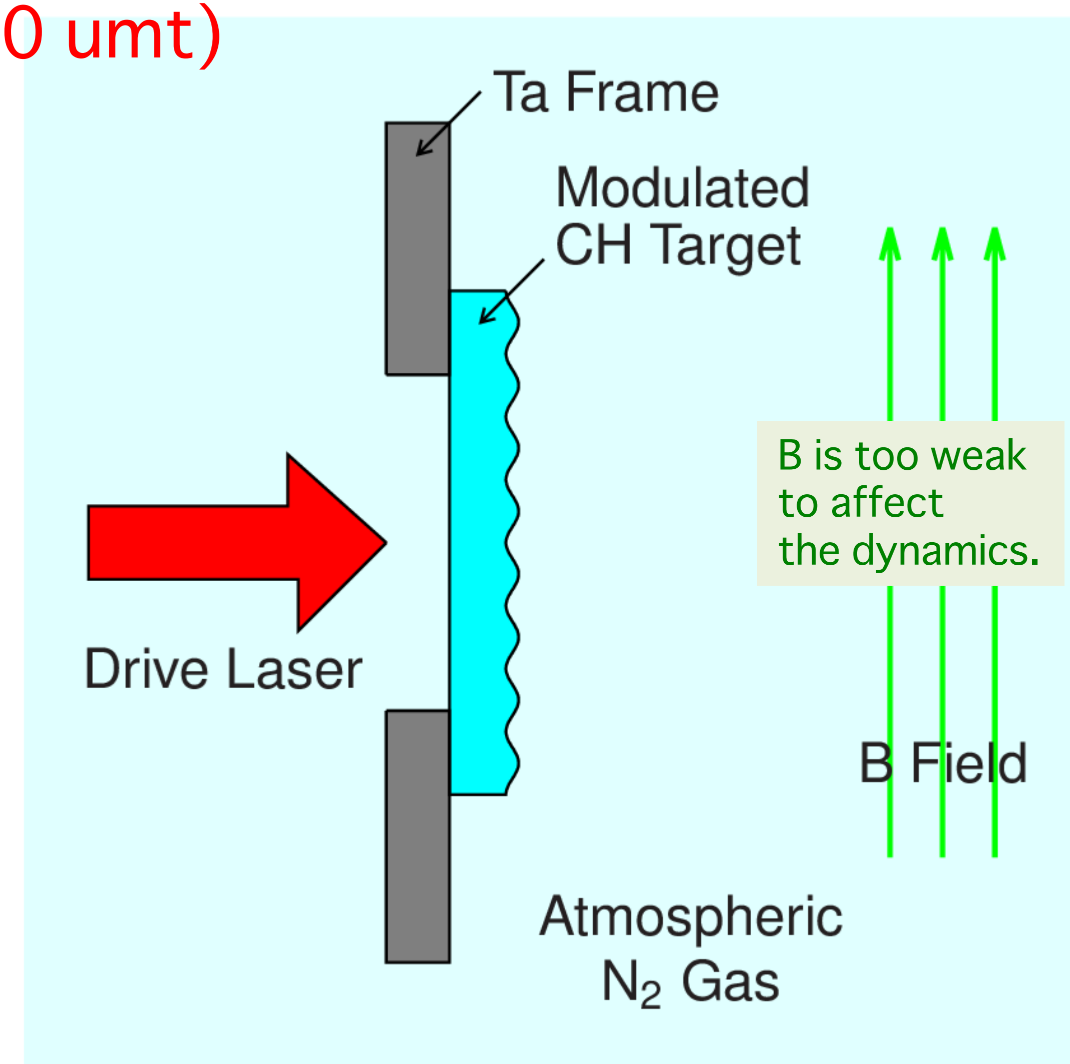

Why laser experiment? --- It is because of magnetized plasma and high Mach number.

EXP

- Initial Interface
  - Modulated CH Foil (50 umt)
    - Wavelength: 150 um
    - Amplitude: 7.5 um
  - Nitrogen Gas
    - Pressure: 5 Torr
- Magnetic Field
  - Neodymium Magnet
    - Strength: 0.2 T
- Laser-Driven Shock
  - GEKKO Laser
    - Energy: 0.2-0.7 kJ
    - Pulse: 2.5 ns

- Experimental Setup

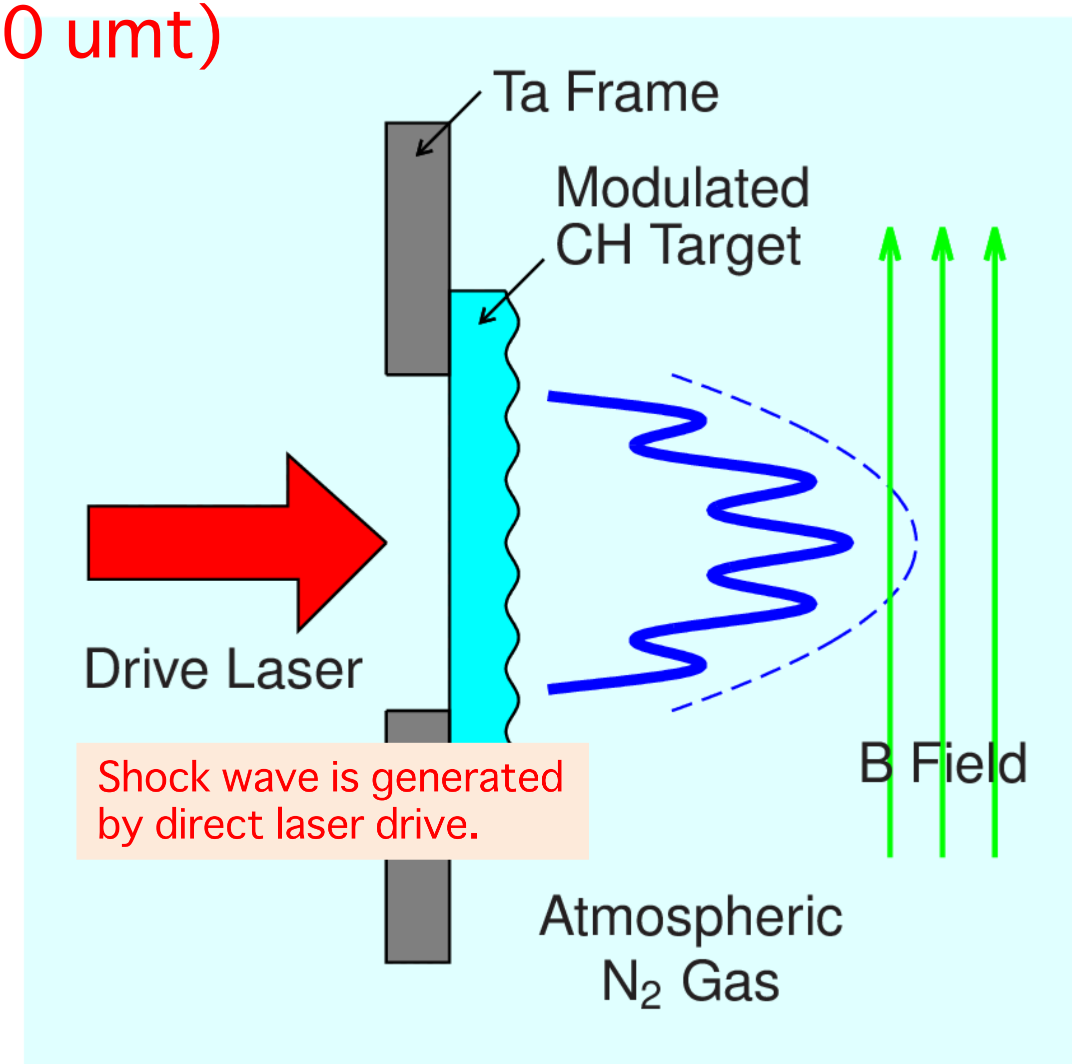

Shock wave is generated by direct laser drive.

EXP

Both of the transmitted shock and interface velocities depend on the laser intensity.

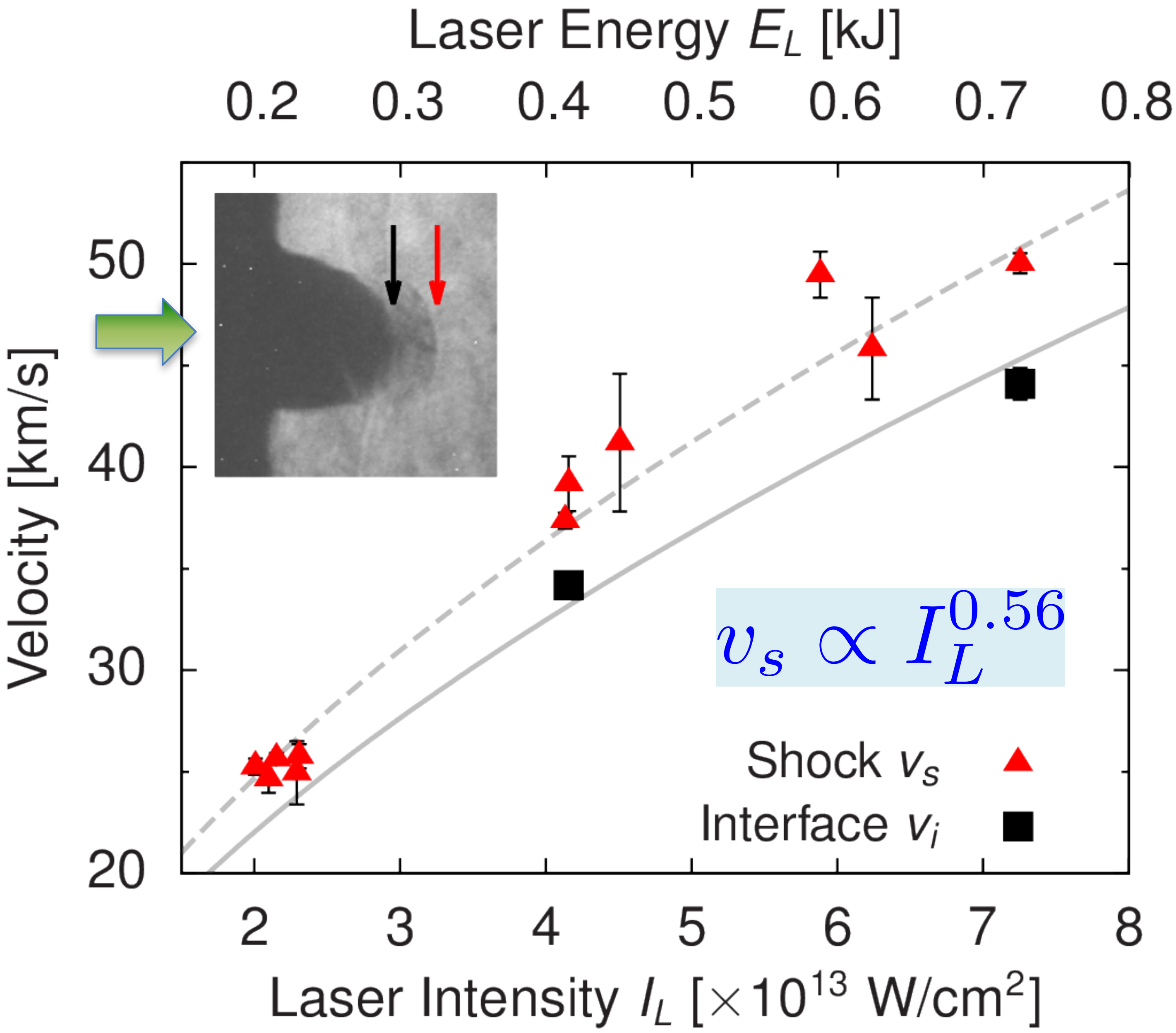

Evolution of RMI growth observed successfully by optical measurements.

EXP

- Snapshot Taken by Optical Shadowgraphy

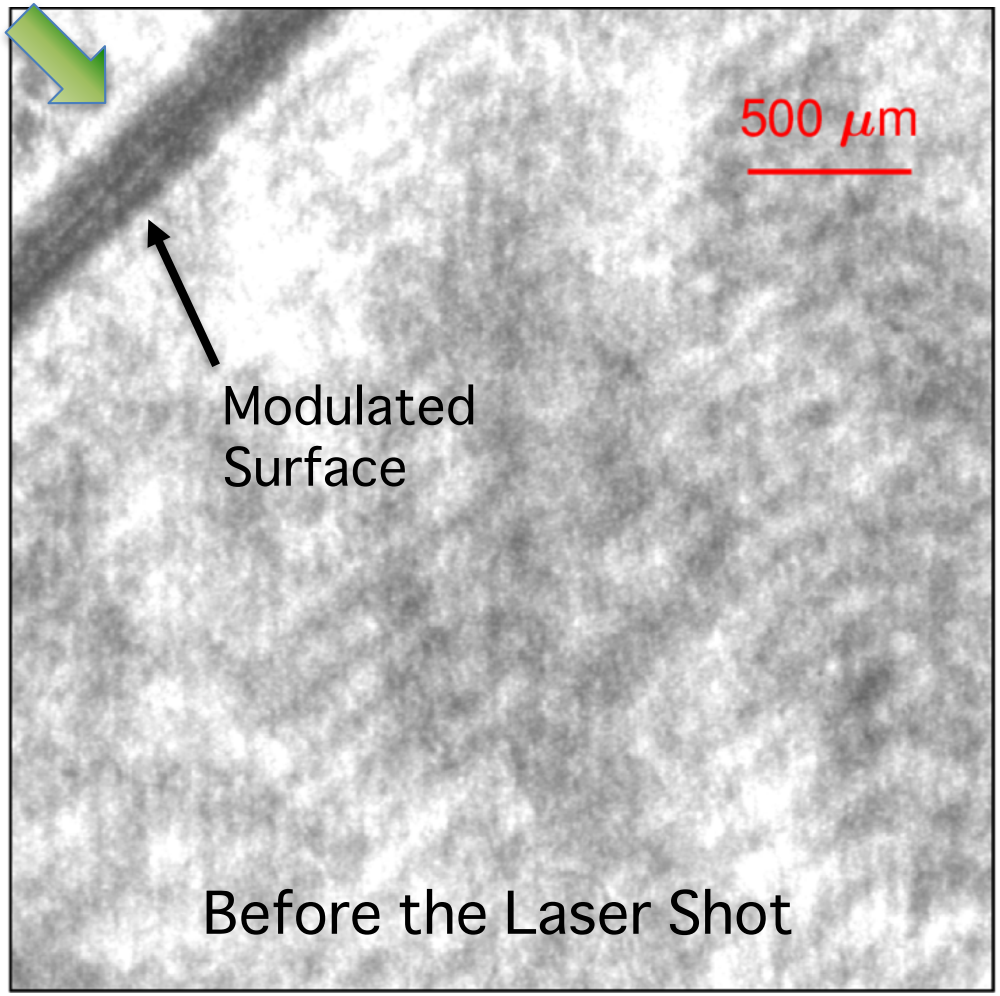

Evolution of RMI growth observed successfully by optical measurements.

EXP

- Snapshot Taken by Optical Shadowgraphy

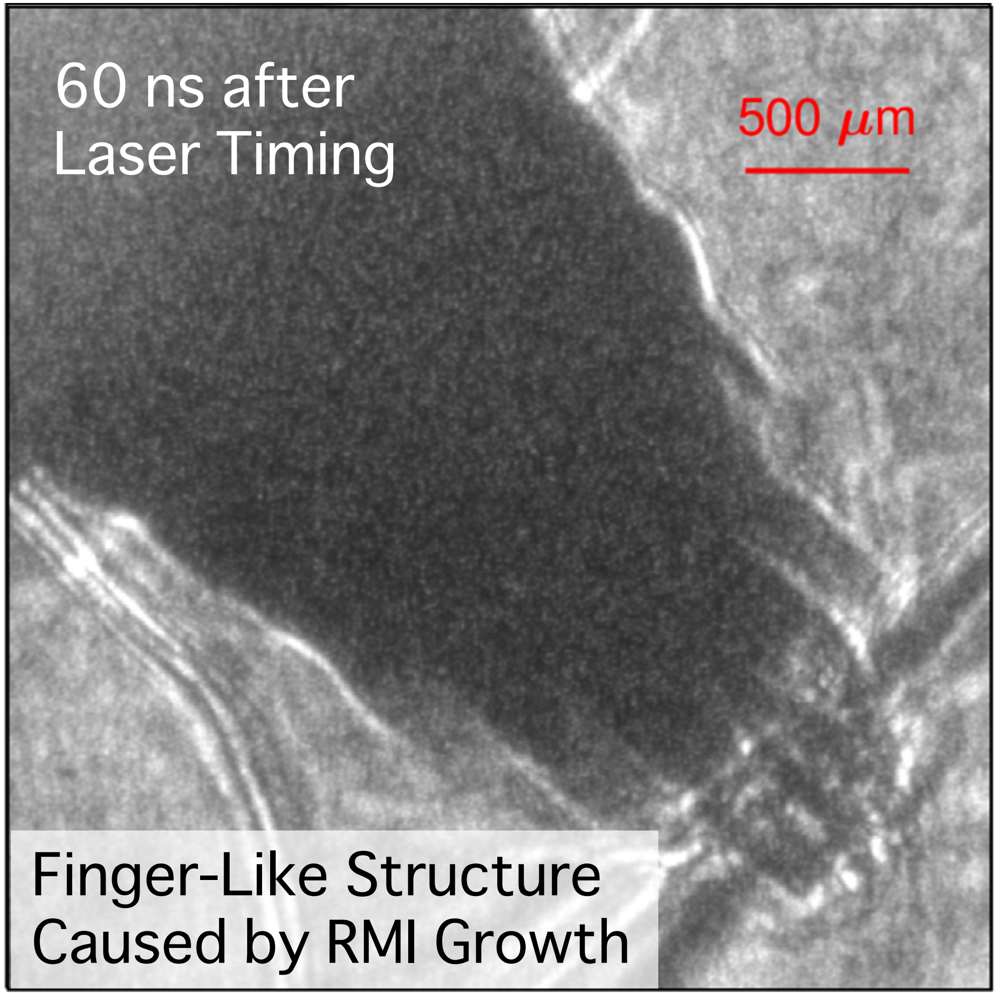

Evolution of RMI growth observed successfully by optical measurements.

EXP

- Snapshot Taken by Optical Shadowgraphy

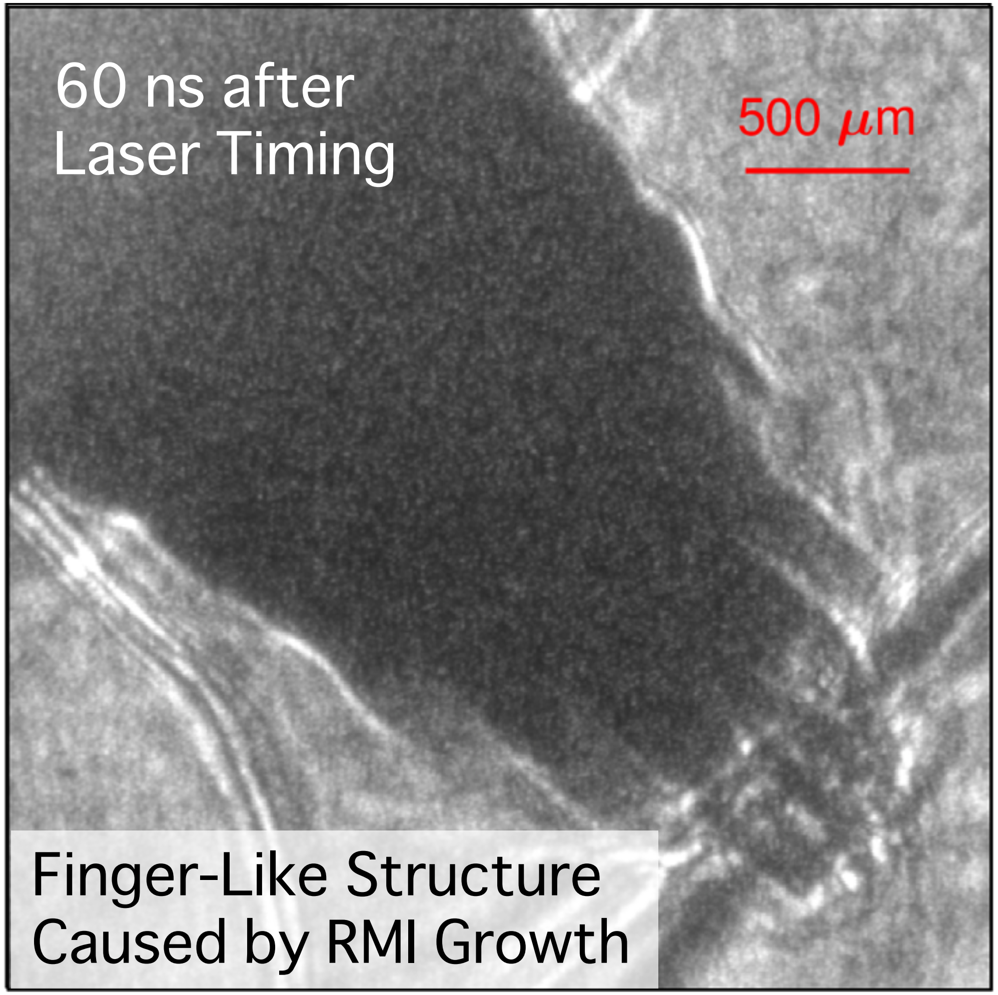

- Phase reversal at the very beginning was observed in the past GEKKO experiment.

Shigemori+ 2000

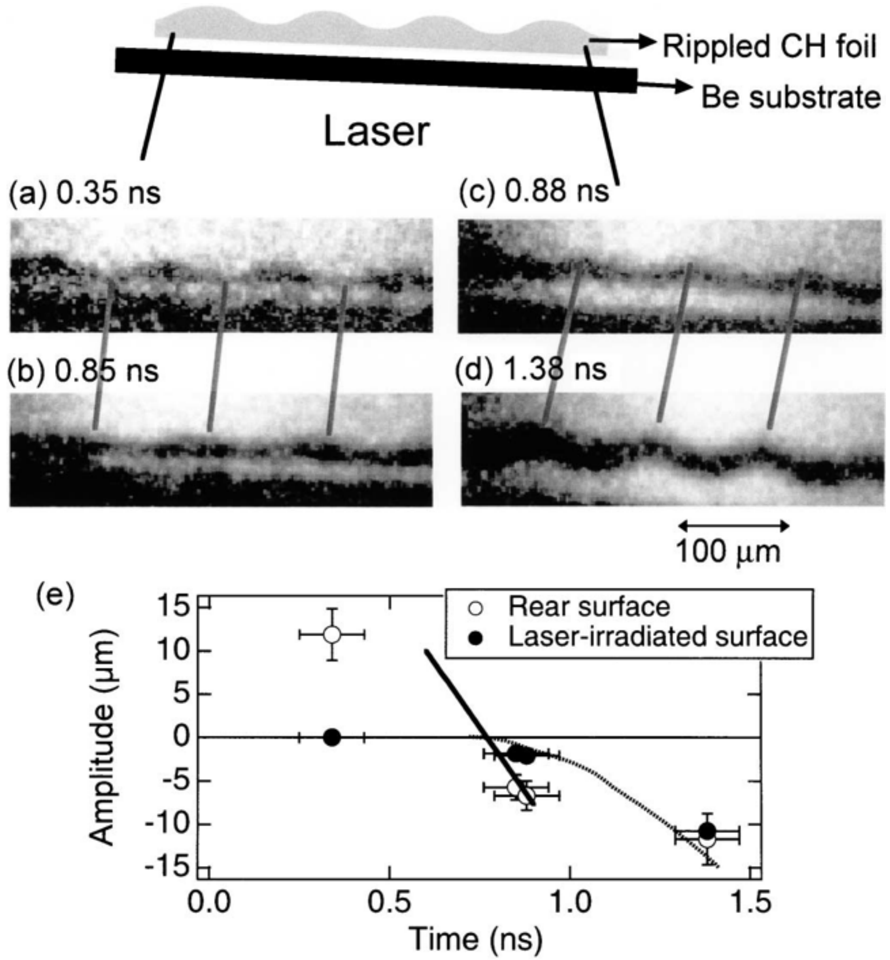

EXP

Growth velocity of the surface fluctuation can be evaluated from snapshots of the "fingers".

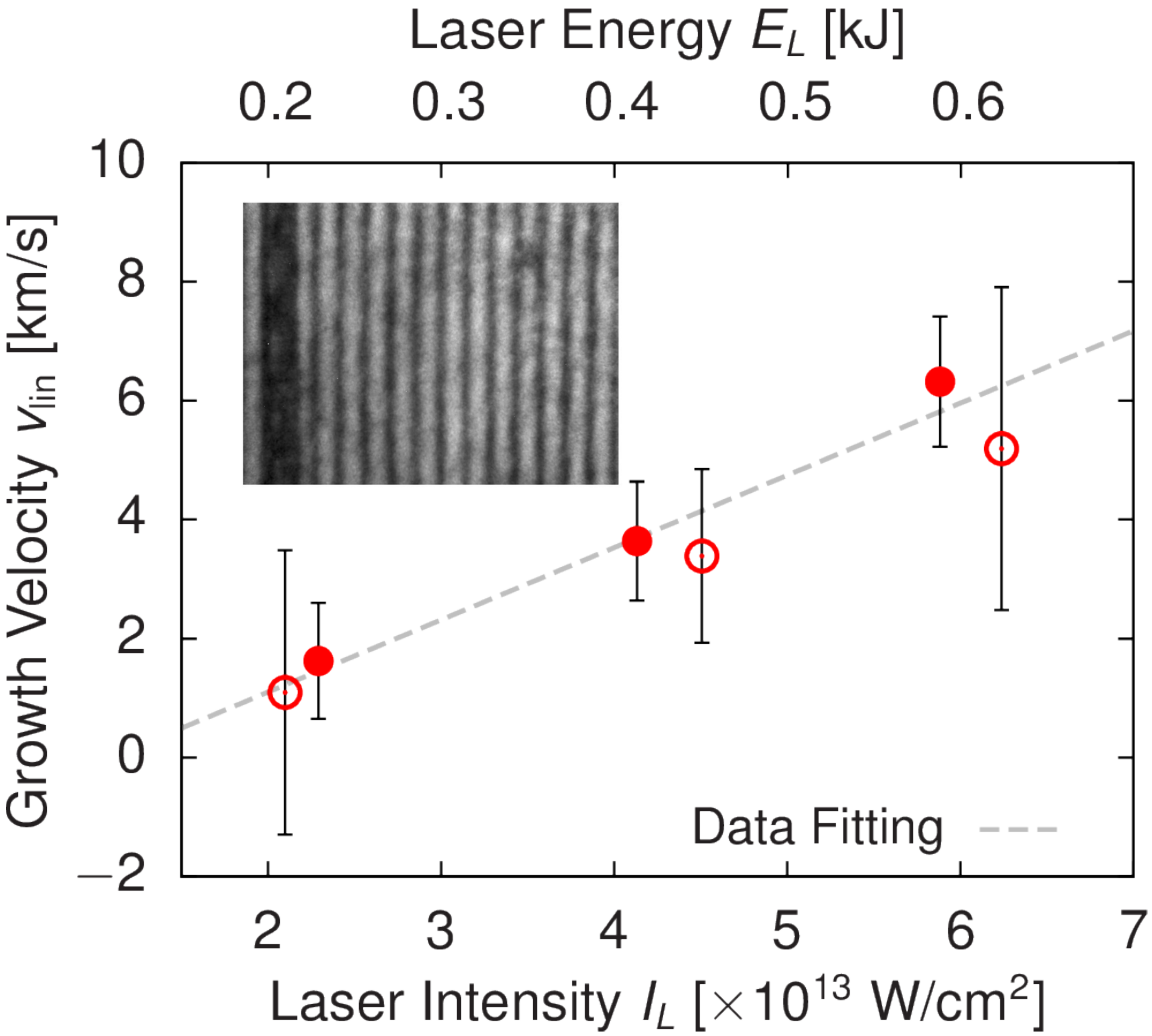

EXP

Measured growth velocities are comparable or larger than the model prediction.

- Wouchuk-Nishihara Formula
  - With a Help of the Interface Velocity from an Empirical Fit

$$\frac{v_{\mathrm{lin}}}{k\psi_0 v_i} \approx -0.16$$

$$\frac{\rho_2}{\rho_1} = 10^{-5}$$

$$M_i = 5$$

$$v_i \sim 15 \left(\frac{I_L}{10^{13}\ \mathrm{W/cm}^2} \right)^{0.56}$$

Meyer & Blewett 1972

$$\frac{v_{\mathrm{MB}}}{k\psi_0 v_i} = \frac{A^*}{2}\left(1 + \frac{\psi_0^*}{\psi_0}\right) \approx -0.20$$

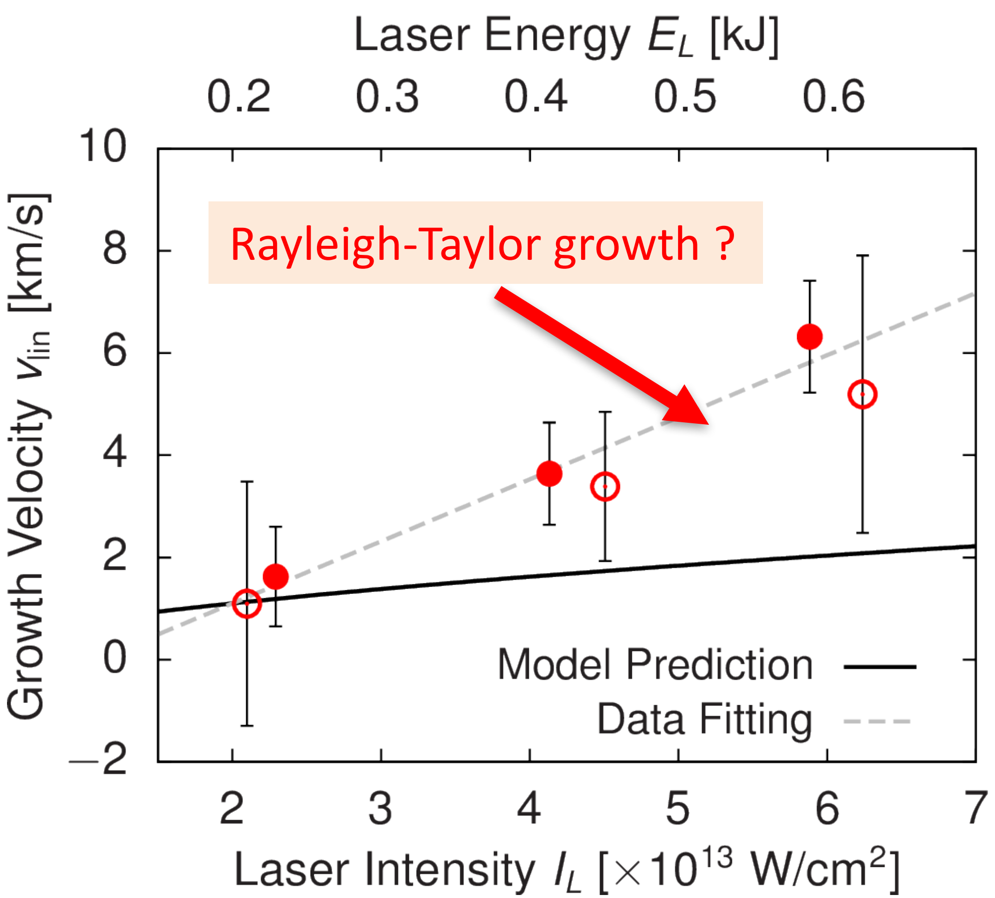

Measured growth velocities are comparable or larger than the model prediction.

EXP

- Wouchuk-Nishihara Formula
  - With a Help of the Interface Velocity from an Empirical Fit

$$v_i \sim 15 \left(\frac{I_L}{10^{13}\ \mathrm{W/cm^2}} \right)^{0.56}$$

- Future Work
  - Amplified Field Measurement (B-Dot)
  - RMI + RTI (Early Phase)

$$\frac{v_{\mathrm{lin}}}{k\psi_0 v_i} \approx -0.16$$

$$\frac{\rho_2}{\rho_1} = 10^{-5}$$

$$M_i = 5$$

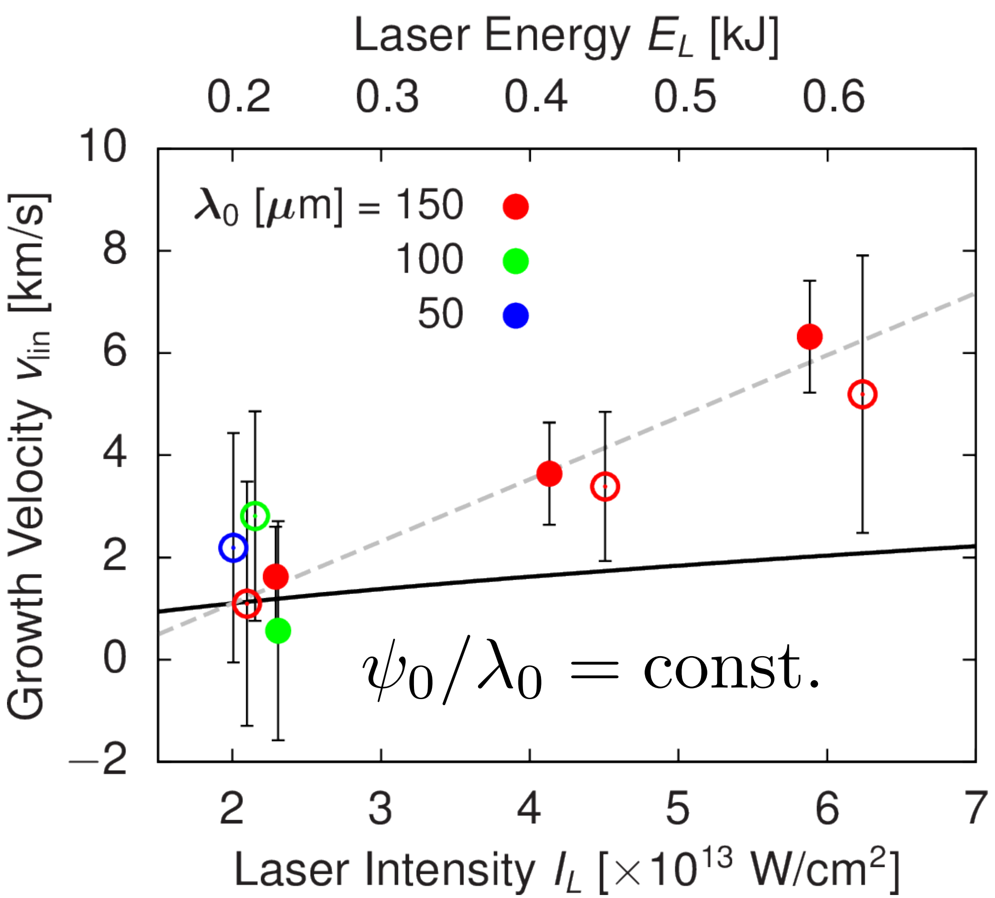

3. Anisotropic Thermal Conduction

GEKKO Experiment in Osaka

Matsuo+ PRE 2017

Bottom Line: Anisotropic thermal conduction affects flow dynamics even when the plasma beta is large.

Anisotropic thermal conduction affects flow dynamics even when the plasma beta is large.

EXP

- Large Plasma Beta: Lorentz force is negligible.
- But the dynamics can be modified by B field via "confinement of plasma thermal energy".
- Hall Parameter

$$\omega_{ce}\tau_{ei}$$

- Ablation Plasma

$$\omega_{ce}\tau_{ei} \sim 1$$

$$\frac{\kappa_{\perp}}{\kappa_{||}} \sim 0.1$$

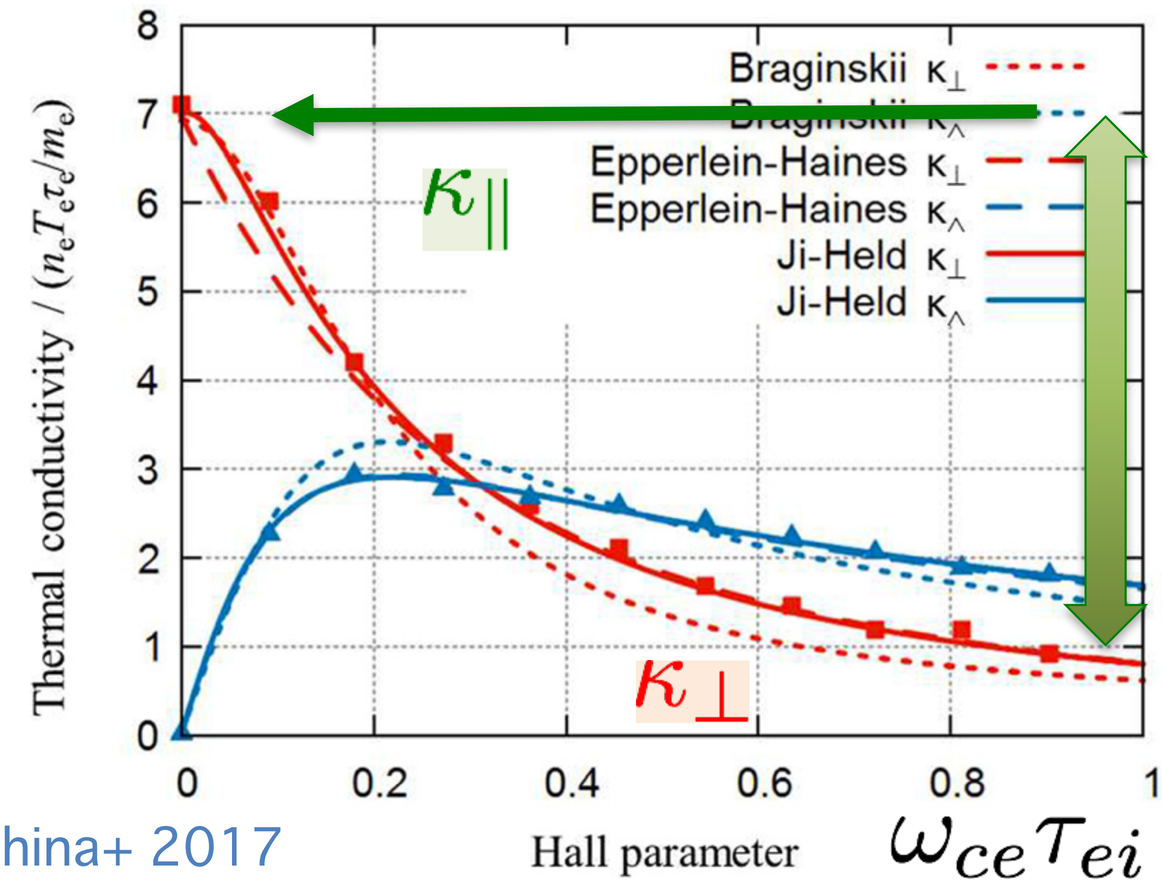

Asahina+ 2017

EXP

Non-uniform heat flow is formed on corrugated planar target in strong B field.

1. Modulation on Ablation Side of Target
2. Non-uniform Field Distribution Generated by Plasma Flow
3. Thermal Energy Kept for Longer Timescale at Stronger Field Region
4. Enhance the Modulation

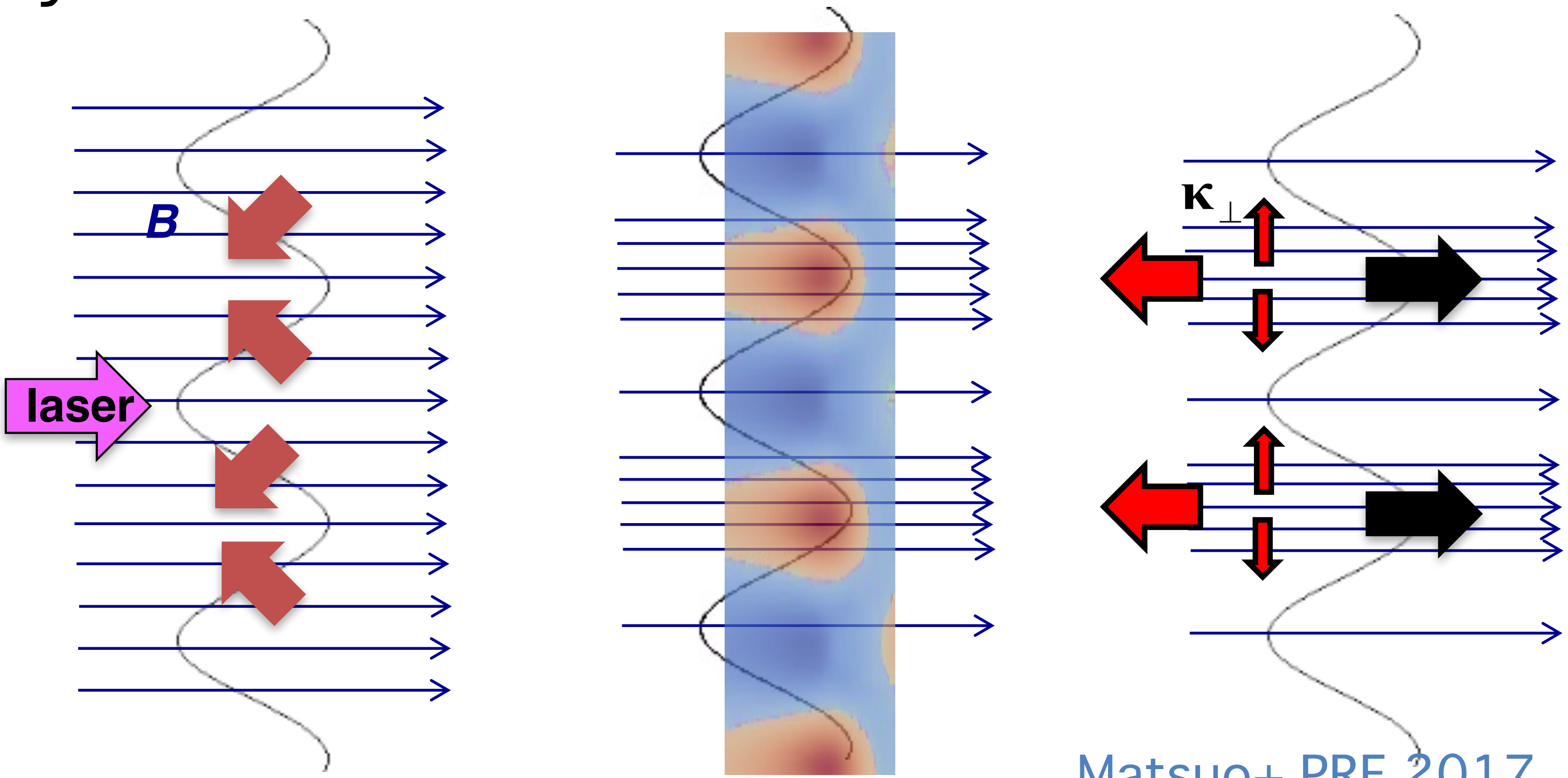

Matsuo+ PRE 2017

Non-uniform heat flow enhances the perturbation growth.

EXP

- Radiation Magneto-Hydrodynamic Simulation (PINOCO-MHD)

Nagatomo+ NF 2015

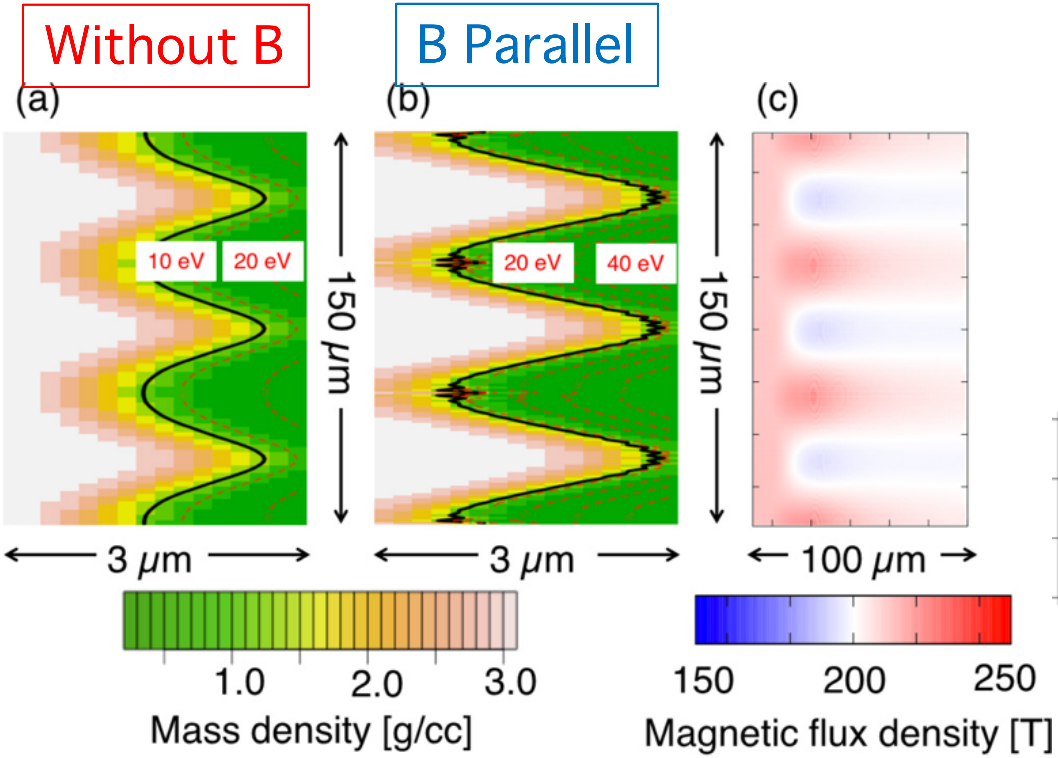

- GEKKO result is in good agreement with the simulation.

Matsuo+ PRE 2017

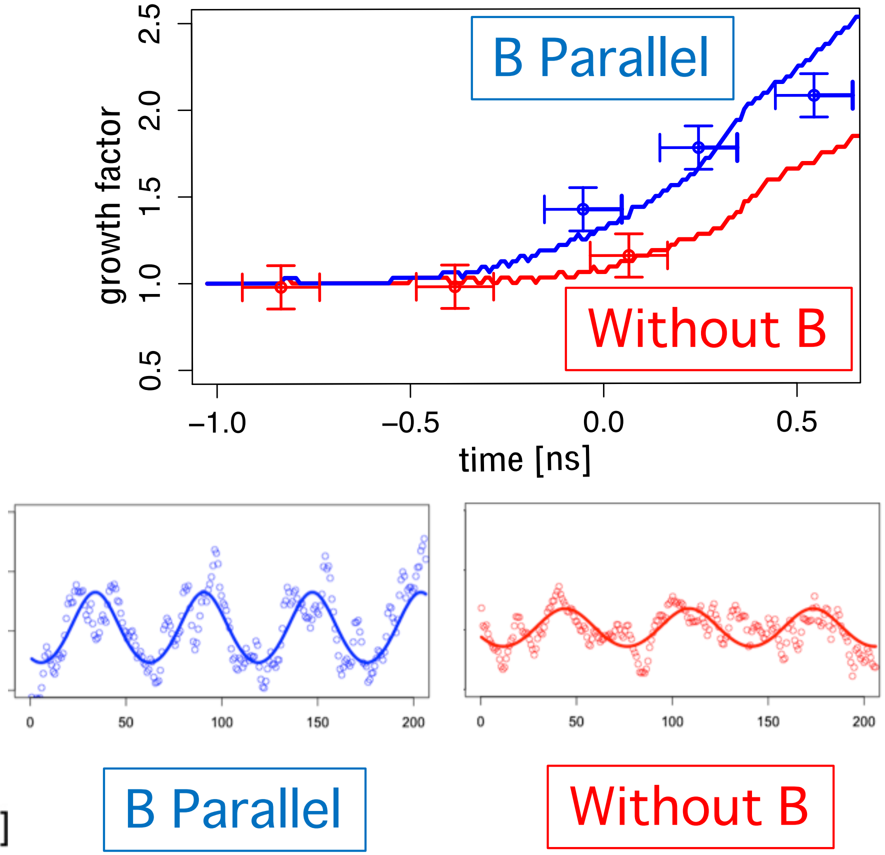

Summary

- We are investigating the magneto-hydrodynamic evolutions of RMI by using both simulations and laser experiments.
- There are 3 interesting features in MHD RMI.
  1. A strong magnetic field can reduce the growth of RMI significantly, where the Alfven (Mach) number is the key controlling parameter.
     Sano+ PRL 2013; Matsuoka+ JNS 2017
  2. Turbulent motions driven by RMI can amplify an ambient magnetic field by many orders of magnitude.
     Sano+ ApJ 2012
  3. Anisotropic thermal conduction can affect hydrodynamic flows even when the plasma beta is much larger than unity.
     Matsuo+ PRE 2017